The effect of ion accumulation owing to water recycling on flotation performance

Mathew Dzingai

A thesis submitted to the Faculty of Engineering and the Built Environment, University of Cape Town, in fulfilment of the requirements for the degree of Master of Science in Engineering, in Chemical Engineering

June 2019

PLAGIARISM DECLARATION

I know the meaning of plagiarism and declare that all the work in this document, save for the properly acknowledged, is my own. This thesis has been submitted to the Turnitin module and I confirm that my supervisor has seen my report and any concerns revealed by such have been resolved with my supervisor.

Signed by candidate

20/06/2019
Mathew Dzingai

ACKNOWLEDGEMENTS

I would like to outspread my sincere gratitude to the following people, who helped making this study possible:

- Associate Professor Kirsten C. Corin and Dr Malibongwe S. Manono, for their open-door policy, superhuman care, remarkable patience and great humour which made all this work exciting and awesome. Your unwavering technical support and investment in my growth as a researcher was priceless. Thank you for being kind and allowing me the freedom and making me feel welcome. Thank you for sending me to Europe especially New Boliden (Kevitsa mine). Thank you for giving me a chance, words will never be enough to express my gratitude for all that you did for me. My story will never feel complete without your names in it.
- Ngoni Mhonde for being a good friend while I stayed in Finland.
- The Centre for Minerals Research laboratory staff at the UCT: Shireen Govender, Refilwe Moalosi, Nosibusiso Sunduzwayo, Kenneth Maseko, Monde Bekaphi, Lorraine Nkemba, Gary Groenmeyer. Heather Sundstrom thank you for your administrative prowess making sure my living and running costs were run on time and that I didn't have to worry.
- My parent, Getrude Nemutenzi Mufandaedza, who we share the same birthday month and who's always proud of my achievements no matter how small I deem them. She thinks I am a genius and that's all I remember whenever adversities are hipped against my progress. Your love is priceless, may God continue to bless you. My father, MHRIP.
- To my friends Simbarashe H. Nyakunuhwa for being the big brother and friend, showing me some cool places in Cape Town, great technical discussions and invaluable "nerdy" talks that we enjoyed indulging in, while working on weekends! Lucia Dzinza for being the big sister and being generous and kind towards me. Lisa L. October for being the nice friend and for being "my soft skills expert". Rešoketšwe M. Manenzhe for allowing me to call you Shoki and for being the humoured friend. Blessing Hellen Chirume for the laughs and believing in me. Laylaa Ebrahim for being such a hard worker and assistance with the column tests, and for being awesome. Andrea Molifie thank you for showing me some mineralogical data manipulation and being a good friend
- My 5055Z course mates: Apol, Tanaka, Dineo and Noli we shared some cool moments, all the best in your studies.

SYNOPSIS

With the drive to reduce water usage globally, the mining sector must reassess its water usage as it has in the past contributed greatly to environmental degradation due to effluent discharge, tailing disposal and process water seepage into the water-table. Mineral beneficiation entails different unit operations; amongst them is froth flotation. Froth flotation is a multifaceted complex process which is water intensive and to manage water usage, the global mining industries are now recycling water. The recycled water may contain deleterious ions that affect the mineral surface, pulp chemistry and reagent action, hence the need to establish whether threshold concentrations exist beyond which the flotation performance will be adversely affected. This is of paramount importance in informing appropriate recycle streams and allowing simple, cost-effective water treatment methods to be applied.

To better understand the influence of water recycling in flotation, a low-grade Cu-Ni-PGM sulphide ore was used. This study investigated the effects of increasing ionic strength as well as increases in specific ion concentrations to determine whether these selected ions had beneficial or deleterious effects on the flotation process. Copper and nickel were the target metals, floated as chalcopyrite and pentlandite, respectively. Their recovery and grade under different conditions was used as a measure to quantify whether a threshold ion concentration existed. The key performance indicators used were: (a) water recovery, (b) solids recovery, (c) valuable metal recovery, (d) grade of the recovered concentrates and (e) electrical conductivity.

While a complex background water chemistry of 3 SPW was maintained for the spiking tests, ion spiking was intended to mimic the recycling of water and the most prevalent ions which would likely be recycled and therefore accumulated, such ions as: Ca^{2+}, Mg^{2+}, NO_3^-, SO_4^{2-} and $S_2O_3^{2-}$. These ions were chosen based on speculation from relevant literature that they might impact the flotation performance due to their influence on pulp chemistry and reagent interaction.

This was achieved by conducting sequential batch flotation and electrical conductivity (EC) tests. Batch flotation tests were performed to investigate the effect of different ionic strength conditions on the overall flotation performance. The same ionic strengths and spiking concentrations were used for froth (or foam) column studies with a focus on tracking the ion concentration distribution between the froth and the slurry (or solution) by means of measuring the EC of each of the froth and the pulp (solution) phases. The differences implied whether the ions were selectively concentrated at the air-water or solids-water interphases in a 3-phase system or likewise at the

- Special mention goes to the New Boliden Kevitsa Oy and Benjamin Musuku for supplying the ore and reagent samples as well as for hosting me during my on-site work, not presented within this thesis.

This Project has received funding from the European Union H2020 programme under grant agreement No. 730480

bubble surface or within the solution for a 2-phase system. This distribution of ions was linked to the other key performance indicators.

Increasing ionic strength; 3, 5 and 10 SPW respectively, resulted in an increase in water recovery in the order 3 SPW < 5 SPW < 10 SPW, indicating an increase in froth stability due to inhibition of bubble coalescence at high ionic strength. There was, however, no significant effect on the valuable metal recovery. Most of the nickel was recovered in the copper circuit which was expected as on-site conditions were not maintained at the laboratory scale, no lime was added to adjust the pH in the copper circuit and an EDTA chelating agent was not included in the nickel circuit.

Spiking 3 SPW with 800 ppm Ca^{2+} results in considerably higher water recovery per unit solids recovered compared to 3 SPW, 5 SPW, 400 ppm Ca^{2+}, 350 ppm Mg^{2+}, 700 ppm Mg^{2+}. 400 ppm Ca^{2+} resulted in the highest copper and nickel grade and was deemed the threshold for this study while for Mg^{2+} threshold lies outside of the range considered for this study. 10 SPW shows a decrease in the copper and nickel grade while the copper and nickel recoveries were not significantly impacted. The presence of the Ca^{2+} and Mg^{2+} at high concentrations leads to gangue activation which as a consequence will result in decreased grade.

880 ppm NO_3^- gave the highest copper and nickel grade compared to 3 SPW while increasing the $S_2O_3^{2-}$ from 60 to 78 ppm resulted in an increase in nickel grade. 1200 ppm SO_4^{2-} and 880 ppm NO_3^- were deemed the threshold concentration for these anions, above which the flotation performance declines, while for $S_2O_3^{2-}$ the threshold lay outside the range considered for this study.

This study has shown that the accumulation of ions within plant water, owing to recycling, is, in general, beneficial to flotation. This study has also shown that there is a concentration for each ion beyond which it is no longer beneficial to flotation. While this finding is clearly ore and ion dependent, it gives an indication as to the need for water treatment and considering the threshold concentrations found, may direct operations to suitable treatment methods for their systems.

GLOSSARY

Cu	copper
Ni	nickel
PGE	platinum group element
PGM	platinum group metal
Pt	platinum
ppm	parts per million
rpm	revolutions per minute
SIPX	sodium isopropyl xanthate
TDS	total dissolved solids
UCT	University of Cape Town
µm	micrometres
µS	micro Siemens
wt.	weight
C1	first concentrate (with C2 being the second, C3 being the third, etc.)
CCC	critical coalescence concentration
cm	centimetres
CMR	Centre for Minerals Research
g	grams
g/t	grams per ton
HG	high grade
I.S.	ionic strength
kg	kilograms
L	litres
L/min	litres per minute
M	molarity
min	minutes
mg/L	milligrams per litres
mm	millimetres
mL	millilitres
EC	electrical conductivity
NFG	naturally floatable gangue

CONTENTS

LIST OF TABLES

LIST OF FIGURES

CHAPTER 1

1 INTRODUCTION

This study considers the recycling of plant water within mineral processing concentrators, with specific focus on selected ions and the impact that these ions will have on flotation performance of a Cu-Ni-PGM low grade ore. Copper and nickel grades and recoveries as well as solids and water recoveries were used as indicators for performance.

1.1 Background and conceptualization

Water scarcity and environmental degradation are global issues. The mining sector has become the central focus as it contributes greatly to environmental degradation by waste disposal processes, caused by tailings disposal and process water seepage into the water-table (Haggard et al. 2015). A closed water circuit refers to green mining whereby the main focus is on recycling water, minimizing effluent discharge while meeting production targets. In order to address process water issues, the closed water circuit is being considered by many operations and in some cases is already in use, (Schreithofer et al. 2017; Muzinda and Schreithofer, 2018).

The recycling of water in mining processes may cause ions and other water components to accumulate (Slatter et al. 2009; Muzenda, 2010). There are ions such as Ca^{2+}, Mg^{2+}, NO_3^- and sulphates present in water that that may be deleterious to the flotation process owing to their effects on sub-processes of flotation (Craig et al. 1993; Cho and Laskowski, 2002; Manono et al. 2016). However, there is limited literature as regards the concentration thresholds beyond which ions common in process would result in adverse effects on flotation. This thus necessitates investigations into specific ions and their concentration in relation to froth flotation performance. The influence of specific inorganic ions on mineral flotation is multifaceted and different ions may play various roles; that is, either beneficial or detrimental to the flotation-concentration process (Li et al. 2017). The cationic and anionic spiking of synthetic plant water to levels above those currently found on actual operations is the main focus of this investigation.

1.2 Scope and Limitations

Finkelstein and Lovell (1972); Davis et al. (1975); Bradshaw et al. (1998a) suggested that frothers, depressants and activators in addition to collectors, dissolved ions and other chemical species affect flotation performance. Part of the trident factors of flotation operating parameters, adapted from Klimpel (1996) shown in **Figure 2-3**, demonstrated that grinding environment also has a substantial effect on flotation performance while Ikumapayi et al. (2012); Muzinda and Schreithofer, (2018), demonstrated that certain ions have potentially adverse effects on flotation performance.

In this study, the grinding environment will be maintained; that is, the mill and grinding media, as well as the milling duration will be maintained as constants. The ions under study are limited to Ca^{2+}, Mg^{2+}, SO_4^{2-}, NO_3^- and $S_2O_3^{2-}$. With regards to reagents; collector, depressant and frother type and dosage are kept constant throughout the study to match those used on site.

The flotation performance will be evaluated with the following as the key indicators:

- The water recovery to the concentrate.
- The solids recovery to the concentrate.
- The recovery of the valuable mineral.
- The grade (purity) of the recovered concentrate.
- Recovery of metal viz. ions distribution
- 2-phase and 3-phase column studies will be carried out.

2 LITERATURE REVIEW

2.1 Froth Flotation

The theory of froth flotation is complex and it involves three phases; solids, liquid and air with many sub-processes and interactions (Finkelstein and Lovell, 1972; Wills and Napier-Munn, 2006). Flotation selectively explores differences in the surface properties between minerals, the primary property exploited is the hydrophobicity associated with different mineral surfaces. Flotation is defined as a physico-chemical separation method which depends on differences in wettability between the valuable (target) mineral and the non-valuable (gangue) material (Wills and Napier-Munn, 2006). Air bubbles are introduced into the finely ground slurry before-which reagents would have been added to enhance the hydrophobicity (water repelling effect) of the desired mineral and exploit primarily the differences in the exposed surface mineral properties. The differences in properties are only exploitable on exposed mineral surfaces.

It is common practice that single stage semi-autogenous (SAG) mills or autogenous (AG) milling are used size reduction and as a consequence surface exposure for a variety of ore types with the advantages of being comparatively low capital cost and flexible for future expansion (Okuyama et al. 2002).

Wills and Napier-Munn (2006) demonstrated that the hydrophobic mineral is usually transferred to the froth phase, leaving the hydrophilic gangue in the pulp phase or tailings. The function of reagent addition is to enhance the overall selectivity of the flotation process. The relationship between recovery and grade is a trade-off that needs to be managed according to operational constraints and is incorporated in the management of an optimum froth stability.

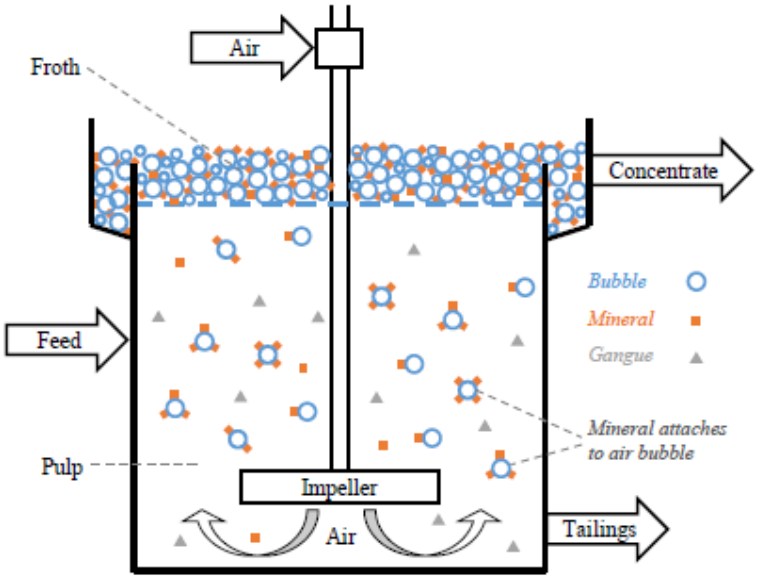

Figure 2-1 Conventional flotation cell (Hu, 2014)

Figure 2-1 shows a schematic of a conventional flotation cell used in industrial lab operations. Wills and Napier-Munn (2006) suggested that the flotation process happens through: (i) selective attachment of particles to air bubbles (or true flotation), (ii) entrainment in the water which passes through the froth and (iii) physical entrapment between particles in the froth attached to air bubbles (often referred to as (aggregation).

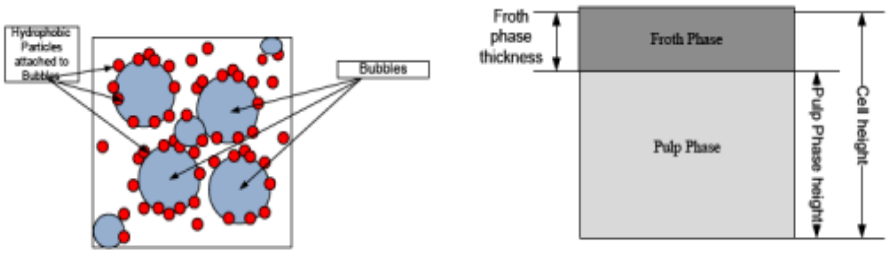

Figure 2-2 Froth and pulp phase with air bubble laden with hydrophobic particles (Hu, 2014)

The particle-bubble attachment of the hydrophobic particles is depicted in **Figure 2-2,** however oftentimes complete separation of gangue from valuable minerals is unachievable. While the target mineral reports to the froth by true flotation, other composite material may be naturally floatable or be entrained in the upward swarm of bubbles. This makes the addition of reagents (depressants, activators, frother and collectors) pertinent to enhance the hydrophobicity of the desired mineral (Bradshaw et al., 1998).

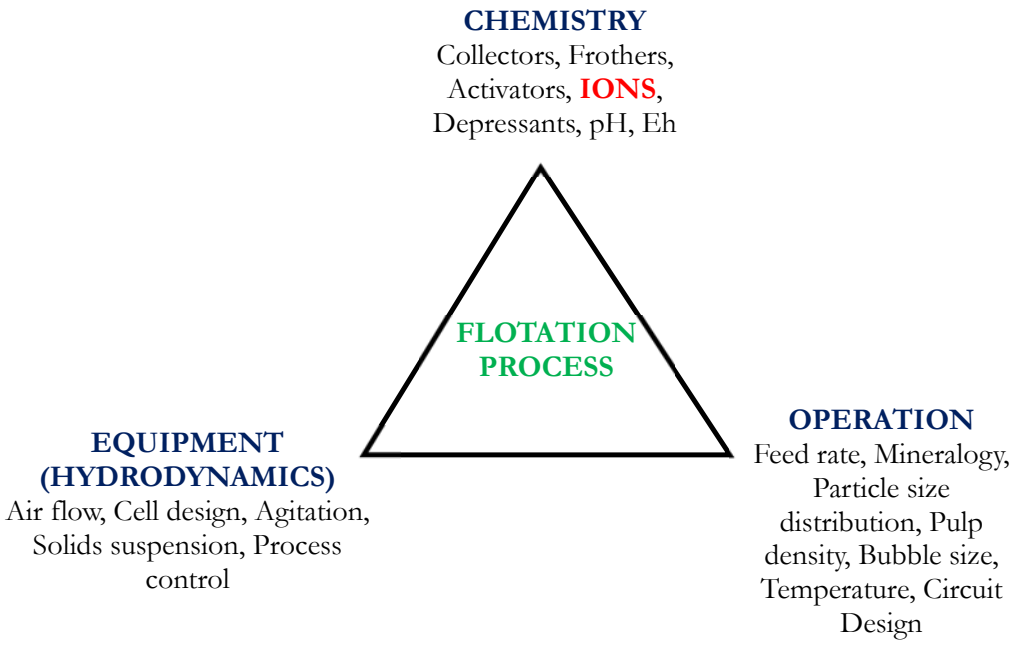

Figure 2-3 Interrelated flotation components in four main categories; a. Flotation system, b. Equipment components, c. Operation components and d. Chemistry components (adapted from Klimpel (1995))

Figure 2-3 shows the flotation system and highlighted in red are the main components of interest to this study; as such, ions will be discussed in detail later in this chapter. Due to the complex nature of the froth flotation, there are many variables that need to be controlled to get the desired outcome. Prior to froth flotation, the ore is first subjected to comminution, which is a size reduction process. The comminution process consists of two stages; crushing and grinding to achieve the appropriate liberation within the desired Particle Size Distribution (PSD).

Crushing is a dry process and it involves reducing Run Of Mine (ROM) to suitable size range that can be transported to concentrators. Grinding is a wet process performed to further liberate the desired material from its associated gangue and it is traditionally achieved by abrasion of the ore using rods (generally used in a laboratory set-up) or balls in different milling equipment (Wills and Napier-Munn, 2006). Usaini et al., (2014) defined liberation as the release of valuable material from its associated gangue material at the coarsest possible particle size hence when the mineral is not liberated from its associated gangue it is said to be locked. Sufficient liberation is required for successful downstream processes.

2.2 The Froth Phase

The air-water interface and its stability are of paramount importance in ensuring that the recovery of the target mineral is adequately conceivable. The froth is created by air introduction during the flotation process. When the froth is not stable, there is consequential bubble bursting leading to valuable mineral loss to the pulp phase and reporting to the tailings. As a result, the flotation cell efficiency in such instances is greatly affected. When the froth is too stable the flotation process efficiency is hindered hence there is a trade-off between froth stability and mineral recovered to the concentrate.

The rising air bubbles through the suspended solid particles frequently collide with these solid particles and depending on the surface properties of the particles, the hydrophobic particles get attached to the air bubbles and are carried upwards through the pulp phase and eventually reaching the surface of the slurry forming the froth. Hu (2014) suggested that at the froth-air surface, larger bubbles are prone to coalescence and bursting. Particles that were attached to the bubble fall through the froth and can re-attach to other bubbles in the pulp phase. Bradshaw (1997) added that the increased bubble loading; as the air is dispatched into the cell is in itself the outcome of a more fundamental process, the increased hydrophobicity of the mineral particle which may be the result of the collector-mineral adsorption process.

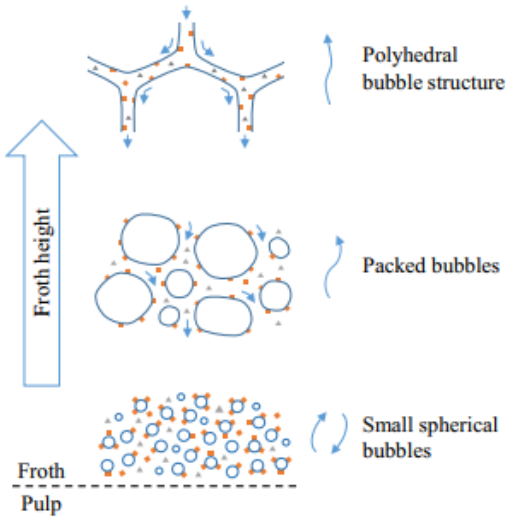

Figure 2-4 Froth structure at different froth height, (Hu, 2014)

Figure 2-4 is a schematic representation of the froth structure at different levels in the froth phase. Fast floating (hydrophobic) particles result in increased rate of liquid drainage during froth flotation.

2.3 The Pulp Phase

After milling, the slurry is added to the flotation cell, make-up water is added to the desired level of the float cell. The water-solids mixture is referred to as slurry. The slurry is then subjected to agitation at appropriate impeller speed. This agitation will keep the solids in suspension throughout the flotation process. The water-solids suspension is referred to as the pulp phase.

Muzenda (2010) suggested that a flotation cell is typically composed of 80-85 wt.% water and 15-20 wt.% solids. When air is introduced, it causes the pulp's effective volume to expand allowing generation of bubbles in the pulp phase. To avoid overflowing of the pulp, air introduced into the float cell is controlled by a control valve, the hydrophobic particles attach to air bubbles in the pulp phase (Wills and Napier-Munn, 2006). For hydrophobic particle-bubble attachment to take place, the contact angle and surface tension should thermodynamically possess a decreasing change in free energy and to achieve optimal attachment, the particle diameter and bubble diameter should be comparable (Finkelstein and Lovell, 1972; Chau, 2009; Kawatra, 2009).

Contact angle varies from a fraction of a degree to several degrees and this is fundamentally important for bubble-particle attachment and the angle depends on the mineral. The contact angle can be evaluated from Young's equation (**Equation 2.1**) based on the surface tension (Celik and Somasundaran, 1980; Chau, 2009).

$$Y_{SA} = Y_{SW} + Y_{WA}Cos\theta \quad ---------- \quad 2.1$$

Where $\mathbf{Y_{SA}}$ – solid-air interfacial tension, $\mathbf{Y_{SW}}$ – solid-water interfacial tension, $\mathbf{Y_{WA}}$ – water-air interfacial tension and $\boldsymbol{\theta}$ – contact angle

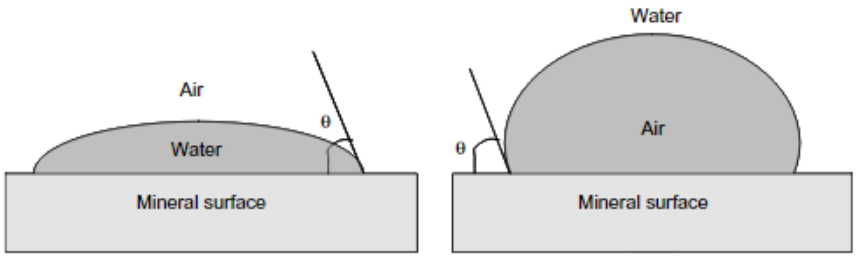

Figure 2-5 Particle-water (left) and Particle-bubble (right) attachment in the pulp phase adapted from Celik and Somasundaran (1980); Chau (2009)

Figure 2-5 shows, schematically, the interaction in the pulp phase while agitation is carried out to homogenize the collector-water-ore system (left) and subsequent reagents before the air introduction (right). Before the introduction of air, the water-collector phase surrounds the mineral

surface, this improves its hydrophobicity such that when the air is introduced, it attaches to the air bubbles formed and moves towards the top-surface of the pulp phase to form the froth.

2.4 Entrainment

The recovery of hydrophilic gangue material during flotation is a problem in mineral beneficiation. Kirjavainen (1996) conducted a review and analysis of factors controlling the mechanical flotation of gangue minerals and suggested that the degree of entrainment depends on a number of factors including; fineness of the feed, water recovery and other process variables such as slimes coatings and composite particles via known mechanisms i.e entrapment and entrainment.

Entrainment depends on particle size and particle density (Savassi et al., 1998; Wills and Napier-Munn, 2006). The amount of water recovered during flotation is not correlated to the degree of entrainment. It was shown by Wang et al. (2016) that the degree of entrainment also depends on the interaction between gas flow rate and froth height combined with particle density.

Adapted from Savassi et al. (1998), the degree of entrainment is defined as the ratio of the solids that are recovered by entrainment and water recovered. When the water recovery and the entrainment recovery is linear, the degree of entrainment becomes independent of water recovery. The degree of entrainment is expressed as a classification function for the i^{th} size fraction on the basis of the pulp as shown in **Equation 2.2**.

$$ENT_i = \frac{mass\ transfer\ of\ entrained\ particles\ of\ the\ i^{th} size\ interval\ to\ the\ concentrate}{mass\ transfer\ of\ water\ to\ the\ concentrate} \quad ---------- 2.2$$

Equation 2.2 represents a more general form of the degree of entrainment (ENT_i). The mass transfer to the concentrate is mostly quantified on the basis of pulp, feed or tailings (Savassi et al., 1998).

Wiese, (2009) developed a procedure in order to determine the respective floatable and non-floatable gangue material that will report to the recovered concentrates by either true flotation or entrainment. This procedure entails depressant addition in specified dosages and as such three basic assumptions were made: (i) average sulphur content of 36.45% was assumed for the sulphide minerals that reports to the concentrates, (ii) at 500 g/t depressant dosage, all the floatable gangue will be depressed meaning only entrained gangue will report to the concentrate at this depressant dosage, and (iii) full liberation is assumed for all sulphide minerals from their gangue material. The total mass of gangue material in the concentrate is therefore the mass of the concentrate minus

the mass of the sulphide minerals. At a depressant dosage of 500 g/t, it is found that all naturally floatable gangue is depressed and the only gangue remaining in the concentrate is that recovered by entrainment. As such, the gradient is calculated from the total gangue versus water recovery curve at 500 g/t depressant and this is used to determine the entrainment factor. This entrainment factor is then used to determine the gangue mass reporting to the concentrate at 0 g/t and 100 g/t depressant dosage.

2.5 Flotation reagents

Flotation reagents are added to the slurry to manipulate mineral surface chemistry and enhance differences in hydrophobicity between the valuable mineral and gangue material, facilitating the separation of gangue from valuable minerals (Bradshaw et al., 1998a). Reagent suites for flotation typically consists of collectors, depressants, frothers and occasionally activators (Davis et al., 1975; Wiese, 2009).

Different ores have different minerals and they behave differently in the presence of chemicals (reagents) and this led Bradshaw et al. (1998b) to assert that; it is difficult to isolate and quantify the interaction of each reagent with the minerals. Due to flotation's complexity and its reagent dependence, more and more specialized chemicals are being developed with a specific focus of altering the surface properties of mineral particles of interest and enhance their recovery (Bulatovic, 2007).

2.5.1 Frothers

Frothers are heteropolar surface active chemicals and are used to lower the surface tension of water by acting at the air-water interface. Khoshdast (2011) suggested that there are four classification methods which are commonly used to categorize frothers, which are mainly based on pH-sensitivity, solubility, frothing/collecting ability, and selectivity/frothing-power relationship. Frother efficiency is dependent upon pH of the pulp and as such they are divided into three categories shown in **Table 2-1**. The acidic frothers' effectiveness is reduced when the pulp pH is increased from acid to alkaline. Acidic frothers can be further divided into two groups i.e phenols (cresol and pine oil) and alkysulfonates (Khoshdast, 2011; Hearn et al., 2015).

Neutral frothers' performance is invariant with changes in pH and these are the most widely used in mineral processing, especially the flotation of sulphide minerals (i.e polyglycol ethers).

Table 2-1 Frother classification at different pulp pH (Khoshdast, 2011)

Acidic	Neutral	Basic
Phenols	Aliphatic alcohols	Pyridine base
Alkyl sulfonates	Cyclic alcohols and Natural oils	
	Alkoxy paraffins	
	Polypropylene glycol ethers	
	Polyglycol ethers	
	Polyglycol glycerol ethers	

When a frother is added to the pulp with air introduced to the flotation cell, the frother molecules are predominantly located at the air-water interface and are oriented in such a manner that the hydrophilic group is attached to the water phase while the hydrophobic (non-polar) is attached to the air bubbles as shown in **Figure 2-6**. An ideal frother should prevent bubble coalescence and be wet enough to be able to remove entrained gangue material.

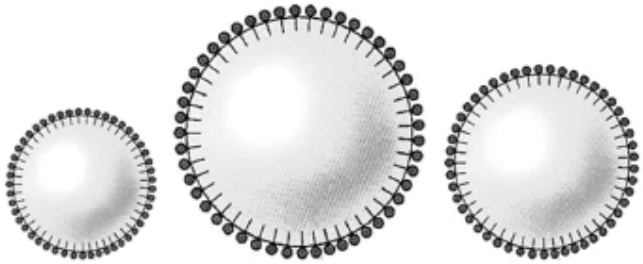

Figure 2-6 Orientation of frother molecules on the surface of bubbles (Khoshdast, 2011)

Figure 2-6 shows a schematic representation of the orientation of frother molecules on the surface of bubbles.

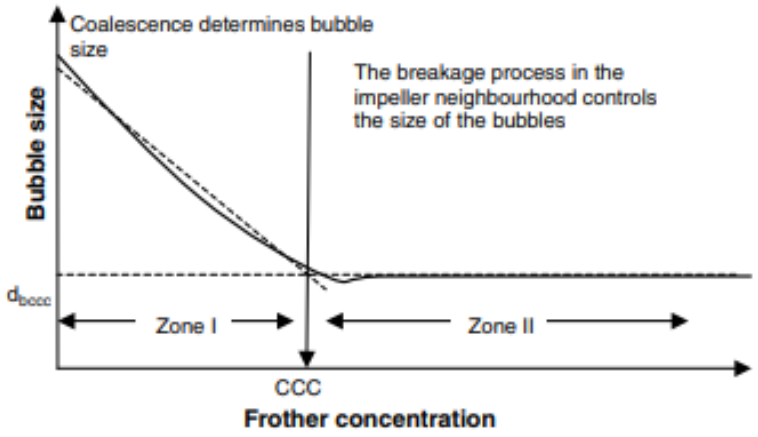

Figure 2-7 Effect of frother concentration on bubble size (Melo and Laskowski, 2006)

Critical Coalescence Concentration (CCC) is another parameter that is used to characterize frothers. Laskowski (2004) determined a relationship between bubble coalescence and frother concentration in solution, i.e as the frother concentration increases, bubble coalescence decreases until a given concentration and this is called the CCC as shown in **Figure 2-7.** For stronger frothers, their CCC values occur at lower concentrations in comparison to weaker frothers (Laskowski, 2004).

2.5.2 Collectors

Collectors are heteropolar molecules that contain an inorganic, active polar group and a non-polar, hydrocarbon chain. Collectors are added to the pulp to impart hydrophobicity to the valuable mineral (Ambrose, 1944). Because collectors render selected (target) minerals water repellent by adsorption of molecules or ions on to the mineral surface (mono layer coverage), this reduces the stability of the hydrated layer separating the mineral surface from the air bubble to such a level that attachment of the particle to the bubble can be made on contact (Wills and Napier-Munn, 2006).

Collectors are generally categorized depending on their ionic charge, i.e nonionic, anionic or cationic collectors. They attach to the mineral surface by either physisorption (physical bonding) or chemisorption (chemically bonded). The nonionic collectors are simple hydrocarbon oils while cationic or anionic collectors consists of a polar group that selectively attaches to the mineral surface and a non-polar, hydrophobic, group that attaches to the air bubbles – the hydrophobic group (Kawatra, 2009).

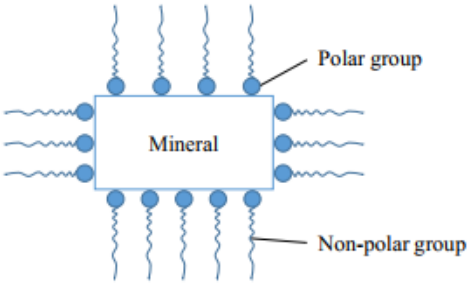

Figure 2-8 Collector adsorption onto the mineral adapted from Wills and Napier-Munn (2006)

Figure 2-8 shows, schematically, an adsorption of a collector, the polar inorganic group which is hydrophilic in nature attaches to the mineral surface, while the alkyl hydrocarbon chain, which is orientated towards the water phase, renders the mineral surface hydrophobic and attaches to an air bubble (Wiese et al., 2005).

2.5.2.1 Xanthate collector

Xanthates are the most commonly used collectors in the flotation of sulphide minerals because of their efficient role in mineral collection and low cost, (Wiese et al., 2005). Xanthates are known to be good collectors for many precious metal sulphides.

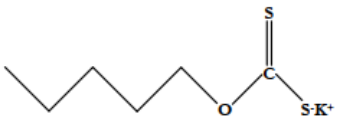

Figure 2-9 General molecular structure of a heterogenous Potassium Amyl xanthate collector adapted from Lotter and Bradshaw (2010).

Xanthates have a generic molecular structure as shown in **Figure 2-9**. Alkyl chains; ethyl-, isopropyl-, isobutyl-, amyl-, and hexyl-xanthate, are some of the most widely used xanthates in industrial flotation of sulphide minerals. The counter ion used in this study is Na^+ which is deemed to have insignificant influence on the ions under investigation, however it should be noted that should the counter ion prove problematic, other counter ions may be considered, such as K^+. Wills and Napier-Munn (2006) suggested that as the xanthate carbon chain length increases it leads to increased xanthate adsorption and thus improved hydrophobicity. The adsorption of a collector occurs by either physisorption and/or chemisorption.

2.5.2.2 Physisorption

The adsorption of collectors through electrostatic and hydrophobic bonding is called physisorption. The Van der Waals interaction is the predominant weak electrostatic force that results in collector adsorption on to the mineral surface.

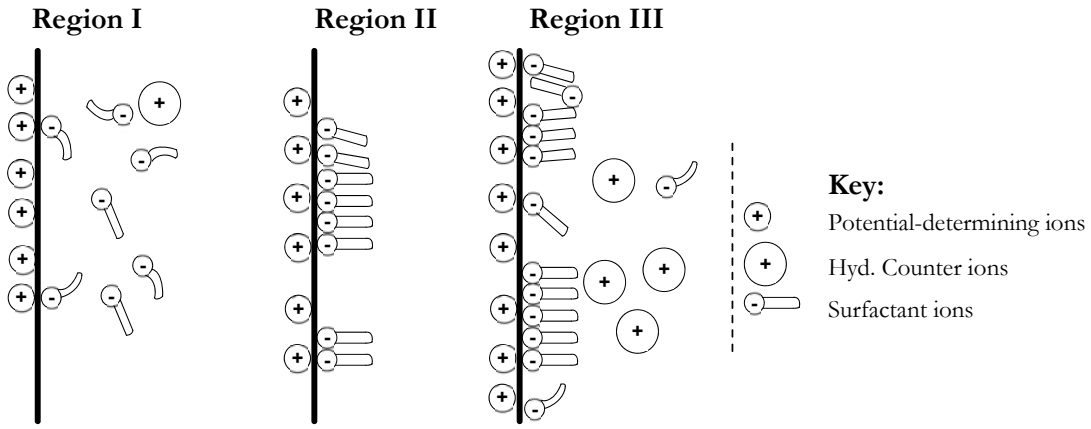

Figure 2-10 Adsorbed surfactant ions in the double layer, showing adsorption as individual ions and as associated hemimicelles, adapted from Ambrose (1944) and Finkelstein and Lovell (1972)

Figure 2-10 illustrates how anionic collectors often adsorb in the electrical double layer (Ambrose, 1944; Finkelstein and Lovell, 1972). **Region I** represent the specific adsorption by electrostatic force of attraction, **Region II** is the specific adsorption plus hemimicelle formation (when surface active cations are adsorbed as individual ions on a negatively charged surface through specific adsorption and electrostatic forces of attraction (Gu et al., 1988)) and finally **Region III** is the hemimicelle formation.

2.5.2.3 Chemisorption

Chemisorption is defined as the formation of covalent bonds between collectors and metal ions on the mineral surface. This process is generally accepted as electrochemical in nature where it occurs by separate electron transfer reactions in which the anodic reaction involving the collector is coupled with a cathodic reaction which is the reduction of oxygen (Buckley and Woods, 1997). This suggests that electrochemical techniques can be used to evaluate the response of mineral surfaces to collectors.

Xanthate adsorption on to the mineral surface and chemical interaction with metal ions results in the formation of hydrophobic metal xanthates (**Equations 2.3 to 2.5**). These can easily be oxidised to dixanthogen with certain minerals under appropriate conditions (Buckley and Woods, 1997; Wiese, 2009)

$$2X^- + ½O_2 + H_2O \rightarrow X_2 + 2OH^- \quad (2.3)$$

$$2X^- + Cu^{2+} \rightarrow CuX(s) + ½X_2 \quad (2.4)$$

$$2X^- + 2Fe^{3+} \rightarrow 2Fe^{2+} + X_2 \quad (2.5)$$

2.5.3 Modifiers

Modifiers are specific chemicals that enhance the collector attachment onto the mineral surface. A good combination of collector/depressant for a specific target mineral does not mean it will work when the target mineral is changed (Kawatra, 2009).

Modfiers can be used to control pH and Eh as well as act as chemical activators; they are inorganic compounds (Finkelstein and Lovell, 1972). A commonly used activator is copper sulphate ($CuSO_4$), for base metal sulphide flotation. CaO is used as a pH modifier mainly due to its availability and low cost, however, Ca^{2+} from CaO dissociation may influence the flotation system hence a sodium based alkali such as NaOH may be considered. Sodium sulphide is an Eh modifier, which is used as a sulphidising reagent for tarnished or oxidised ores (Bradshaw, 1997).

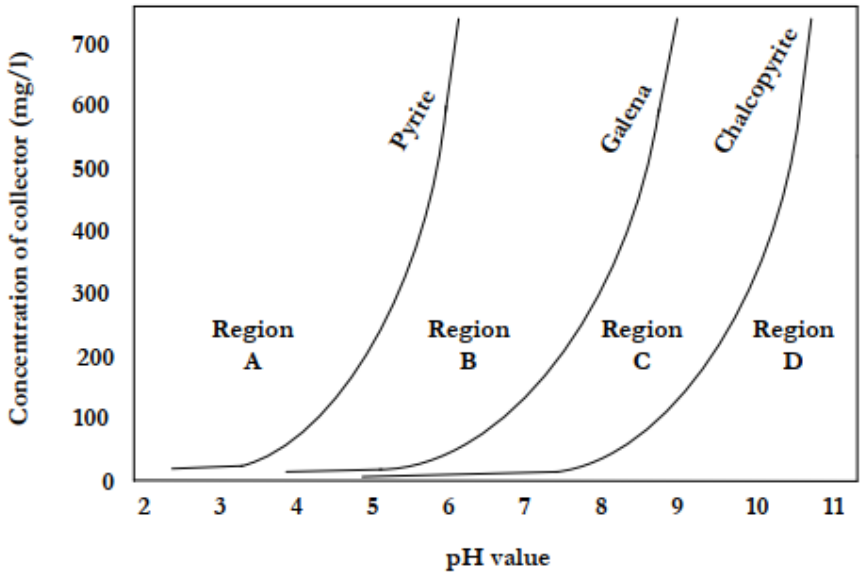

Figure 2-11 pH response curves for sulfhydryl collector adsorption on different sulphide minerals (Finkelstein and Lovell, 1972; Kawatra, 2009)

Figure 2-11 shows curves that mark the boundary for pyrite, galena and chalcopyrite when they are sufficiently hydrophobic to float. It is important to note that both xanthates (e.g SIPX) and dithiophosphates (e.g Aerophine 3418A) exhibit similar curves as pH varies at the same time as the concentrations for each type of collector (Finkelstein and Lovell, 1972; Kawatra, 2009).

The three minerals shown in **Figure 2-11** will float in region A. As pH increases into region B, collector adsorption increases making both pyrite and galena susceptible to flotation. Further increase in pH will result into chalcopyrite flotation in addition to pyrite and galena in region C. As pH keeps increasing into region D, no mineral is hydrophobic enough to float and there is no collector adsorption in this region (Finkelstein and Lovell, 1972; Kawatra, 2009)

2.5.3.1 Depressants

For sulphide mineral flotation, organic depressants are commonly used. Finkelstein and Lovell (1972) noted that, in cases where the collector, in addition to adsorbing to valuable minerals, adsorbs onto gangue minerals, depressants are added to enhance the hydrophilicity of the gangue and thus ensure that only the valuable minerals float. Bradshaw et al. (1998) also suggested that depressants are used to reduce the floatability of naturally floatable gangue materials. Typical depressants used in industry are long chain polysaccharides, most commonly, Guar Gum and Carboxymethylcellulose (CMC)

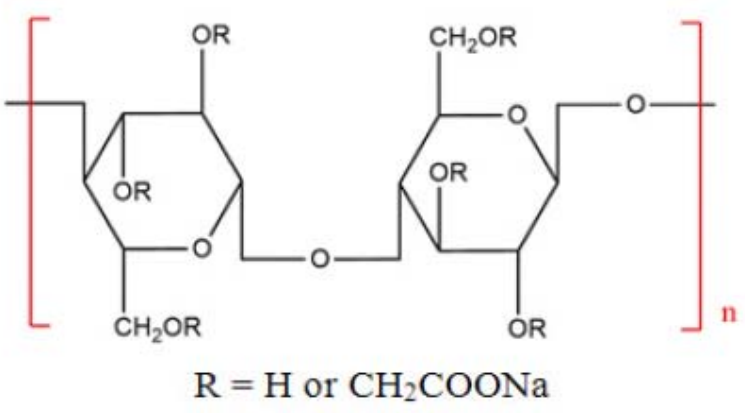

Figure 2-12 Structure of CMC (Runpeng et al., 2018)

CMC is a biodegradable polysaccharide, (Qiu et al., 2018) with the structure shown in **Figure 2-12**. Burdukova et al. (2008) suggested that CMC is an anionic polysaccharide. CMC molecules have a strong negative charge, when it comes in contact with gangue material it imparts a negative charge resulting in dispersed pulps (Wiese, 2009). The counter ion to the negatively charged ligand is usually sodium.

2.6 Ionic Strength and flotation impact

It is known that the reagents described in **Section 2.5**; collector and depressants, are affected by the ionic nature of the solution in their interaction with mineral particles (Craig, et al., 1993; Levay et al., 2001; Muzenda, 2010; Corin et al., 2011; Manono et al., 2012, 2018; Laskowski and Castro, 2017). These ion-reagent-particle interactions could in turn impact both the pulp and froth phase phenomena. Therefore, it stands to reason that the inorganic electrolytes present in process water may affect interactions occurring in the pulp phase and in turn the implications of these effects could be seen in the froth phase.

The mining industry uses vast amounts of water from exploration through mining to closure. Water is considered a scarce resource and should be carefully managed. Mining operations are mostly located in water scarce regions and do not have access to fresh water, there is thus a need for recycling. It is, therefore, imperative to undertake studies to understand the impact of water recycling and how to manage the impact of inorganic ions that get recycled together with the water. South African mining operations are located in water scarce regions forcing them to make use of non-potable and other brown/grey water sources to maintain their operations.

Recycling alleviates the need for large amounts of fresh water and/or dependence on water suppliers. In Finland, however, while the operations are not located in water scarce regions, owing to past water pollution by the pulp and paper industry, the suspended solids disposed to the environment increased exponentially alongside paper production until the early 1970s (Katko et al., 2006). Finland's environmental restrictions on discharge water are incredibly strict, this forces operations to recycle for zero effluent. Added to this is persistent and large seasonal variation. During winter months, temperatures drop significantly, tailings dams freeze over and shorten the recycle stream to only a few hours, changing the quality of the recycled water. As the seasons change and the ice thaws, there is a large flush of water followed by the summer months in which temperatures are higher and the water quality changes again. **Figure 2-13** shows historical data for Kevitsa mine's recycled water and the level of ions.

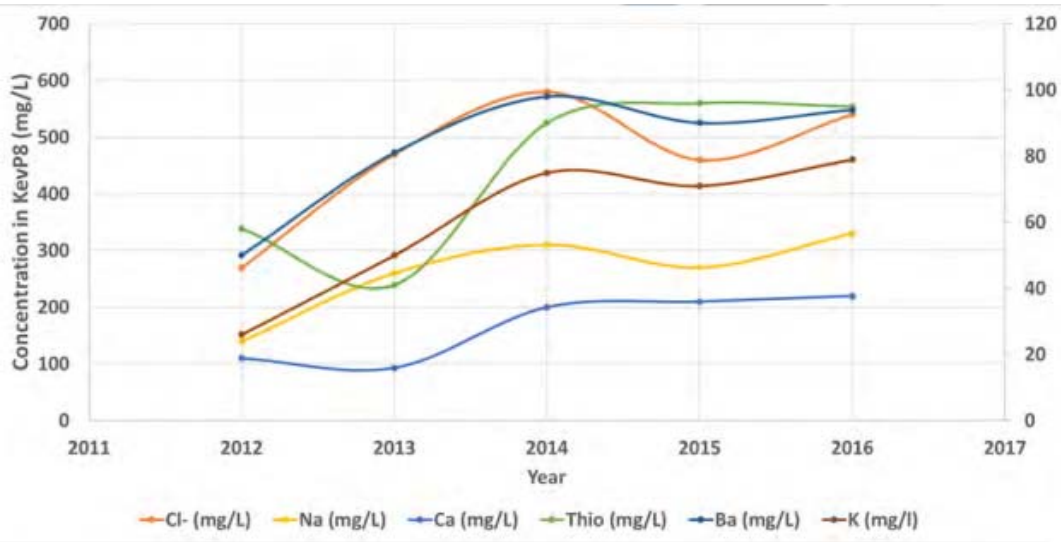

Figure 2-13 Kevitsa historical ions distribution (Schreithofer, 2018)

This investigation seeks to understand the cyclic seasonal variations and its impact on flotation performance as the predominant recycled ions keep changing in concentrations.

The ionic strength of a solution is the measure of the concentration of electrolytes dissolved in that solution and is calculated from **Equation 2.6**. Recycled water is usually obtained from tailings dams, where the typical contaminating species are: SO_4^{2-}, Cl^-, F^-, Mg^{2+}, Ca^{2+}, Na^+, K^+, base metals, collectors, frothers, activators, depressants, colloidal materials such as iron hydroxides, and natural organic material. It is worth noting that some ions exist naturally in water. There are some advantages to recycling process water, these include: the reduced potable water usage and discharge from the plant, and the retention of some reagents, therefore lowering the consumption of reagents (Slatter et al., 2009).

$$I = \frac{1}{2}\sum_{i}^{n}(Z_i^2 C_i) \quad \text{----------} \quad 2.6$$

Where: ***I*** – is the ionic strength

Z – charge of the ion *i*

C – molarity of ion *i*

i – specific ion at which the ionic strength is evaluated

n – number of ions present in a system

Wiese et al. (2005) developed a standard synthetic plant water formula (with a total dissolved solids concentration of 1023 mg/L, and termed synthetic plant water (SPW), more recently referred to as 1SPW) designed to represent a typical water analysis of a PGE concentrator. This water recipe is achieved by adding various chemical salts to de-ionised water (Wiese et al., 2005). The influence of ionic strength on flotation is thus studied by multiplying 1SPW by three, five and ten times as shown in **Table 2-2** (Manono et al., 2012). It is important to note that the original SPW does not contain $S_2O_3^{2-}$ and the spiking with 60 and 78 ppm $S_2O_3^{2-}$ was determined to be suitable from on-site measurements.

Table 2-2 Table Inorganic ions concentration present in synthetic plant water (Manono et al., 2012)

Water type	*Ca^{2+} (ppm)*	*Mg^{2+} (ppm)*	*Na^{+} (ppm)*	*Cl^{-} (ppm)*	*SO_4^{2-} (ppm)*	*$S_2O_3^{2-}$ (ppm)*	*NO_3^{-} (ppm)*	*NO_2^{-} (ppm)*	*CO_3^{2-} (ppm)*	*TDS (mg/L)*	I.S [M]
3 SPW	240	210	459	861	720	-	528	-	51	3069	0.073
5 SPW	400	350	765	1435	1200	-	880	-	85	5115	0.121
10 SPW	800	700	1530	2870	2400	-	1760	-	170	10230	0.242

The presence of ions has been shown to either increase or decrease the floatability of sulphide minerals, depending on both the mineral type and the water chemistry (Slatter et al., 2009; Ikumapayi and Makitalo, 2013).

Ikumapayi et al. (2012) in an investigation of the effect of varying concentration of $Ca^{2+}$and SO_4^{2-} on flotation of pure sulphide minerals in a Hallimond tube with a specific focus on galena and chalcopyrite, showed that 400 mg/L Ca^{2+} and 1400 mg/L SO_4^{2-} were the maximum concentration of the ions beyond which the flotation recoveries were affected. Ca^{2+} resulted in the formation of a hydrophilic layer around the valuable mineral and this affected the flotation performance by inhibiting collector adsorption. This increases the probability of gangue resulting in floating by mechanical carry-over (Konopacka and Drzymala, 2010).

In a study by Muzenda (2010); an investigation on the effect of water quality on flotation performance was conducted. A Denver flotation cell was used for batch flotation tests using different water sources with different Total Dissolved Solids (TDS), Total Suspended Solids (TSS) and Conductivity (Eh). Artificial water was prepared by adding different concentrations of Ca^{2+} ions to demineralized water. It was found in this study that the quality of water has an impact on froth flotation performance particularly recovery and grade. The sensitivity of flotation on water quality implied that there is a need to maintain a certain level of ions that get recycled to the

flotation cells, an increase in the suspended solids (because of high Ca^{2+} ion concentration) results in decreased recoveries and grade.

However a study by Hirajima et al. (2016) concluded that Ca^{2+} ions have a marginal decreasing effect on the flotation of chalcopyrite at low pH and suggested that this marginal effect is owing to the presence of other ions in the saline environment that causes preferential collector attachment to the sulphide mineral. As the pH increased beyond 9, chalcopyrite recovery decreased as both Ca^{2+} and Mg^{2+} ions concentration increased owing to the formation of $Mg(OH)_2$ and $CaCO_3$ which precipitates on the mineral surfaces and thus reducing the mineral surface hydrophobicity. Kirjavainen and Heiskanen (2007) suggested that the presence of ions at high concentration beyond a certain threshold results in modified pulp viscosity which leads to entrainment and reduced grade of the recovered sulphide mineral.

Manono et al. (2017) suggested that ionic strength and the type of cations in solution may potentially have an influence on the extent of gangue activation. Talc which is a magnesium rich phyllosilicate mineral and is a natural gangue component of many base metal sulphides ores is highly floatable. Manono et al. (2016) while investigating the effect of electrolytes present in process water on the flotation behaviour of a Cu-Ni containing ore looked at the effect of ion type focusing on: Na^+, Ca^{2+}, Mg^{2+}, NO_3^-, SO_4^{2-}, Cl^-, using single salts at a constant ionic strength of 0.0213 $mol.dm^{-3}$ (an ionic strength of standard synthetic plant water) and found out that the divalent ions results in a higher water recovery than the monovalent ion which possibly means they have a stronger froth stabilizing power than the monovalent ion. Of the anions, NO_3^- ion resulted in considerable increase in copper and nickel grades at 0.65 % and 1.3 % respectively. This paper is fundamental to this study as the spiking of synthetic plant water recipes with selected ions is done following a similar procedure however using water of different ionic strength and different target concentrations of the spiked ions.

These concerns have led to the proposed spiking mechanisms to ascertain the impact that individually selected ions have on flotation performance.

2.7 Ore Mineralogy

Kevitsa is situated in Finnish Lapland, 142 km north-northeast of Rovaniemi, the capital of Finnish Lapland and approximately 140 km north of the Arctic Circle in Sodankyla Municipality. New Boliden Kevitsa Mining Oy's Cu-Ni-PGM concentrator recycles 90-95 % of its water (Schreithofer et al. 2017). Their water contains various ions and compounds: Ca^{2+}, Na^+, Mg^{2+}, K^+, SO_4^{2-}, and

residual reagents that accumulate. This accumulation of residual reagents results in seasonal variations in the flotation performance (Muzinda and Schreithofer, 2018).

Table 2-3 shows bulk mineralogy data for the Kevitsa Cu-Ni-PGM ore. In winter the temperatures at Kevitsa mine can get to -30 ºC or lower and this causes the concentration of the ions to drop as most of the ions will be locked within the frozen ice waters in the tailings dam. In summer, as temperature rises above 0 ºC, the ice-caps in the recycled water melts and the concentration of the ions that get recycled to the plant increases. This affects the quality of the water that is recycled and ultimately the flotation performance keeps changing as seasons changes between winter and summer.

Table 2-3 Feed mineralogy data

Mineral	Mass %
Cu-sulphides	1.1
Ni-sulphides	0.8
Pyrrhotite	2.0
Olivine	7.7
Enstatite (OPX)	7.8
Augite (CPX)	28.1
Tremolite	33.8
Serpentine	1.5
Talc	0.2
Chlorite	6.8
Biotite/Phlogopite	0.8
Plagioclase Feldspar	2.4
K-Feldspar	0.1
Quartz	0.3
Calcite	0.5
Dolomite	0.2
Fe-oxides	5.9
Other	0.3

Sequential flotation which entails conditioning for copper first and recover the first two concentrates followed by stopping the air flowrate, reconditioning for nickel at the same pulp density and recover the remaining four concentrate was done on this ore to ascertain which point in the flotation cell does the most copper and nickel get recovered.

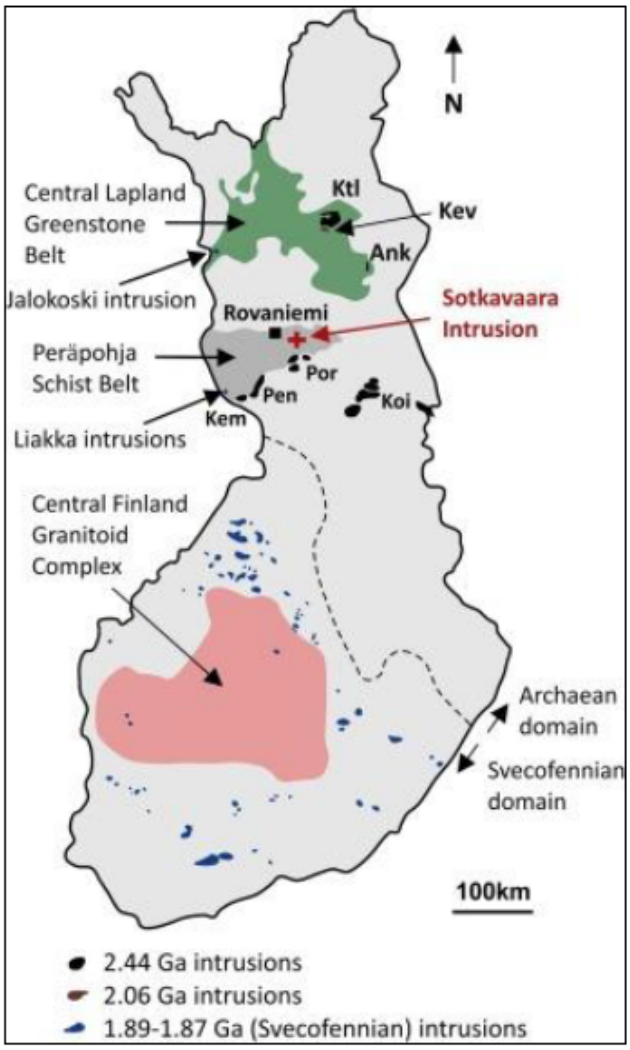

Figure 2-14 Kevitsa ore deposit relative to the Central Lapland Greenstone Belt adapted from Gray et al., (2016)

Figure 2-14 shows the location of ore source. For the Kevitsa ore, the sulphides account for less than 5% of the overall deposit's mineralogy. Chalcopyrite is the primary copper bearing mineral of interest while pentlandite is the nickel bearing mineral of interest (Gray et al. 2016). 20% of the nickel and up to 10% of the copper is contained in the non-sulphide minerals, this qualifies the ore body as low grade. Schreithofer and Muzinda (2017) found that pyroxene is the most abundant non-sulphide gangue mineral. The most abundant sulphide gangue mineral is pyrrhotite (Gray et al. 2016; Musuku et al. 2016).

3 OBJECTIVES, HYPOTHESIS AND KEY QUESTIONS

3.1 Problem statement

Froth flotation is a water intensive process. The drive for recycling process water is multifaceted and there is need to adhere to any country's environmental policy or legislation in which the operation takes place while not compromising the overall flotation performance. Recycling leads to a build-up of ions some of which can be deleterious and have a negative impact of flotation performance. The effect of such ion accumulation is a topic of great interest and the influence they have on flotation performance should be understood for proper control and management of water quality and its associated effects within the process.

The following ions are investigated in this project: Ca^{2+}, Mg^{2+}, SO_4^{2-}, NO_3^- and $S_2O_3^{2-}$ under varying spiking conditions. Spiking is done in such a manner as to get an understanding of what happens when a specific ion's concentration is increased up to certain levels while keeping other ions that make-up the synthetic plant water constant. These studies are different to single salt studies as they maintain the complex background of the original SPW recipe while only increasing the concentration of one ion (salt) at a time. The flotation procedure presented in this study is done sequentially so as to mimic plant procedure; that is, copper is recovered first before conditioning for nickel flotation.

3.2 Objectives

Considering how the selected water hardening ions affect the flotation efficiency, the objectives of this study are:

1. To investigate the effect of selected divalent cations on the flotation response of copper and nickel in terms of recovery and grade.
2. To investigate the effect of selected anions on flotation efficiency with regards to copper and nickel grade and recovery
3. To determine a threshold concentration for the selected ions beyond which the flotation performance will be adversely affected.

3.3 Research Hypothesis

The following is hypothesized:

1. For any given ion, there is a threshold concentration beyond which flotation performance (as measured by recovery and grade of valuable minerals) is adversely affected. This is because as increases in ion concentrations have a positive effect on froth stabilization (as implied by increases in water recovery) due to the affinity of the ions for gangue activation (as implied by increases in solids recovery without corresponding increases in valuable mineral recovery) which results in dilution of the concentrates.
2. It is possible to determine the distribution of ions between the pulp and froth phase; this is because the EC in water is a measure of its ability to conduct current. Current can be carried by ions in an electrolyte solution, the more ions there are in solution the higher the EC

3.4 Key Questions

1. How does the increase in ionic strength (3, 5 and 10 SPW) affect flotation performance?
2. How does spiking Ca^{2+} and Mg^{2+} affect flotation performance of a Cu-Ni-PGM ore?
3. How does spiking SO_4^{2-}, NO_3^- and $S_2O_3^{2-}$affect the flotation performance of a Cu-Ni-PGM ore?
4. Is there a concentration of the selected divalent cations and the selected anions (between 3 and 10 SPW) beyond which the flotation performance is adversely impacted?
5. What is the ions distribution across the pulp and the froth phase?

3.5 Sustainable Development Goals for the project

The SDGs addressed in this project are 6,12,13 and 14. The respective mission of these goals are; ensure clean water and sanitation for all; responsible production and consumption; climate action; and conserve and sustainably use land and oceans resources, The United Nations, 2015). This research seeks to address environmental, industrialization and sanity sustainable development goals. Recycling entails reduction of detrimental ions that seep into the water table, the growing awareness and knowledge will ensure compliance with SDGs

4 EXPERIMENTAL DETAILS

4.1 Ore Sampling and Preparation

A Cu-Ni-PGM ore was sourced from Finland. The ore was reduced to -1 mm particle size using a TM Engineering Terminator jaw crusher, homogenised and split using the rotary splitter to equal 1.0 kg portions. The mill was charged with 20 stainless steel rods of varying diameter (6 x 16 mm, 8 x 20 mm and 6 x 25 mm), at 66 wt. % solids, the synthetic plant waters (3, 5 and 10) were prepared from the inorganic salts based on Wiese et al. (2005) proposed water recipe (1 SPW) shown in Table **2-2** and **Table 4-4** shows the complete recipe for the ions' spiking. The milling curve shown in **Figure 4-1** a grind size of 70% passing 75 µm would be achieved after 10 minutes of wet milling. The chosen grind size is representative of the grind used on site. For each test, a 1.0 kg ore sample and 650 ml of the desired specific plant water shown in **Table 4-4** was added to the mill. The mill drive speed was maintained at 47 rpm for all tests.

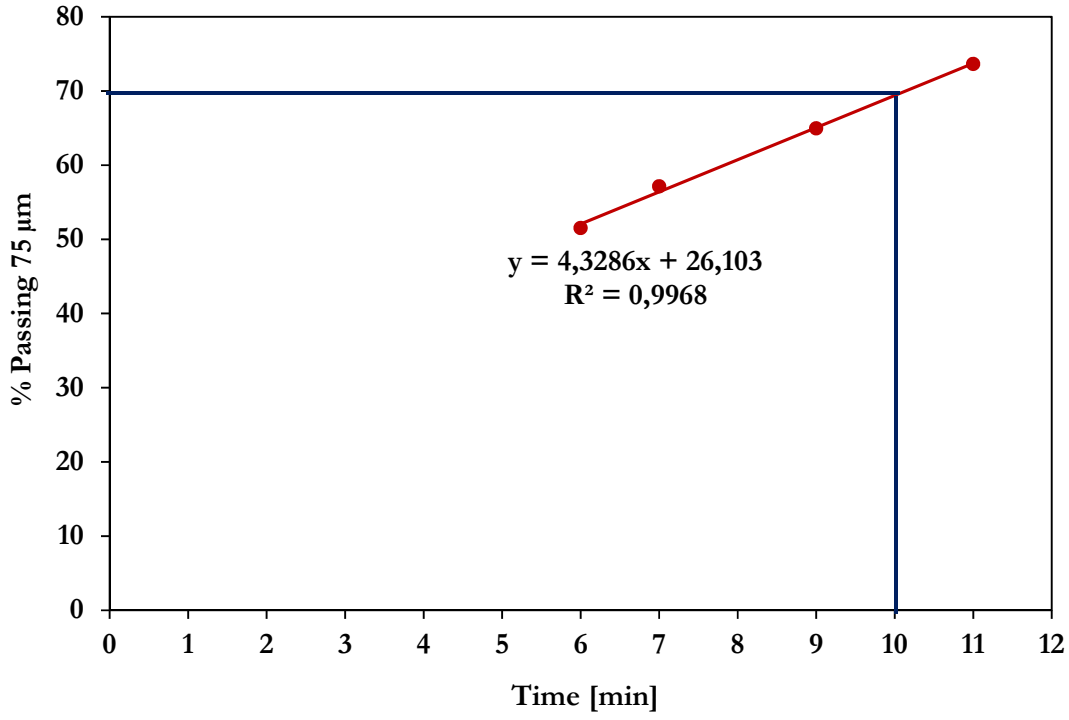

Figure 4-1 Milling curve

4.2 Ore Characterisation – QEMSCAN and XRF

Quantitative Evaluation of Materials by Scanning Electron Microscopy (QEMSCAN) was used to measure the mineralogical variability and textural characterization. Bulk mineralogy composition, sulphide liberation and association of different Kevitsa feed samples were determined using QEMSCAN analysis. Representative samples were split into 1 g aliquots using a Quantachrome microrifler. The blocks were prepared by mixing the aliquots with graphite and resin and then curing. Quality check of the cured blocks was done using optical microscopy. Polishing was done using a series of grinding and polishing papers until a final product of 1 μm polish. Carbon coating of the final polish was done to diffuse electrons off the surface of the sample once inside the QEMSCAN. All the analysis were run at 25 kV and 10 nA, with a field size of 500 microns at a pixel spacing of 1 micron for the Trace Mineral Search (TMS) and a field size of 1500 microns for the gangue mineralogy search at a pixel spacing of 4 microns.

Two Bruker X-Flash 6130 detectors were used for compositional analysis. Backscatter detection calibration (BSE values) are related at Z = 13.0 mm where three standards were used: (1) quartz at BSE 42; (2) copper at BSE 130; and (3) gold at BSE 232. A mineral library called Species Identification Protocol (SIP) was used to reclassify all minerals with user-specified criteria to match the X-ray spectra and BSE data from a measurement point to a mineral species. Each mineral phase within the SIP Editor file consists of "must-have" and "may-have" lists.

Compulsory elements (those that make up the formula of a mineral) are assigned within the "must-have" list, whereas other elements common to a particular mineral phase are assigned in the "may-have" list. It is important to note that for this study no assaying of PGMs was carried out. The Platinum Group Metal (PGMs) are recovered together with the sulphides in the Kevitsa ore so sulphides recovery can be used as a proxy for PGM recovery (Musuku et al., 2016). Kevitsa ore is similar in composition to the South Africa Merensky ore.

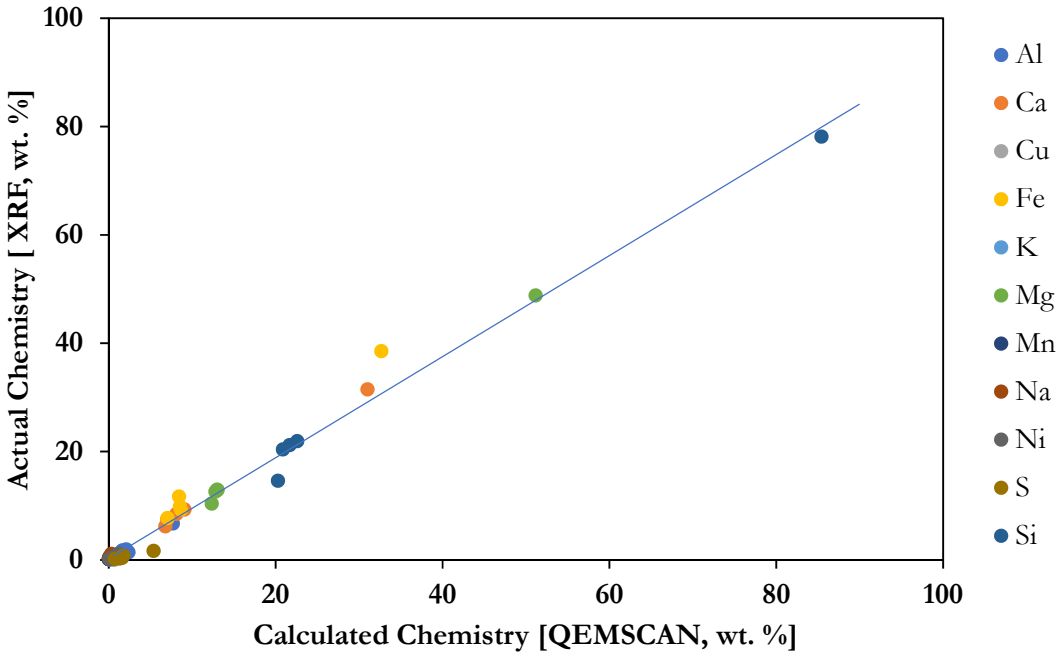

Figure 4-2 Feed bulk mineralogy showing assay reconciliation

Figure 4-2 shows the validation that was done between the chemical assay by XRF, and QEMSCAN based on its mineral protocol. Strong correlation is shown as most of the points lie on the line of best fit.

4.3 Reagents Preparation and Storage

All reagents were supplied by New Boliden Kevitsa.

4.3.1 Collector

Table 4-1 summarises the properties of the collectors used. Sodium dithiophosphinate (generally known as Aerophine) was used as a Cu collector. Aerophine 3418A was dosed at 5 g/t per run as supplied, not corrected for active content. When not in use, it was stored at 9°C. A 1% (w/v) solution of Sodium Isopropyl Xanthate (SIPX) was prepared daily prior to experiments due to its decompositional nature and dosed at 50 g/t (to recover C_3 and C_4) and 30 g/t (to recover C_5 and C_6) sequentially. Residual xanthate solution was discarded as outlined by the material safety data sheet and laboratory rules.

Table 4-1 Chemical properties of the collectors used

Collector	Chemical formula	Molecular weight (g/mol)	Purity (%)
SIPX	$(CH_3)_2CHOCS_2Na$	158	97
Aerophine 3418A	$(C_4H_9)_2PS_2Na$	232	50

4.3.2 Depressant

A polysaccharide depressant, carboxymethyl cellulose (CMC) supplied as a sodium salt with a molecular weight of 323 000 g/mol was used sequentially; **Figure 4-3**, as gangue depressants at 100% purity and was supplied as granules. A 1% (w/v) solution was prepared and stirred for two hours using a magnetic stirrer to allow complete dissolution. The CMC dosage was varied at two dosage levels of 35 g/t for gangue depression in the copper flotation circuit and 15 g/t for gangue depression in the nickel circuit. CMC solution was prepared every 5th day and, when not in use, stored at -15 ^{0}C. Residual CMC solution was discarded as outlined by the material safety data sheet and laboratory rules.

Table 4-2 Chemical properties of depressant used

Frother	Chemical formula	Molecular weight (g/mol)	Purity (%)
CMC	$C_8H_{15}NaO_8$	323 000	100

4.3.3 Frother

Nasfroth 240 was used for all the experimental runs, the frother was dosed as supplied, at 20 g/t for copper flotation and 10 g/t for nickel flotation as shown in **Figure 4-3**. The frother was stored at room temperature after use. **Table 4-3** summarises the chemical properties of the frother.

Table 4-3 Chemical properties of the frother used

Frother	Chemical formula	Molecular weight (g/mol)	Purity (%)
Nasfroth 240	$C_4H_9(OC_2H_4)_3OH$	206	100

4.4 Sequential Batch Flotation

Aerophine was used specifically to target chalcopyrite since it is more selective than SIPX and hence better suited for the recovery of the fast-floating chalcopyrite (Schreithofer and Muzinda , 2017)**. Figure 4-3** shows the reagent addition flowsheet for sequential batch flotation carried out in a 3 L Barker cell (**Figure 4-4**). The conditions, the sequential addition of collectors, depressant and frother together with conditioning times, were selected to mimic plant operational conditions. A 20 min transfer time from mill to flotation cell was maintained and synthetic plant water was added to attain a solids concentration of 35 wt.% solids.

The impeller speed was set and maintained at 1200 rpm. Air flow was maintained at 7 L/min and froth height/pulp level was controlled manually and kept constant at 2 cm by continuously adding make-up water at 60-seconds intervals. One 50 mL feed sample was taken before commencement of each flotation procedure and 2 50 mL tailings samples were taken at the end of each test to mass balance and determine metal grades and recoveries. In total, six concentrates were collected by scraping the froth every 15 seconds into a collecting dish at 5, 10, 17.5, 25, 37.5 and 50 min (C_1, C_2, C_3, C_4, C_5 and C_6 respectively).

With airflow off, collector; Aerophine 3418A was added to the slurry at 5 g/t and conditioned for 2 minutes. The 1 % solution depressant; was then added at 35 g/t of CMC and allowed a conditioning time of 2 minutes. 20 g/t of Nasforth 240 was added and allowed to condition for 2 minutes after which the air supply was opened at 7 L/min. Two concentrates; C_1 and C_2 were collected at 5 and 10 min respectively, targeting copper as shown in **Figure 4-3**. The air flow was then turned off.

SIPX at 50 g/t was added while air was off and allowed to condition for 2 minutes. 15 g/t CMC was added and allowed to condition for 2 minutes. Nasfroth 240 at 10 g/t was added and allowed 2 minutes conditioning time after which air was tuned-on at 7 L/min allowing collection of two further concentrates (C_3 and C_4) targeting nickel. After C_4, the air was turned off, further SIPX at 30 g/t was added and allowed 2 min conditioning time after which air was turned on and a further two final nickel concentrates were collected (C_5 and C_6).

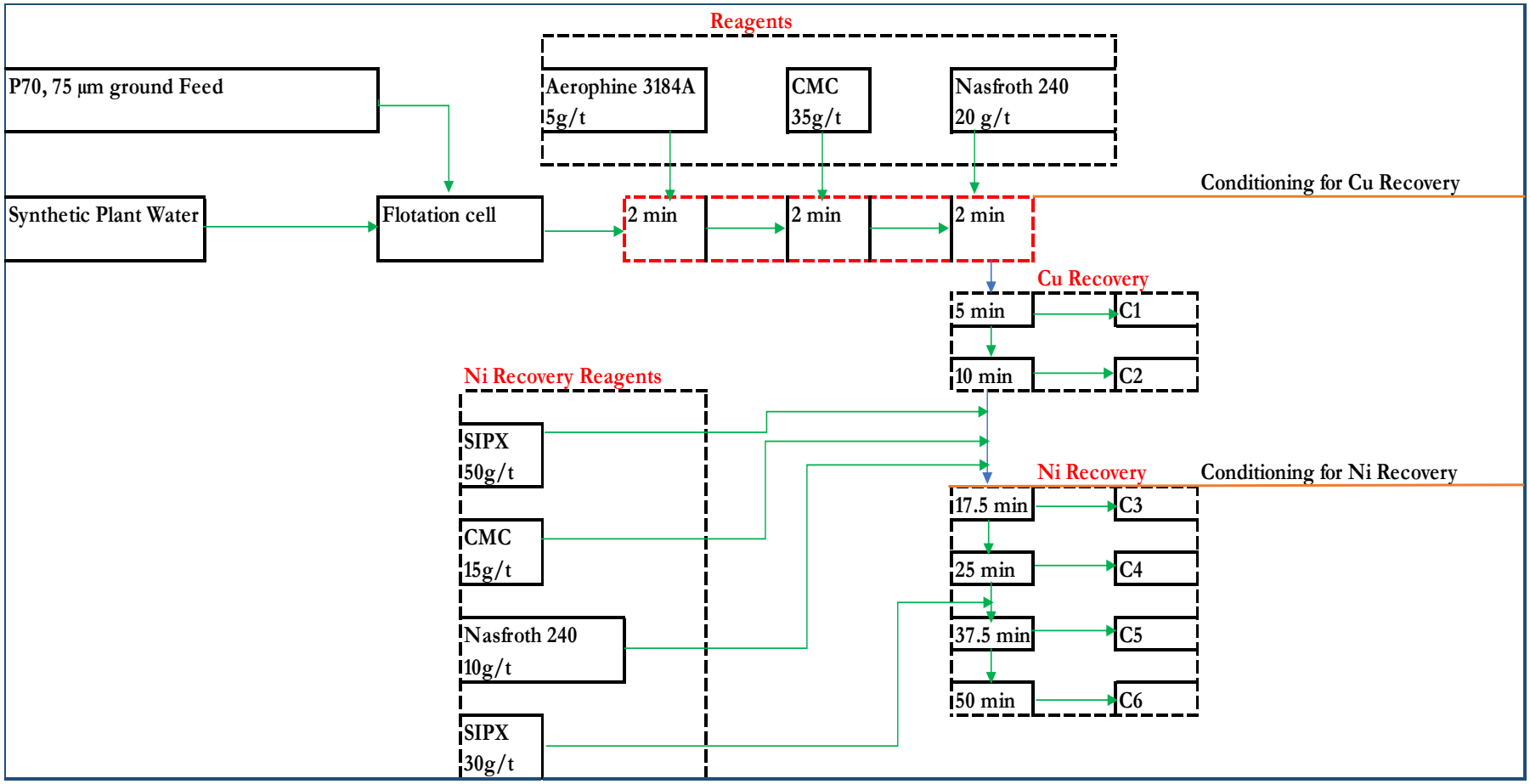

Figure 4-3 Reagents addition flowsheet and sequential steps for Cu and Ni recovery

The amount of water and solids recovered were measured using an electronic balance during each of the tests. The tests were performed in duplicates to confirm reproducibility. Concentrates, feed and tailings samples were filtered, dried and weighed. The dry flotation products were then sent for analysis to determine the amount of copper and nickel. Copper and nickel content analysis was done using a Bruker S4 Explorer XRF Spectrophotometer.

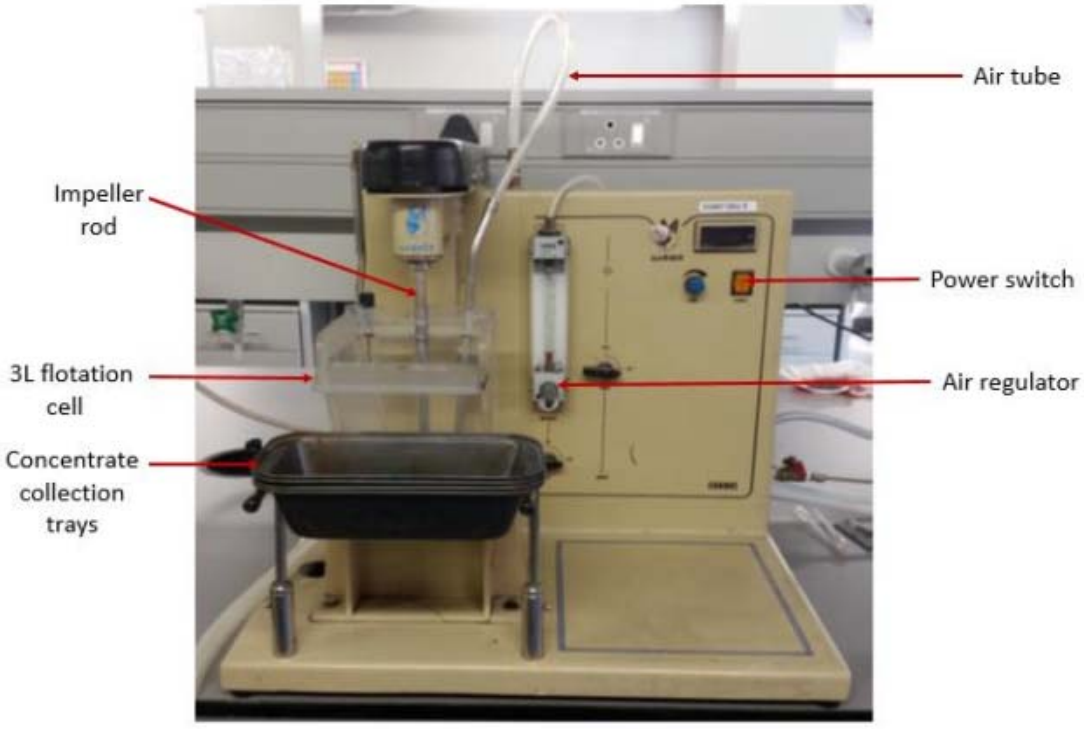

Figure 4-4 Barker flotation cell used for sequential batch flotation tests

4.5 2-Phase Foam Column

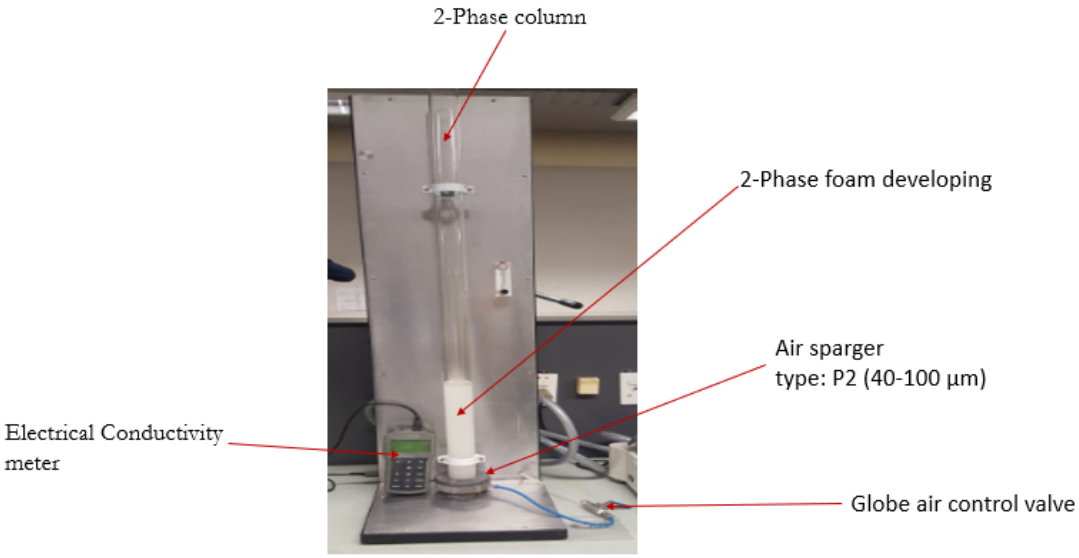

Figure 4-5 2-Phase Foam Column set up

Figure 4-5 shows a 2-phase foam column set up. The desired SPW was mixed with 10 ppm Nasfroth 240 prior to adding the mixture into the column. No other reagent was used for the 2-phase programme. The 200 cm column was first filled with solution (SPW and frother) to the desired initial level and this height was noted in all instances. The air was introduced at 3 L/min from the bottom of the column through a control globe-valve maintaining 200 kPa, a synthetic air sparger with constant pore size, type P2 (40-100 µm) was fitted at the bottom of the column to allow air flow through to the column. The foam was allowed to develop, and the time taken to reach an equilibrium foam height was noted.

Electrical Conductivity (EC) in water is a measure of its ability to conduct current. Current can be carried by ions in an electrolyte solution, the more ions there are in solution the higher the EC. No sample was collected from 2- and 3-phase flotation column studies as these were done for the purposes of EC investigations.

The foam was removed using a vacuum pump into a collecting flask and the conductivity, used as a measure of ionic strength, was measured using a HANNA Instruments' conductivity multi-probe.

4.6 3-Phase Froth Column

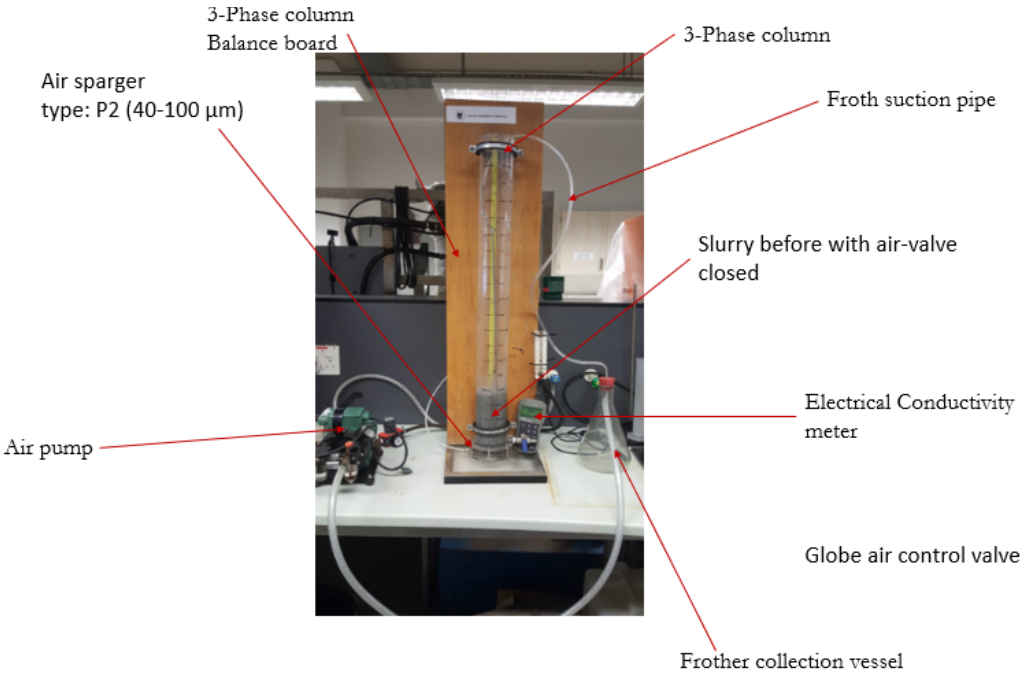

Figure 4-6 3-Phase Froth Column set up

Figure 4-6 shows the experimental set up for a 3-phase froth column. 400 mL of slurry was thoroughly stirred in a 500 mL beaker to condition the 10 g/t Nasfroth 240 and 2.5 g/t Aerophine 3418A before being transferred to the column; this was meant to be replicated for the copper circuit only. The initial height of the slurry in the column was noted before air was introduced. Air was introduced to the column at a flow rate of 3 L/min from the bottom of the column through a constant pore size air sparger, type P2, which allowed the development of the froth phase until an equilibrium froth height was attained. A control globe-valve was used to maintain the air flowrate at 200 kPa. This height was noted. A vacuum pump was used to remove the froth after an equilibrium froth height was achieved. A conductivity probe was used to measure both slurry and froth conductivity as was done in the 2-phase system.

4.7 Plant Water Preparation

As the process water recycling cycles increase, the ions present will increase or decrease depending on the ore type and other chemical conditions within the pulp. 3, 5 and 10 SPW recipes were adapted from the 1 SPW recipe developed by Wiese et al., (2005) with the concentrations of the respective ions multiplied three, five and ten times. The synthetic plant waters were prepared by adding varying amounts of inorganic salts to de-ionised water. All salts were supplied in powder-form by Merck. It is important to note that the original SPW does not contain $S_2O_3^{2-}$ and the spiking with 60 and 78 ppm $S_2O_3^{2-}$ was determined to be suitable from on-site measurements.

As a means of considering the increase in concentration of one ion at a time while maintaining a complex background process water matrix, ions were spiked to represent the accumulation of that one ion over and above all other ions present. This spiking was informed by actual site water compositions. 3 SPW was considered best to represent average current on site TDS levels and was thus used as the baseline experiment. All spiking tests were therefore done with this baseline of the complex background process water matrix at the 3 SPW level. Standard SPW ionic concentrations are shown in **Table 4-4**. The spiking of inorganic salts for the respective ions is also shown. Each ion was spiked to the level of 5 and 10 SPW respectively. Note that Cl^- was used as the counter-ion for the cations and Na^+ the counter ion for the anions, these ions were shown to have minimal impact in studies conducted by Manono et al. (2016) and are deemed to not compete with the ions of interest for the purposes of this study.

It is important to note that the original SPW does not contain $S_2O_3^{2-}$ and the spiking with 60 and 78 ppm $S_2O_3^{2-}$ could possibly introduce unusual complexity in the system.

Table 4-4 Synthetic Plant Water (SPW) and spiking

	Water type	*Ca^{2+} (ppm)*	*Mg^{2+} (ppm)*	*Na^{+} (ppm)*	*Cl^{-} (ppm)*	*SO_4^{2-} (ppm)*	*$S_2O_3^{2-}$ (ppm)*	*NO_3^{-} (ppm)*	*NO_2^{-} (ppm)*	*CO_3^{2-} (ppm)*	*TDS (mg/L)*	I.S [M]
	3 SPW	240	210	459	861	720	-	528	-	51	3069	0.073
	5 SPW	400	350	765	1435	1200	-	880	-	85	5115	0.121
	10 SPW	800	700	1530	2870	2400	-	1760	-	170	10230	0.242
5 SPW	$MgCl_2$	240	**350**	459	1049.85	720	-	528	-	51	3398	0.087
10 SPW	$MgCl_2$	240	**700**	459	1531.10	720	-	528	-	51	4229	0.123
5 SPW	$CaCl_2$	**400**	210	459	1141.48	720	-	528	-	51	3509	0.085
10 SPW	$CaCl_2$.	**800**	700	459	1851.48	720	-	528	-	51	5109	0.156
5 SPW	Na_2SO_4	240	210	647.2	861	**1200**	-	528	-	51	3737	0.087
10 SPW	Na_2SO_4	240	210	1117.8	861	**2400**	-	528	-	51	5408	0.122
5 SPW	$NaNO_3$	240	210	772.3	861	720	-	**880**	-	51	3734	0.082
10 SPW	$NaNO_3$	240	210	1554.6	861	720	-	**1760**	-	51	5397	0.106
5 SPW	$Na_2S_2O_3$	240	210	479.3	861	720	**60**	528	-	51	3149	0.074
10 SPW	$Na_2S_2O_3$	240	210	485.4	861	720	**78**	528	-	51	3173	0.075

KEY

Cations under investigation

Anions under investigation

4.8 Analysis of Means

First developed by Ott (1967); Analysis of means (ANOM) is a statistical method that is used for comparison purposes between the treated means and the overall mean. This is used to check the significance, if any, between the means in comparison to the grand mean. Treated means is the average/mean of the groups under investigation. The grand mean is defined as the sum of all the means of the samples under consideration divided by the number of means.

The ANOM compares the samples' mean to the grand mean and boundary lines called the Upper Decision Line (UDL) and Lower Decision Line (LDL). The UDL shows a positive statistical difference while the LDL shows a negative statistical difference both of which are compared to the grand mean. A typical ANOM chart has 3 lines: the UDL, the grand mean and the LDL.

It is important to note that Ott (1967) introduced the ANOM technique based on a series of tests following the pioneering work of Halperin (1955) in trying to control a group of means instead of considering them individually. The assumed level of confidence of these tests was 95%. As with confidence interval estimation, when computing the UDL and LDL, add and subtract a measure of sampling error around the statistic of interest. That is, **Equation 4.1** represents the generalized equation for evaluating the UDL and LDL.

$$\bar{\bar{y}} = \pm h_{c,n_j} \sqrt{\left\{ \frac{S_p^2 (c-1)}{n} \right\}} \quad \text{---------- 4.1}$$

Where:

c = number of groups of study

j = representation of a particular group

n_j = sample size for group j

n = total number of observations where all of the sample sizes are equal i.e $n = n_1 + n_2 + \ldots\ldots + n_c$

$\bar{\bar{y}}$ = overall or grand mean i.e $\bar{\bar{y}} = \frac{\overline{x_1} + \overline{x_2} + \cdots + \overline{x_c}}{c}$

S_p^2 = pooled variance, an estimate of the inherent variability in the data computed by averaging the c group variances $S_p^2 = \frac{S_1^2 + S_2^2 + \cdots + S_c^2}{c}$

h_{c,n_j} = critical value of Nelson's h statistic with c groups and equal observations per group obtained from the table of the h statistic

This leads to the UDL being calculated as shown in **Equation 4.2**

$$UDL = \bar{\bar{y}} + h_{c,n_j}\sqrt{\left\{\frac{S_p^2(c-1)}{n}\right\}} \quad \text{----------} \quad 4.2$$

The LDL is evaluated using **Equation 4.3**

$$UDL = \bar{\bar{y}} - h_{c,n_j}\sqrt{\left\{\frac{S_p^2(c-1)}{n}\right\}} \quad \text{----------} \quad 4.3$$

4.9 Reproducibility

Sequential batch flotation and 2 and 3-phase column tests were performed in duplicate for every condition tested in this study to determine and minimise the standard error associated with experimental results. Solids recovery, water recovery, and metal recoveries and grades were the variables which were key in determining whether performed duplicate tests were reproducible or not. The sample standard error was calculated for every condition and the sample standard error was calculated simply by dividing the sample standard deviation by the square root of the sample size.

For all batch float data presented in this thesis, the calculated standard error was found to be within accepted limits of < 5%. Note that the values presented for each condition are the average values between tests which were performed in duplicate and the error bars represent the standard error (**Equation 4.4)** between duplicate tests.

$$S = \sqrt{\frac{1}{N-1}\sum_{i=1}^{N}(x_i - \bar{x})^2} \quad \text{----------(4.4)}$$

5 RESULTS

5.1 Bulk Mineralogy

The Kevitsa ore type is a low-grade Cu-Ni-PGM ore from which copper is recovered as chalcopyrite and nickel as pentlandite, the two primary Base Metal Sulphides (BMS) present in this ore. A survey conducted by Gunn and Benham (2009) found that among others, Merensky Reef, Bushveld Complex, South Africa; Great Dyke, Zimbabwe; J-M Reef, Still Water Complex, USA; and Munni Munni Complex, Western Australia had typical grades of 5-7 g/t Pt+Pd, which were considered to be low grade and this has been used as a basis to distinguish between high grade and low grade ore in this study, since the Kevitsa Cu-Ni-PGM ore feed grades are less than 5-7 g/t Pt+Pd it is therefore classified as low grade ore. Usaini et al. (2014) defined liberation as the release of valuable material from its associated gangue material at the coarsest possible particle size hence when the mineral is not liberated from its associated gangue it is said to be locked.

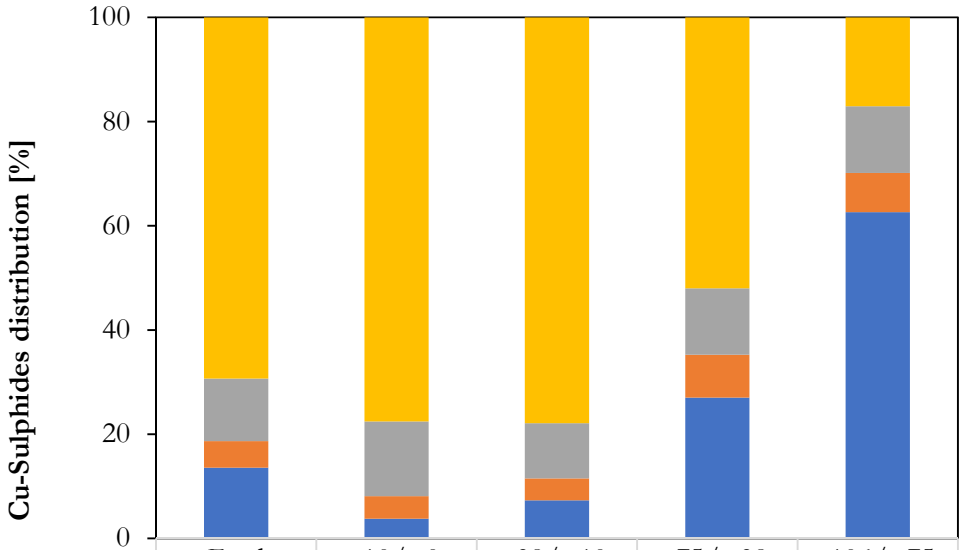

	Feed	-10/+0	-38/+10	-75/+38	-106/+75
Liberated	69,32	77,54	77,86	51,99	17,06
HG Middlings	12,01	14,33	10,62	12,75	12,79
LG Middlings	5,08	4,34	4,22	8,22	7,53
Locked	13,58	3,79	7,30	27,04	62,62

Figure 5-1 Liberation by size fraction of the Base Metal Sulphide (BMS) content of Cu-Sulphides constituting of mostly chalcopyrite.

From **Figure 5-1,** size by size distribution of Cu-Sulphides for the feed sample is illustrated, where, Liberated > 90 % by area, high-grade middlings, 60-90 % by area, low grade middlings, 30-60 % by size and locked < 30 % by area. The best Cu-sulphide liberation is observed at -38 µm size fraction. Higher size fractions have less chalcopyrite liberation.

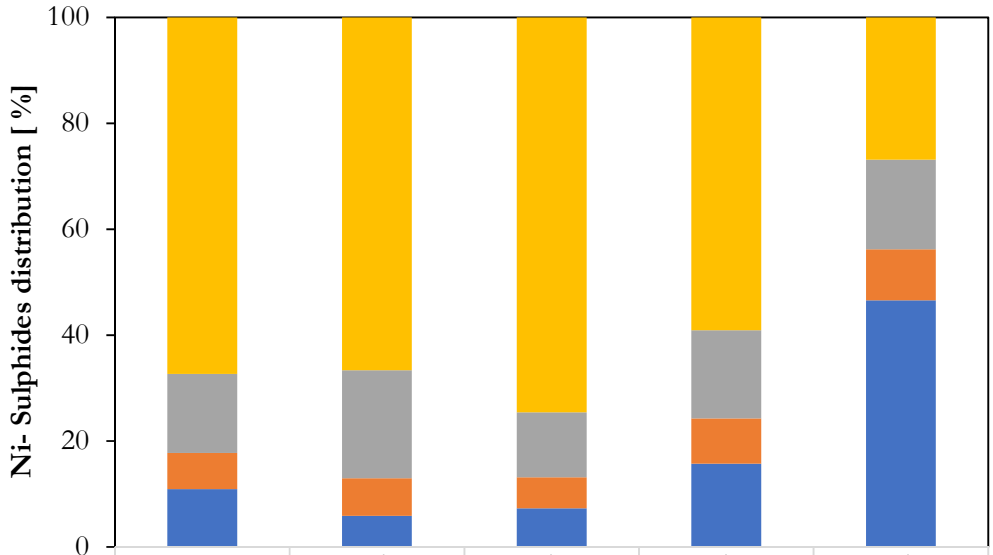

	Feed	-10/+0	-38/+10	-75/+38	-106/+75
Liberated	67,32	66,62	74,55	59,08	26,85
HG Middlings	14,93	20,41	12,28	16,66	16,93
LG Middlings	6,81	7,09	5,87	8,56	9,63
Locked	10,95	5,88	7,30	15,70	46,59

Figure 5-2 Liberation by size fraction of the Base Metal Sulphide (BMS) content of Ni-Sulphides constituting of mostly pentlandite.

From **Figure 5-2,** size by size distribution of Ni-sulphides for the feed sample is illustrated, where, Liberated > 90 % by area, high-grade middlings, 60-90 % by area, low grade middlings, 30-60 % by size and locked < 30 % by area. The best Ni-Sulphide liberation is observed at -38/+10 µm size fraction. Higher and lower size fractions have less pentlandite liberation

5.2 Flotation response upon increasing ionic strength of Synthetic Plant Water: 3, 5 and 10 SPW

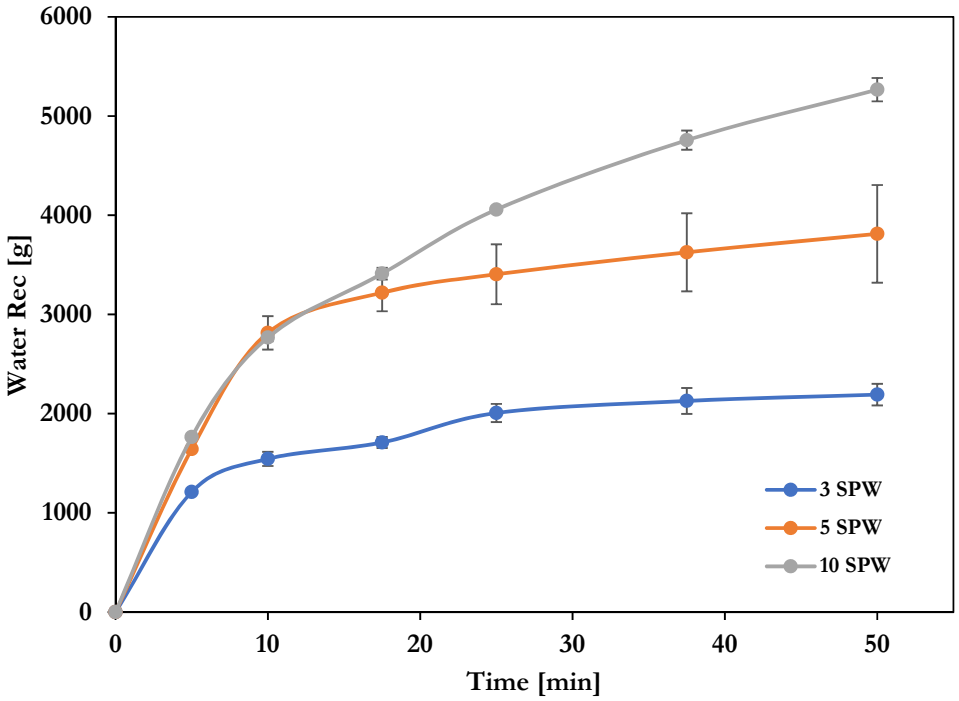

Figure 5-3 Water recovery vs time for 3, 5 and 10 SPW

As the ionic strength increases, the amount of water recovered also increases, **Figure 4-2**. During the first 10 minutes, 5 SPW and 10 SPW have the same rate and they result in the same amount of water recovered. This is notably higher than the kinetics and amount of water recovered with 3 SPW. However, beyond 10 minutes, 10 SPW continues to recover more water than 3 and 5 SPW, while 5 SPW tends to level off. 3 SPW recovers the least water.

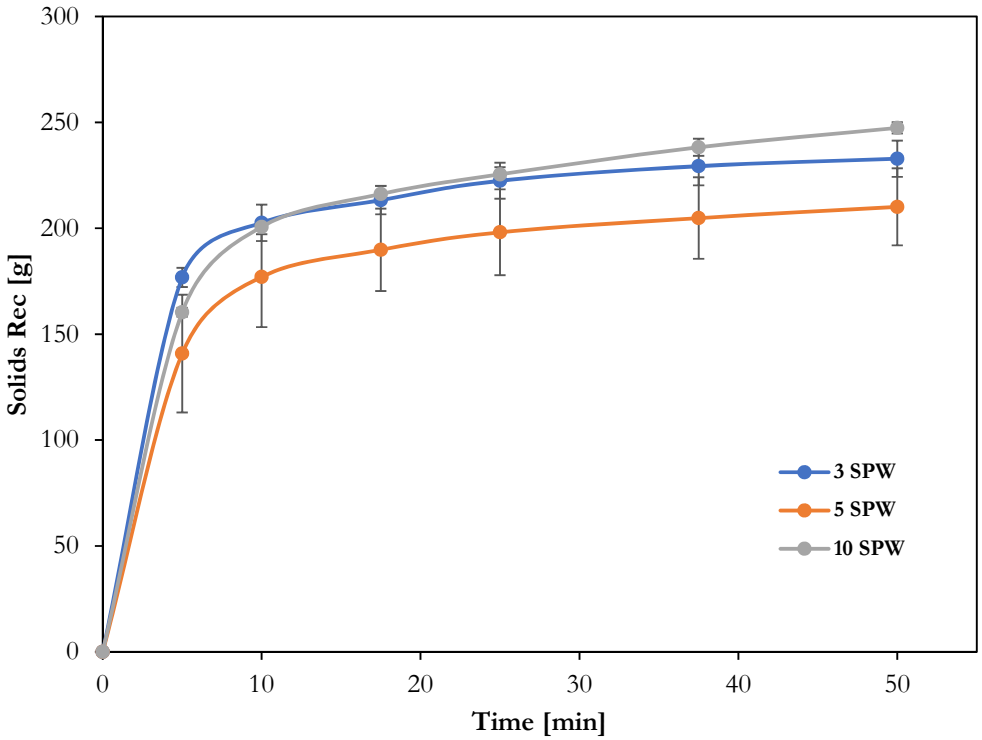

Figure 5-4 Solids recovery vs time for 3, 5 and 10 SPW

Overall, 10 SPW recovers more total solids than 3 and 5 SPW. It can be seen from **Figure 5-4** that as the flotation time increases from 0 to 50 minutes, there is a general increase in recovery of the solids cumulatively to the concentrates. According to the error shown, 3 and 5 SPW recovers almost the same amount of solids at the end of the flotation time. Within the first 40 min, 3, 5 and 10 SPW recovers almost the same amount of solids to the concentrate.

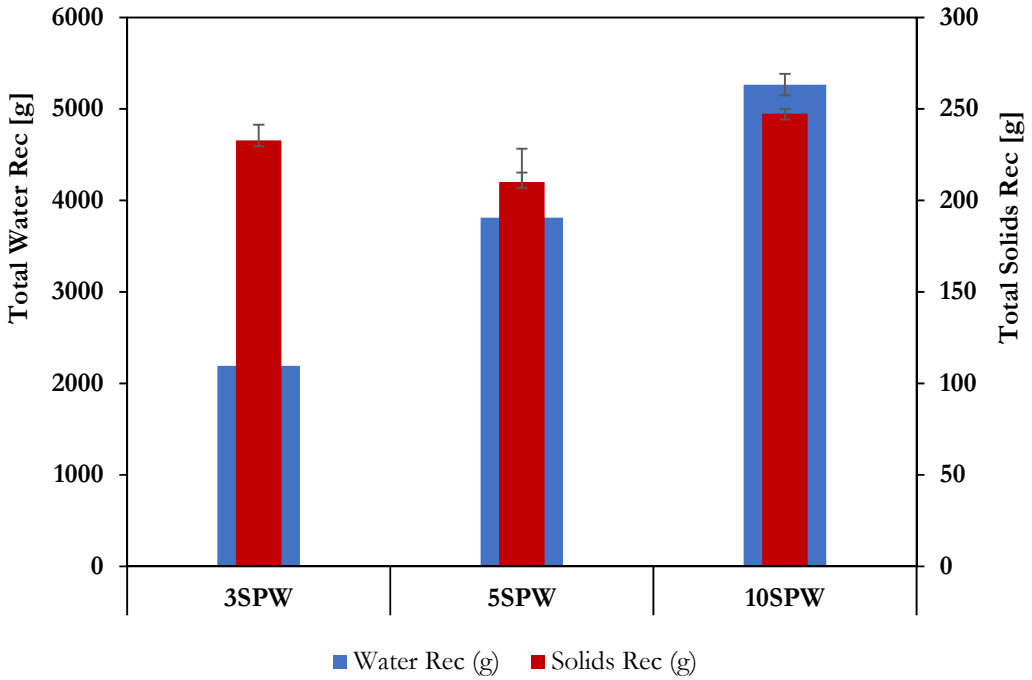

Figure 5-5 Total water and solids recovered for 3, 5 and 10 SPW

Figure 5-5 shows the effect of changing water quality on the total final recovered water and solids. The general trend observed here is that; as the ionic strength of water increases water recovery also increases however the same cannot be said with regards to solid recovery. 5 SPW recovers the least less solids than either 3 or 10 SPW. As the ionic strength of water increases from 3 through 5 to 10 SPW, there is a general increase in water recovery, this however does not translate to a linear relationship to the solids recovered. 5 SPW; an outlier, pulls more water than 3 SPW but it has the least mass pull of 210.1 g.

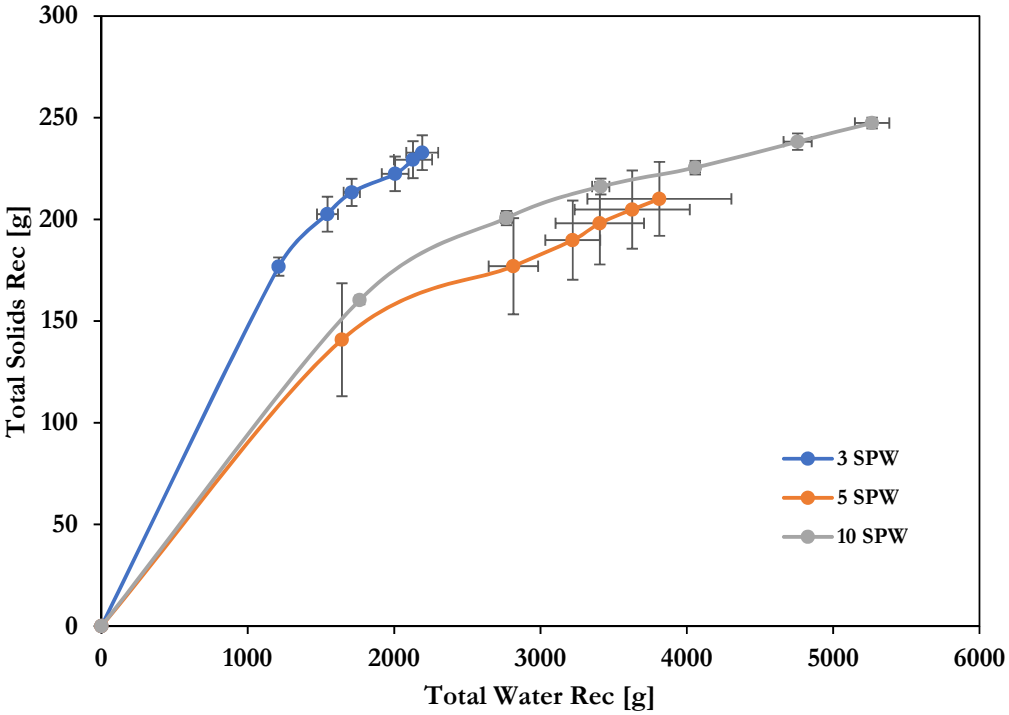

Figure 5-6 Total solids vs water recovery for 3, 5 and 10 SPW

Figure 5-6 shows that as water recovery to the concentrate increases, so does the solids recovery. However, the solids recovery per unit water recovery observed in 3 SPW was higher compared to that observed in both 5 and 10 SPW.

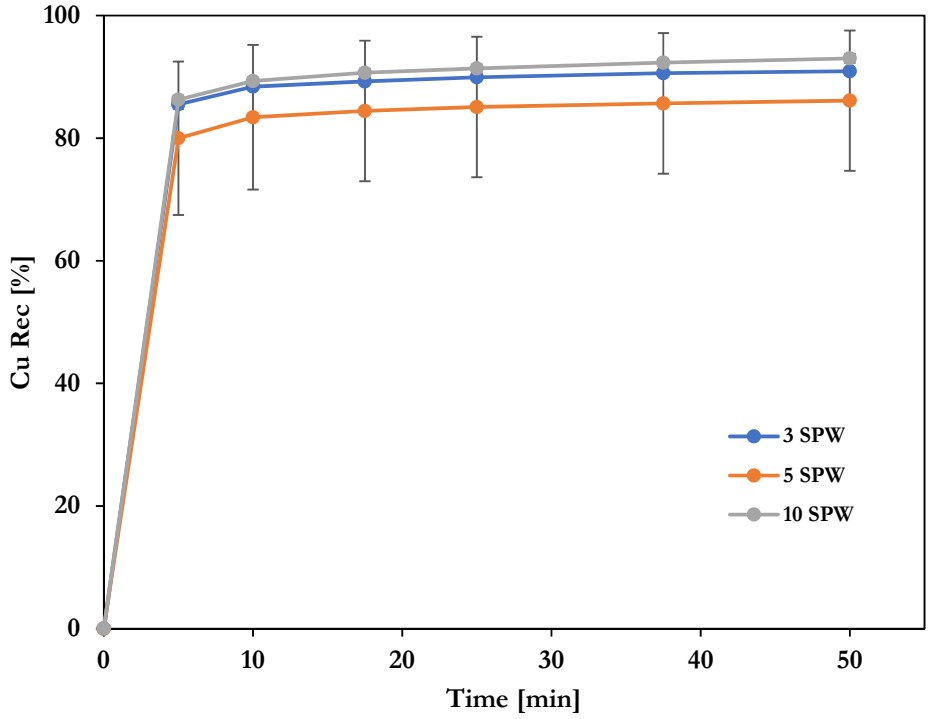

Figure 5-7 Copper recovery vs time for 3, 5 and 10 SPW

As expected, most of the copper is recovered in the first two concentrates. The general trend observed in **Figure 5-7** is that; for the entire flotation time, 3, 5 and 10 SPW exhibit the same copper recovery. Final total copper recovery is noted as being between the same recovery for the three water types considering the overlap of the error bars.

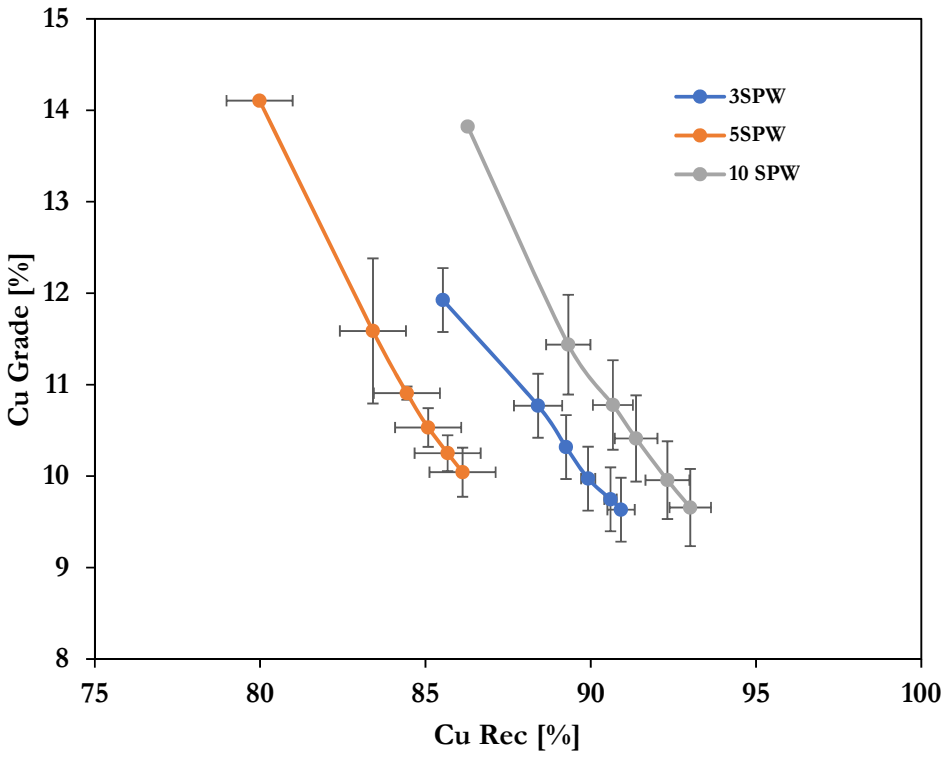

Figure 5-8 Copper grade vs copper recovery for 3, 5 and 10 SPW (note the axis range has been shortened for clarity the y-axis shows 8-15% Cu Grade while the x-axis shows 75-100% Cu Recovery))

From **Figure 5-8**, while the highest final recovery is given by 10 SPW, the highest final grade is given by 5 SPW. As copper recovery increases there is a general decrease in its grade for each specific water type, as expected. For 3 SPW copper grade of the recovered concentrate was 9.6% while for 5 SPW it was 10.0% and 10 SPW gave 9.7%.

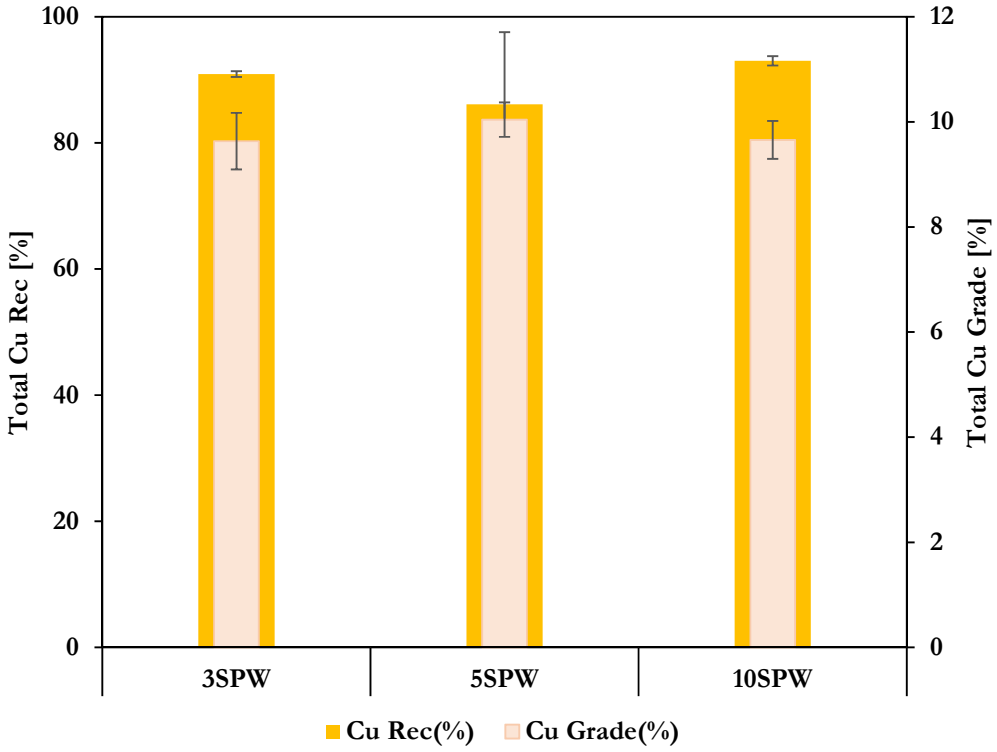

Figure 5-9 Final copper recovery vs. grade for 3, 5 and 10 SPW

Figure 5-9 illustrates the final grade and recovery for copper. Considering the error bars, 3, 5 and 10 SPW have the same overall recovery of copper. 3 SPW shows copper recovery of 90.1% with a grade of 9.6%, 5 SPW has 86.1% with copper grade of 10.0% and 10 SPW has 93% copper recovery with 9.7% copper grade.

Table 5-1 Overall copper recovery for different ionic strengths: 3, 5 and 10 SPW including the std. values

Water [I.S]	Spiking	Cu Rec [%]	Cu Rec [Std_Error]	Cu Grade [%]	Cu Grade [Std_Error]
3 SPW	No spiking	90.9	0.46	9.6	0.54
5 SPW	No spiking	86.1	11.4	10.0	0.33
10 SPW	No spiking	93.0	0.7	9.7	0.36

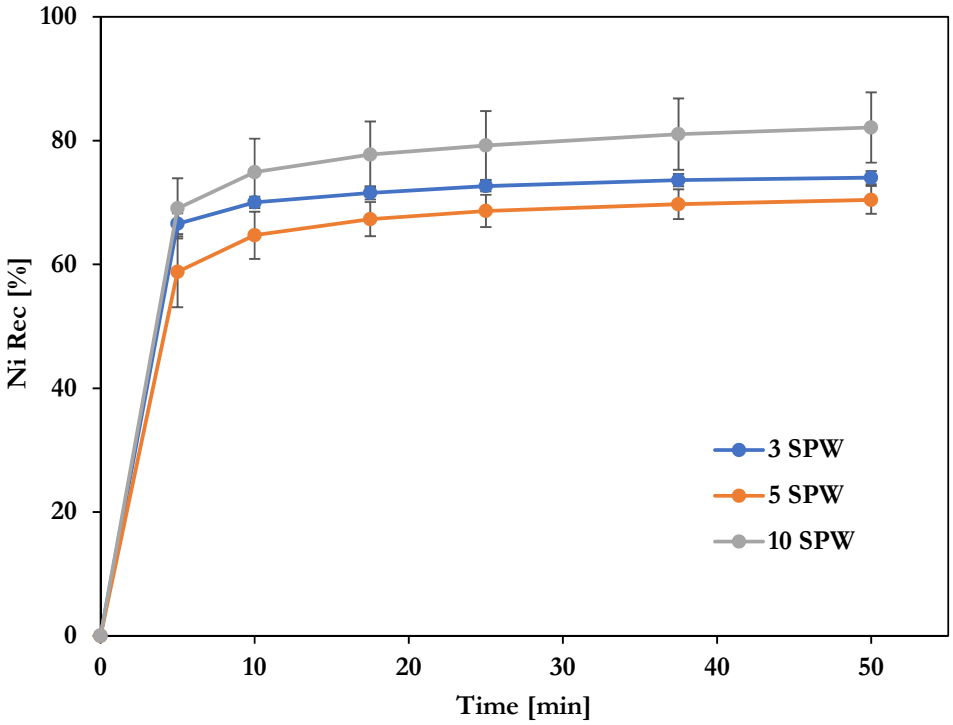

Figure 5-10 Nickel recovery vs. time for 3, 5 and 10 SPW

Figure 5-10 shows the recovery of nickel to the concentrate as a function of froth flotation time, for 3, 5 and 10 SPW. As was the case for both solids and copper recoveries, 10 SPW recovers the most nickel followed by 3 SPW while 5 SPW recovers the least nickel. While the experimental design was intended to be sequential flotation, a significant amount of nickel was recovered to the copper concentrate.

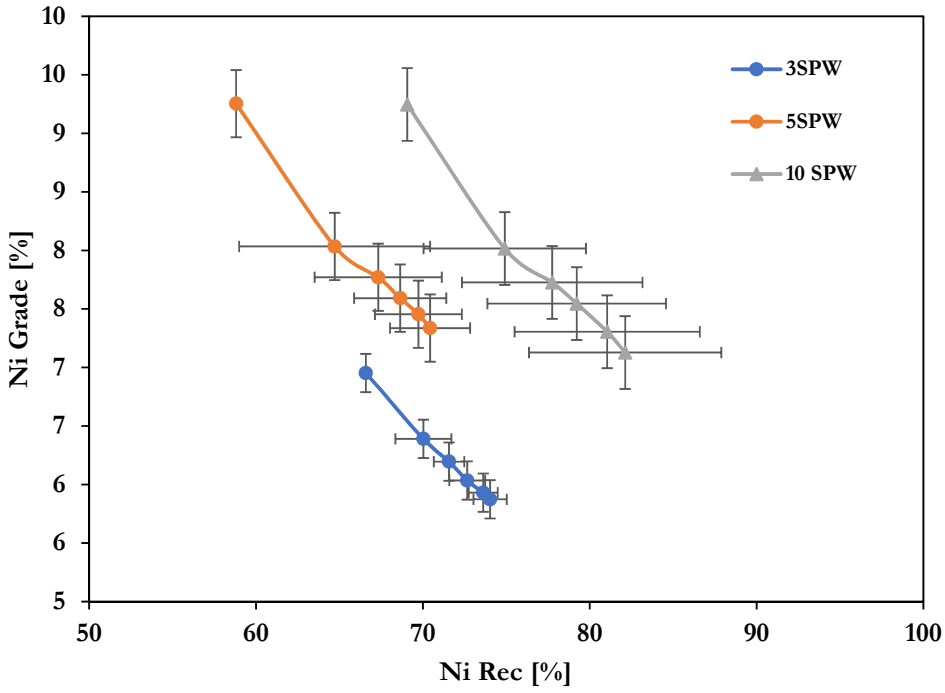

Figure 5-11 Nickel grade vs recovery for 3, 5 and 10 SPW (note the axis range has been shortened for clarity the y-axis shows 5-10% Ni Grade while the x-axis shows 50-100% Ni Recovery))

Figure 5-11 depicts the nickel grade as a function of its recovery. 3 SPW shows that it has the lowest nickel grade-recovery curve compared to 5 and 10 SPW. 3 SPW shows that of the 74.0% nickel recovered it constitutes nickel grade of 5.9%, while 5 SPW has 70.4% nickel recovery with 7.3% nickel grade and 10 SPW recovered 82.1% nickel concentrate with 7.1% nickel grade.

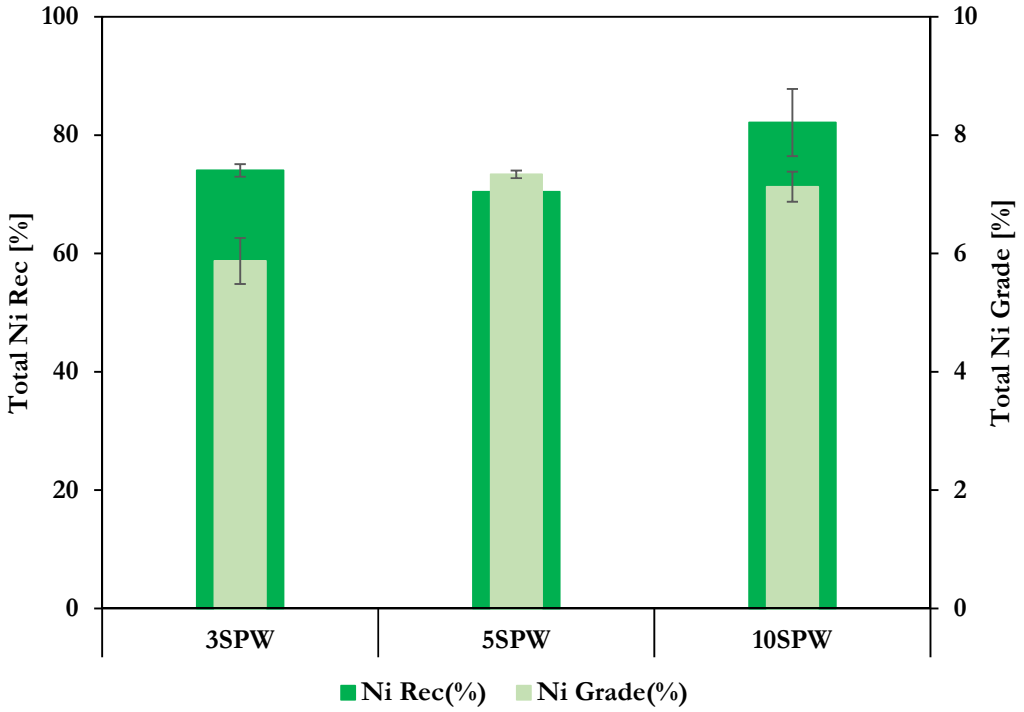

Figure 5-12 Total nickel recovery vs. grade for 3, 5 and 10 SPW

Figure 5-12 illustrates the final grade and recovery for nickel. The highest final nickel recovery was achieved in 10 SPW flotation (82.1%) with the lowest being 5 SPW with a 70.4% nickel recovery, with the highest final grade of 7.3% and the lowest nickel grade being in 3 SPW at 5.9 %. **Table 5-2** illustrates the final nickel recoveries and grades for different synthetic plant water recipes used for this study including the standard error.

Table 5-2 Overall nickel recovery and grade for different ionic strengths including the std. values

Water [I.S]	Spiking	Ni Rec [%]	Ni Rec [Std_Error]	Ni Grade [%]	Ni Grade [Std_Error]
3SPW	No spiking	74.0	1.05	5.9	0.39
5SPW	No spiking	70.4	2.25	7.3	0.06
10SPW	No spiking	82.1	6.68	7.1	0.25

5.3 EC in 2-phase column studies: 3, 5 and 10 SPW

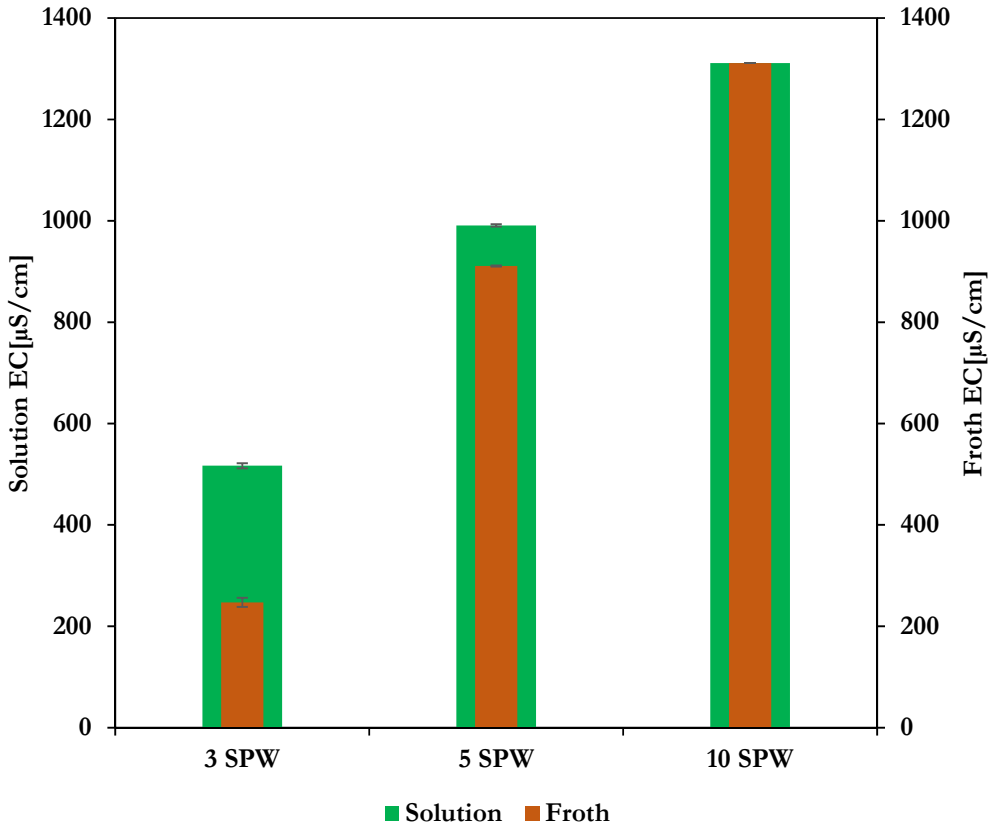

Figure 5-13 2-Phase EC between froth and solution using standard synthetic plant water

Figure 5-13 illustrates the 2-phase column's EC between froth and solution for 3, 5 and 10 SPW. The increase in the difference in EC between the solution and froth is almost proportional to the increase in the ionic strength of the water type used. The difference in EC between the froth and solution in 3 SPW is the highest compared to 5 and 10 SPW. 5 SPW shows a slight difference in EC between the froth and solution in a two-phase system while there is no difference for 10 SPW.

5.4 EC in 3-phase column studies: 3, 5 and 10 SPW

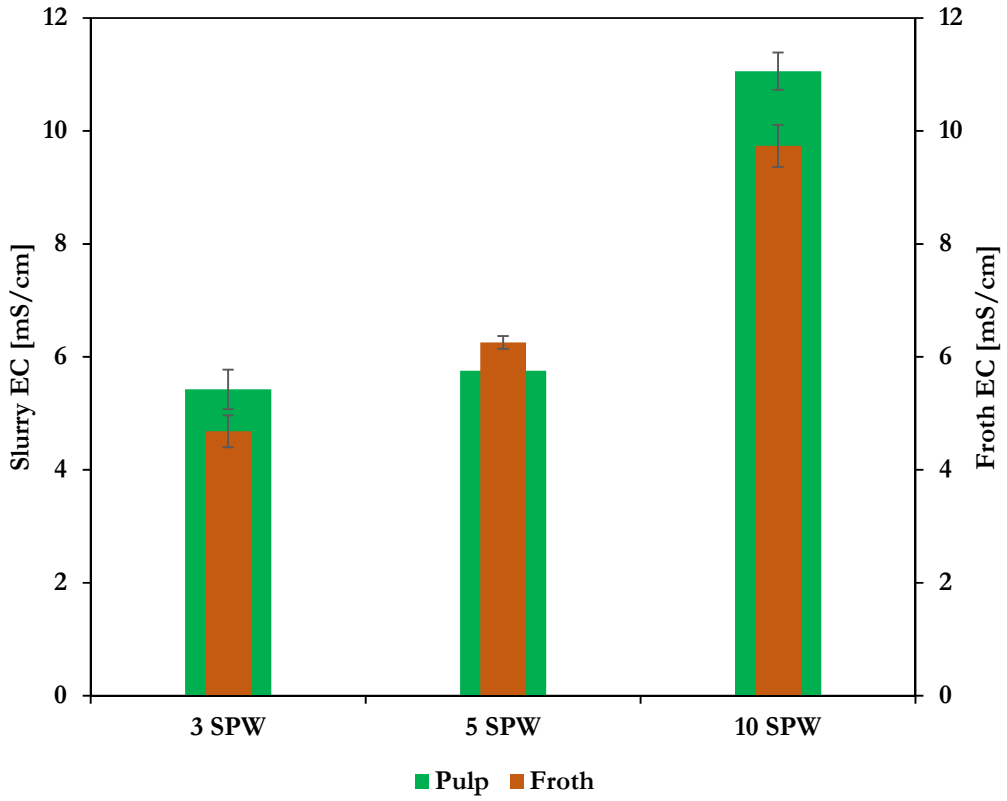

Figure 5-14 3-Phase EC between froth and solution using standard synthetic plant water

The EC in the froth increases as the ionic strength of water increases from 3 through 5 to 10 SPW. The EC in the pulp is the same for 3 and 5 SPW while 10 SPW has the highest EC in the pulp phase. As can be observed from **Figure 5-14,** 3 and 10 SPW show that the EC in the pulp is higher compared to that in the froth phase. 5 SPW shows that the EC in the froth phase is higher than the pulp phase.

5.5 Key Findings: 3, 5 and 10 SPW

- Increasing ionic strength of water increases the water recovered to the concentrate
- 3, 5 and 10 SPW recovered the same amount of copper
- Owing to this investigation being sequential flotation, it is important to note that a significant amount of the nickel is recovered in the copper concentrate.
- 5 SPW is an outlier with regards to nickel recovery/grade upon increase in ionic strength. It does not follow the trend that as the ionic strength increases recovery will also increase
- For 2-phase EC studies, 3 SPW results in higher EC in solution than in the froth while 10 SPW shows the same value of EC in the froth as is in solution.
- For 3-phase EC studies, 3 and 10 SPW show that the pulp EC is much higher than the froth EC while 5 SPW shows that the froth has a high EC than its pulp phase.

6 FLOTATION RESPONSE UPON SPIKING OF 3 SPW WITH Ca^{2+} AND Mg^{2+}

The previous section (**Chapter 5**) considered the effect of increased ionic strength of a complex water recipe on flotation performance (3, 5 and 10 SPW). This section (**Chapter 6**) deals with the effect of spiking Ca^{2+} and Mg^{2+} to the levels of 5 and 10 SPW within a complex baseline of 3SPW (shown in yellow and green respectively, **Table 6-1**). The spiked response is then compared to 3, 5 and 10 SPW although much emphasis is put on the spiked response against 3 SPW (shown in brown, **Table 6-1**).

Table 6-1 Type of water quality used and its accompanying cationic spiking levels

	Water type	*Ca^{2+} (ppm)*	*Mg^{2+} (ppm)*	*Na^{+} (ppm)*	*Cl^{-} (ppm)*	*SO_4^{2-} (ppm)*	*$S_2O_3^{2-}$ (ppm)*	*NO_3^{-} (ppm)*	*NO_2^{-} (ppm)*	*CO_3^{2-} (ppm)*	*TDS (mg/L)*	I.S [M]
	3 SPW	240	210	459	861	720	-	528	-	51	3069	0.073
	5 SPW	400	350	765	1435	1200	-	880	-	85	5115	0.121
	10 SPW	800	700	1530	2870	2400	-	1760	-	170	10230	0.242
5 SPW	$MgCl_2$	240	**350**	459	1049.85	720	-	528	-	51	3398	0.087
10 SPW	$MgCl_2$	240	**700**	459	1531.10	720	-	528	-	51	4229	0.123
5 SPW	$CaCl_2$	**400**	210	459	1141.48	720	-	528	-	51	3509	0.085
10 SPW	$CaCl_2$	**800**	700	459	1851.48	720	-	528	-	51	5109	0.156

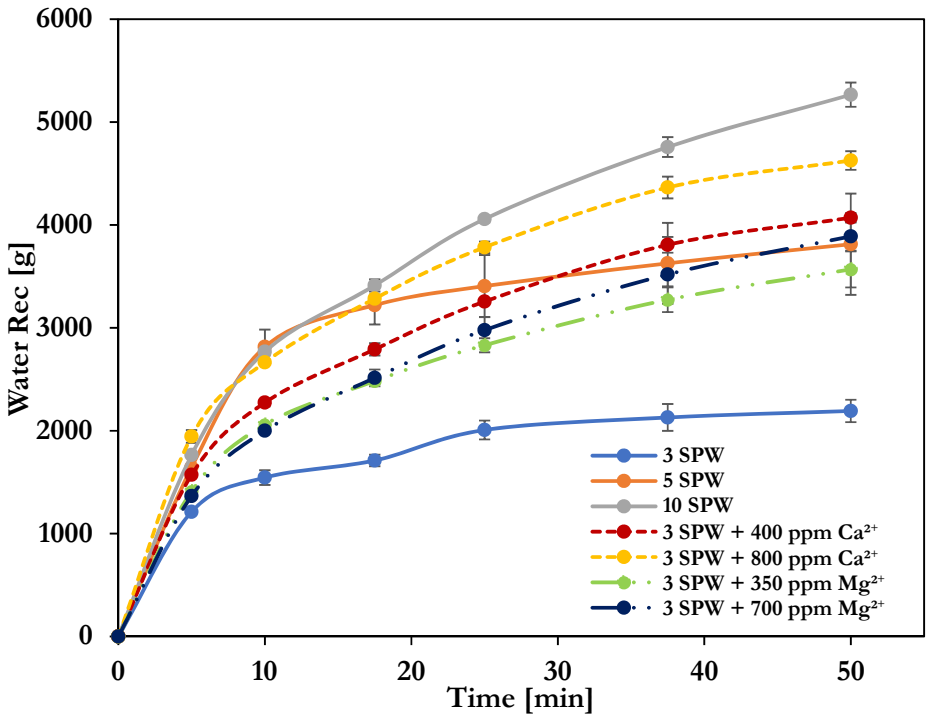

Figure 6-1 Water recovery per flotation time during Ca^{2+} and Mg^{2+} spiking

For 400 and 800 ppm Ca^{2+} and, 350 and 700 ppm Mg^{2+} ion spiking **Figure 6-1** illustrates the effect of the ion on water recovery to the concentrate per unit time. All cation spiking increases water recoveries above that of the 3 SPW. Ca^{2+} increases water recoveries more than Mg^{2+}. 800 ppm Ca^{2+} recovered the most water in comparison to the other spiked cation concentrations and is higher than the water recovery of 5 SPW despite having a lower overall ionic strength than 5 SPW.

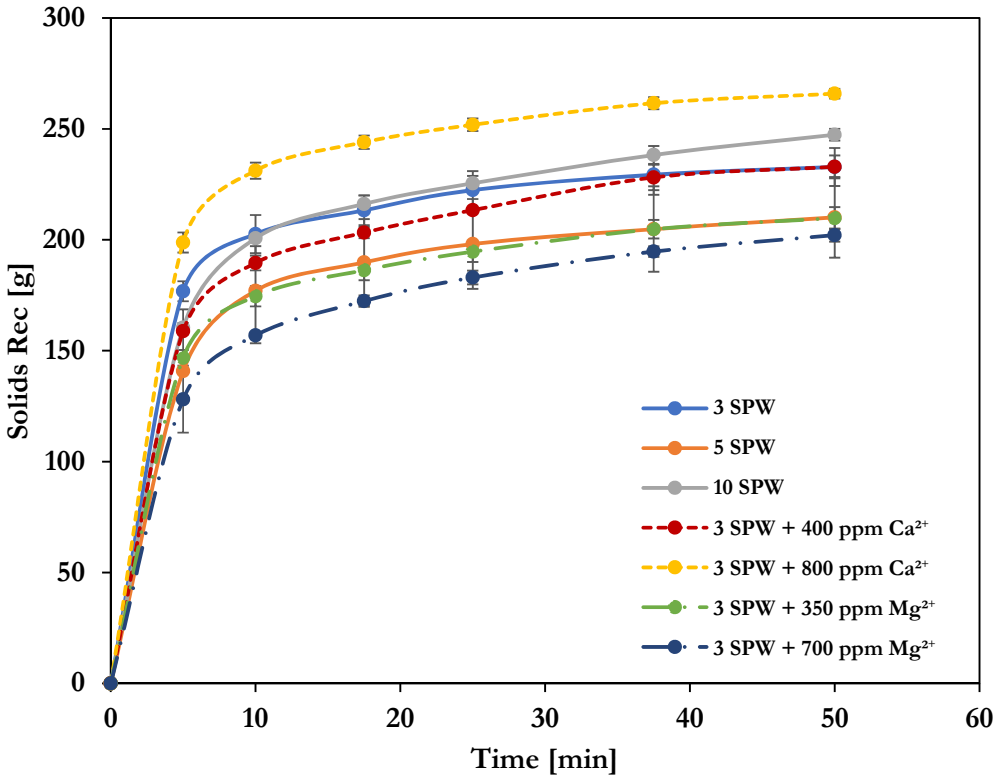

Figure 6-2 Solids recovery per flotation time during Ca^{2+} and Mg^{2+} spiking

As illustrated in **Figure 6-2**, 800 ppm Ca^{2+} ion spiking produced the highest solids recoveries while 700 ppm Mg^{2+} produced the lowest solids. 400 ppm Ca^{2+} after 50 minutes of flotation time pulled the same amount of solids as 3 SPW. A similar trend is observed between 350 ppm $Mg^{2+}$and 5 SPW where they closely track one another and pull the same amount of solids at the end of the flotation time. Mg^{2+} ions clearly shows a dramatic decrease in solids recovery compared to 3 SPW even worse when it is spiked to levels of 10 SPW (700 ppm Mg^{2+}), 350 ppm Mg^{2+} solids recovered are maintained this in the same region as 5 SPW.

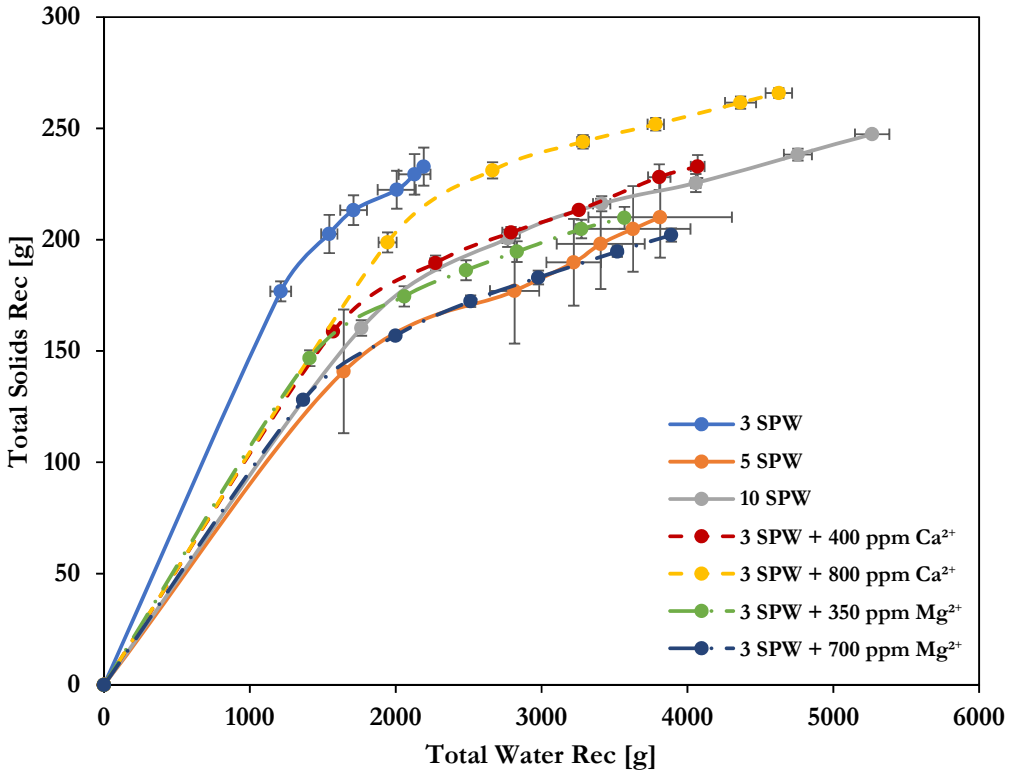

Figure 6-3 Solids-water recovery upon Ca^{2+} and Mg^{2+} spiking

Figure 6-3 shows the response of the solids recovered to the concentrate per water recovery. 5 SPW and 700 ppm Mg^{2+} shows the same amount of total water and solids recovery, both having overlapping error bars. 3 SPW (232.8 g) shows lower amount of solids recovered to the concentrate comparable to 10 SPW (247.4 g) though 10 SPW has the highest total water recovery to the concentrate. 5 SPW recovery water and solids in the same region as 350 ppm Mg^{2+} and 700 ppm Mg^{2+}. 800 ppm Ca^{2+} spiking shows higher total solids recovered per unit water recovery compared to 5 SPW, 350 ppm Mg^{2+} and 700 ppm Mg^{2+}.

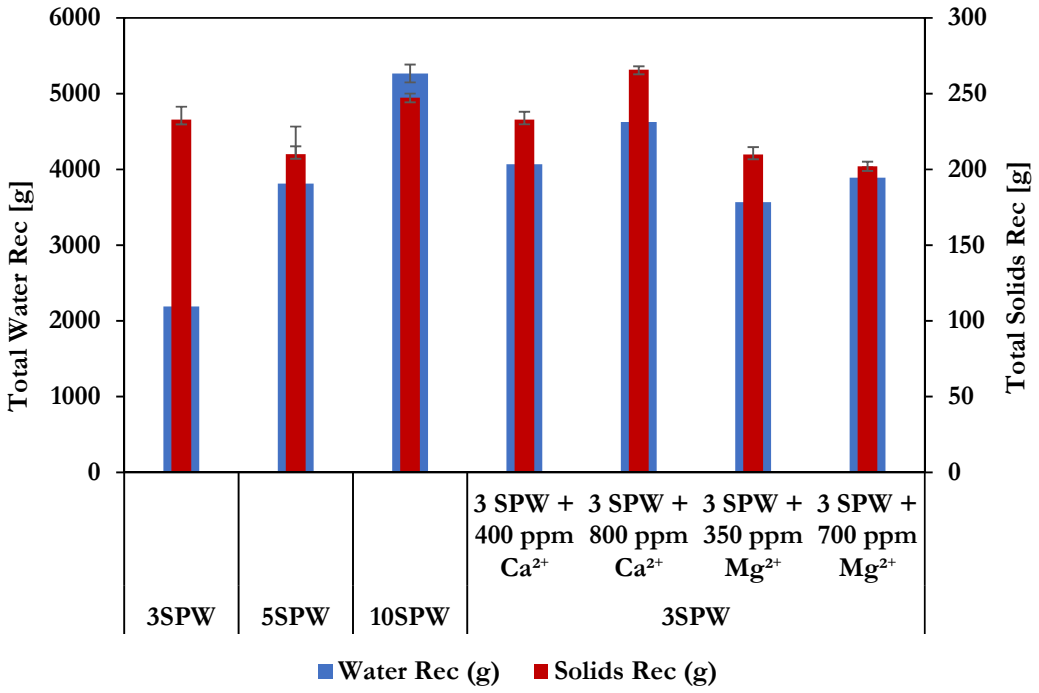

Figure 6-4 Final water recovery vs. solids recovery at different levels of cationic spiking

Figure 6-4 shows the final solids and water recovered to the concentrate. The general trend is that; as the concentration of the specific ion increases, the water and solids recovery increases. 400 ppm Ca^{2+} pulls more water and solids compared to 5 SPW while 800 ppm Ca^{2+} pulls more solids compared to 10 SPW with less water recovery. 700 ppm Mg^{2+} recovers more water compared to 350 ppm Mg^{2+} however despite having a higher ionic strength, 700 ppm Mg^{2+} recovers less solids compared to 350 ppm Mg^{2+}.

Table 6-2 Overall solids recovery per water recovered at different cationic spiking concentrations including the std. values

Water [I.S]	Spiking	Solids Rec [g]	Solids Rec [Std_Error]	Water Rec [g]	Water Rec [Std_Error]
3 SPW	-	232.8	8.6	2192.0	109
5 SPW	-	210.1	18.2	3813.0	492
10 SPW	-	247.4	2.7	5266.4	117.7
3 SPW	400 ppm Ca^{2+}	232.9	5.2	4070.0	47.3
	800 ppm Ca^{2+}	265.9	2.2	4626.6	90.8
	350 ppm Mg^{2+}	209.8	4.9	3568.4	175.6
	700 ppm Mg^{2+}	202.1	3.0	3889.4	139.9

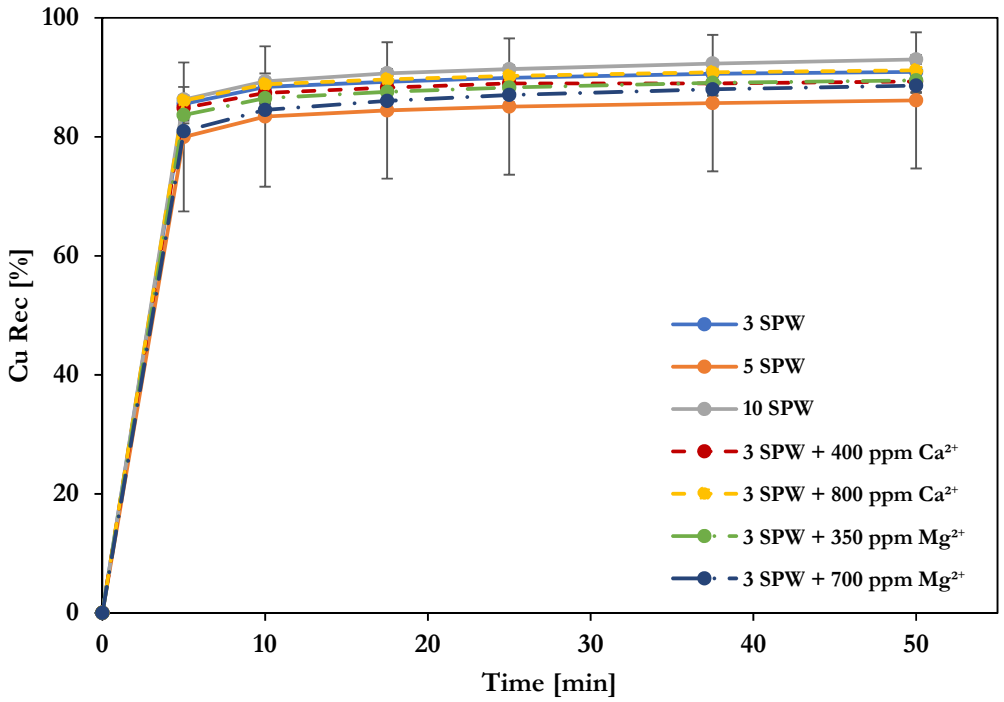

Figure 6-5 Copper vs. time upon cationic spiking

Figure 6-5 shows that there is no distinct differences in copper recovery as the ionic strength water increases. The same is observed when when 3 SPW is spiked to 400 and 800 ppm Ca^{2+}, 350 and 700 ppm Mg^{2+}.

Table 6-3 Water recovery upon cationic spiking of the selected water hardening ions including the std. values

Water [I.S]	Spiking	Cu Rec [%]	Cu Rec [Std_Error]
3 SPW	-	90.92	0.5
5 SPW	-	86.12	11.4
10 SPW	-	93.01	0.7
3 SPW	400 ppm Ca^{2+}	89.30	1.9
	800 ppm Ca^{2+}	91.18	1.6
	350 ppm Mg^{2+}	89.49	1.1
	700 ppm Mg^{2+}	88.61	1.1

At 400 ppm Ca^{2+} spiking, copper recovery is 89.3% which is lower compared to that of 3 SPW (90.9%) but higher than that of 5 SPW (86.1%) but lower than that of 10 SPW (93%). For 800 ppm Ca^{2+} spiking, copper recovery is at 91.18% which is higher than 3 and 5 SPW with a recovery of 90.9% and 86.1% respectively. However, as the concentration of Mg^{2+} increases, copper recovery decreases. At both 350 ppm and 700 ppm Mg^{2+} ionic concentration, the recovery is

89.49% and 88.61% respectively, these recoveries are lower than the baseline synthetic plant water (3 SPW) which has recovery of 90.92%, these recoveries are practically the same.

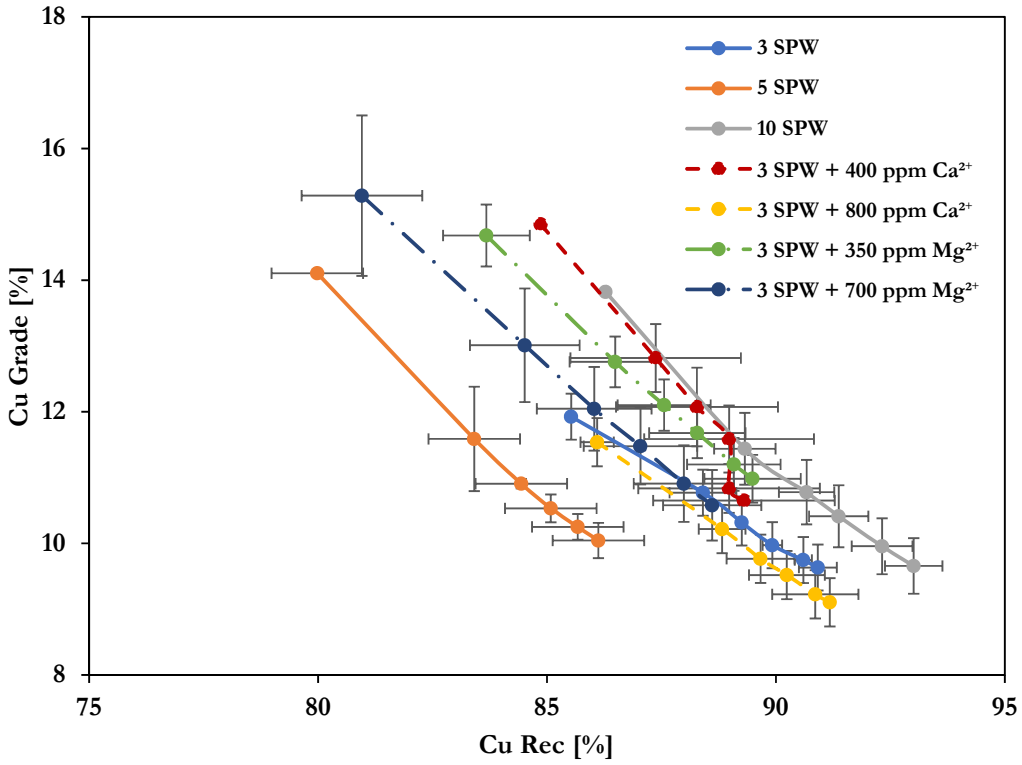

Figure 6-6 Copper grade per copper concentrate recovered at different cationic concentrations (note the axis range has been shortened for clarity the y-axis shows 8-18% Cu Grade while the x-axis shows 75-95% Cu Recovery)

Figure 6-6 shows that 400 ppm Ca^{2+} has slightly higher grade than 3 SPW, however copper grade decreases as the Ca^{2+} ion concentration increases from 400 to 800 ppm. The grade decreases from 10.65% to 9.10%. At 800 ppm Ca^{2+}, the grade is lower than that for 3 SPW (9.63%). This may suggest that 400 ppm Ca^{2+} is the trade-off and beyond which copper grade is evidently affected. With respect to Mg^{2+}, at 350 ppm, the copper grade is higher than that at 3 SPW. At 700 ppm Mg^{2+}, the copper grade is still higher than that at 3 SPW, however it is slightly lower than that at 350 ppm Mg^{2+}. **Table 6-4** shows the breakdown of the copper grade and accompanying standard error values.

Table 6-4 Copper grade upon spiking of the water hardening ions, showing the associated std. error

Water [I.S]	Spiking	Cu Grade [%]	Cu Grade [Std_Error]
3 SPW	-	9.63	0.5
5 SPW	-	10.04	0.3
10 SPW	-	9.66	0.4
3 SPW	400 ppm Ca^{2+}	10.65	0.1
	800 ppm Ca^{2+}	9.10	1.2
	350 ppm Mg^{2+}	10.98	0.4
	700 ppm Mg^{2+}	10.58	0.5

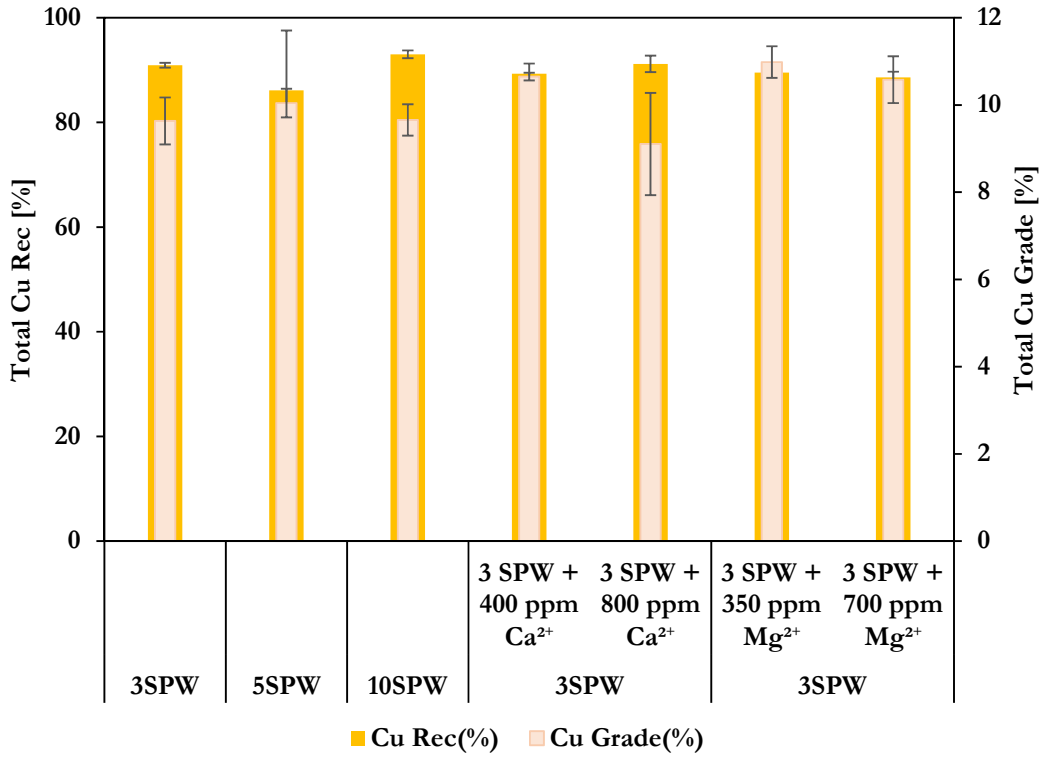

Figure 6-7 Final copper recovery vs. grade at different levels of cationic concentrations

Overall, as can be seen from **Figure 6-7** both Ca^{2+} and Mg^{2+} ions exhibit different effects with regards to copper recovery, that is; as the concentration of Ca^{2+} ion increases, the copper recovery increases however copper grade decreases but as the Mg^{2+} ion concentration increases, there is a slight decrease in copper recovery and this is accompanied by a decrease in grade.

Table 6-5 Overall flotation cell copper recovery-grade performance at different levels of cationic spiking concentrations, including the associated std. errors

Water [I.S]	Spiking	Cu Rec [%]	Cu Rec [Std_Error]	Cu Grade [%]	Cu Grade [Std_Error]
3 SPW	-	90.9	0.5	9.6	0.5
5 SPW	-	86.1	11.4	10.0	0.3
10 SPW	-	93.0	0.7	9.7	0.4
3 SPW	400 ppm Ca^{2+}	89.3	1.9	10.7	0.1
	800 ppm Ca^{2+}	91.2	1.6	9.1	1.2
	350 ppm Mg^{2+}	89.5	1.1	11.0	0.4
	700 ppm Mg^{2+}	88.6	1.1	10.6	0.5

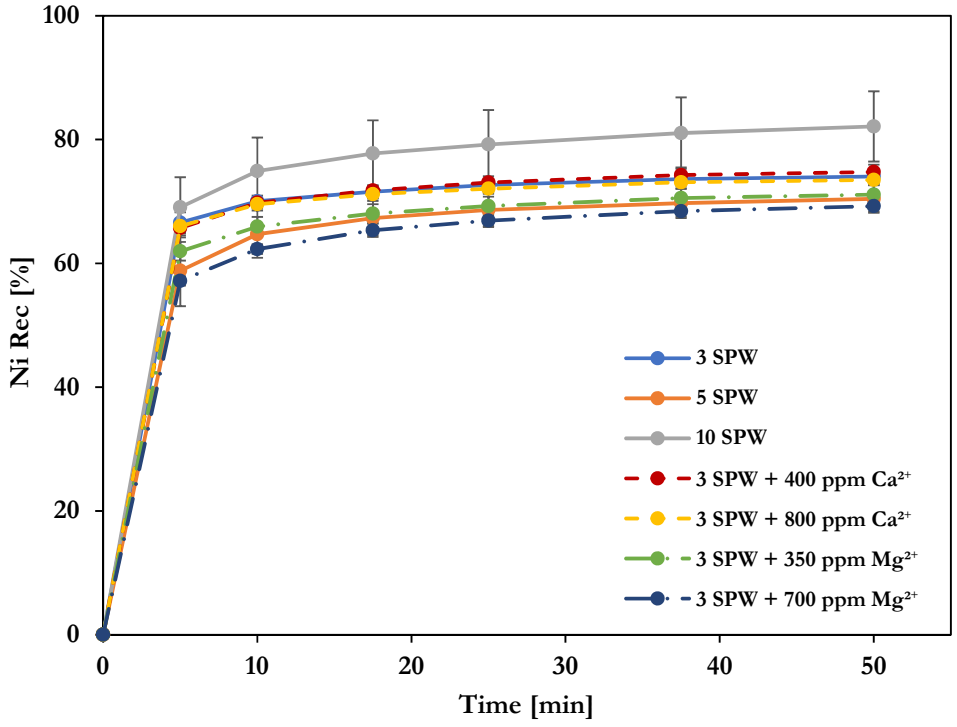

Figure 6-8 Nickel recovery per unit flotation time at different concentrations of cationic spiking

Figure 6-8 shows the nickel recovery per flotation time resulting in 10 SPW (82.1%) recovering the most nickel. The lowest recovery is at 700 ppm Mg^{2+} spiking. 5 SPW (70.4%) recovers lower than 3 SPW (74.0%). Spiking Mg^{2+} from 350 to 700 ppm Mg^{2+} did not influence nickel recovery. **Table 6-6** shows a breakdown of how the spiking affects recovery.

Table 6-6 Nickel recovery upon spiking of water hardening cations including the associated std. errors

Water [I.S]	Spiking	Ni Rec [%]	Ni Rec [Std_Error]
3 SPW	-	74.0	1.1
5 SPW	-	70.4	2.3
10 SPW	-	82.1	5.7
3 SPW	400 ppm Ca^{2+}	74.8	1.2
	800 ppm Ca^{2+}	73.5	0.5
	350 ppm Mg^{2+}	71.1	1.5
	700 ppm Mg^{2+}	69.2	0.9

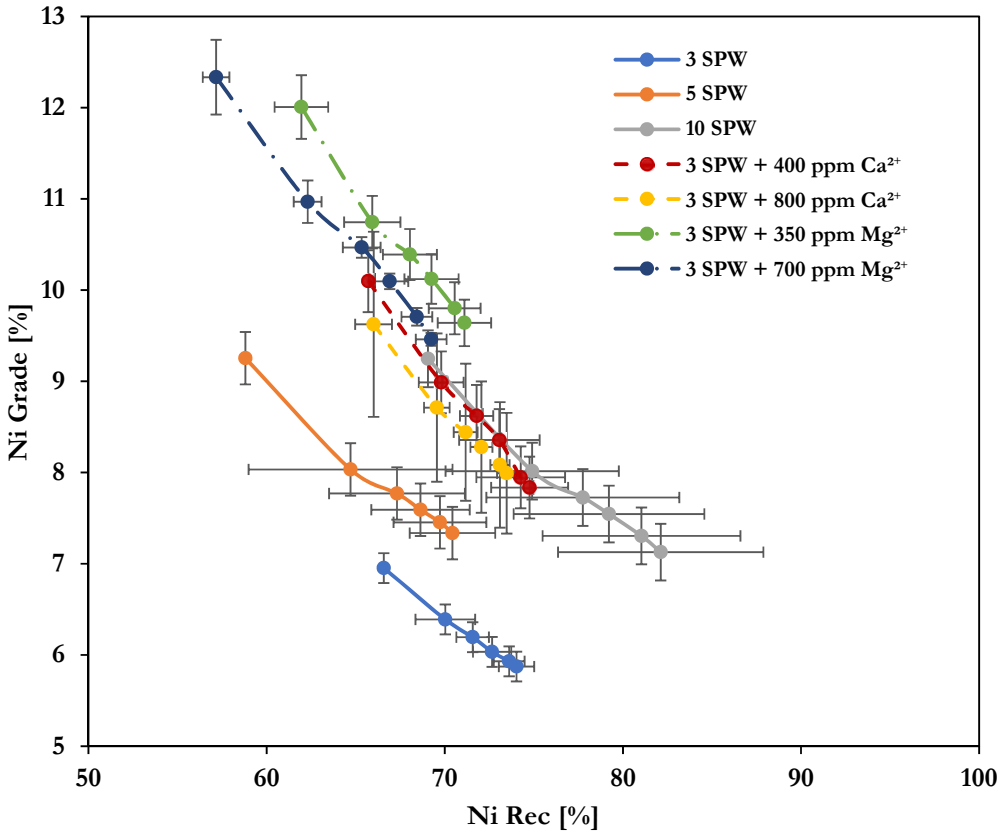

Figure 6-9 Nickel grade per nickel concentrate recovered at different cationic concentrations (note the axis range has been shortened for clarity the y-axis shows 5-13% Ni Grade while the x-axis shows 50-100% Ni Recovery)

Figure 6-9 shows the impact of spiking on the grade of nickel recovered. As the spiking concentration of Ca^{2+} increases from 400 to 800 ppm, the grade increased significantly above the baseline experiment, 3 SPW. Ca^{2+} ion spiking resulted in significantly higher grade compared to 3, 5 and 10 SPW as can be seen from **Table 6-7**. As the Mg^{2+} ionic concentration increases from 350 to 700 ppm, the grade increased much higher above 3, 5 and 10 SPW and even higher than Ca^{2+} spiking. 3 SPW (5.9 %) has the lowest grade, however as the ionic strength of the water used

increases, the grade increases substantially. **Table 6-7** shows a breakdown of the nickel grade and standard error values.

Table 6-7 Nickel grade upon spiking of the selected water hardening ions including the associated std. errors

Water [I.S]	Spiking	Ni Grade [%]	Ni Grade [Std_Error]
3 SPW	-	5.9	0.4
5 SPW	-	7.3	0.1
10 SPW	-	7.1	0.3
3 SPW	400 ppm Ca^{2+}	7.8	0.1
	800 ppm Ca^{2+}	8.0	0.7
	350 ppm Mg^{2+}	9.6	0.3
	700 ppm Mg^{2+}	9.5	0.1

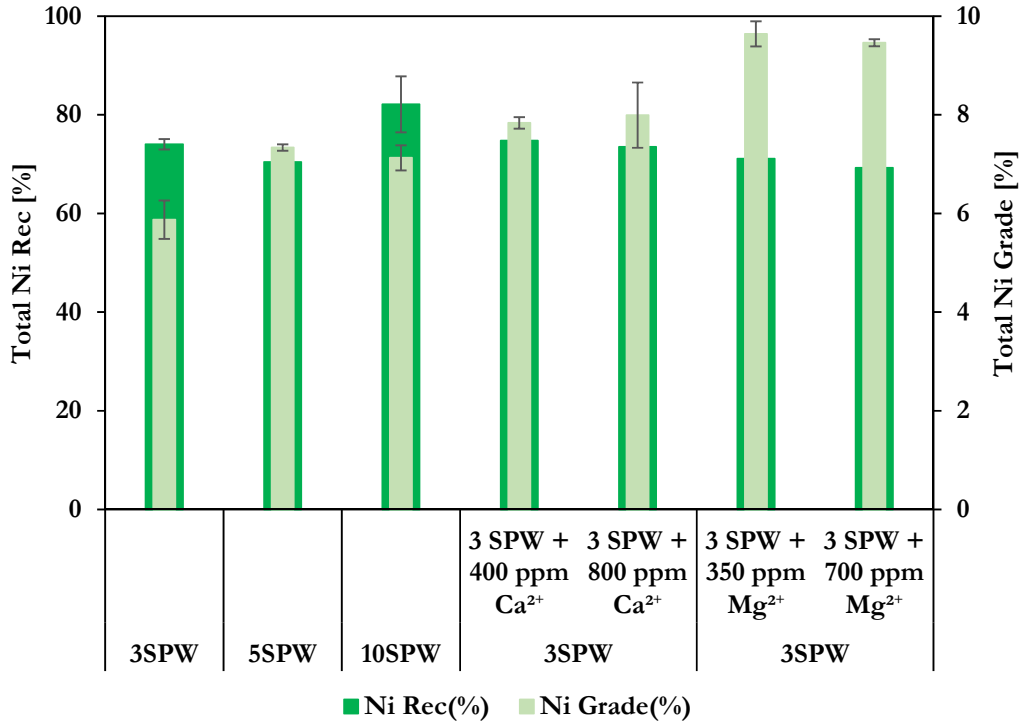

Figure 6-10 Final nickel recovery vs. grade at different cationic spiking concentrations

Overall, the recovery and grade of nickel is shown by **Figure 6-10**. As the concentration of Ca^{2+} ion increases, the nickel recovery is lower compared to 10 SPW but it is within the same region as 3 SPW slightly above 5 SPW. Furthermore, as spiking of Ca^{2+} ion concentration increased, nickel grade increased above that of 3, 5 and 10 SPW. 3 SPW shows the lowest nickel grade compared to the of Ca^{2+} ion grades. 350 and 700 ppm Mg^{2+} presents the highest final nickel grade compared to 3 SPW, 5 SPW, 10 SPW, 400 and 800 ppm Ca^{2+} spiking. **Table 6-8** shows the overall breakdown of nickel recovery and grade including its respective standard error values.

Table 6-8 Overall flotation cell nickel recovery-grade performance at different levels of cationic spiking concentrations including the std. error values

Water [I.S]	Spiking	Ni Rec [%]	Ni Rec [Std_Error]	Ni Grade [%]	Ni Grade [Std_Error]
3 SPW	-	74.0	1.1	5.9	0.4
5 SPW	-	70.4	2.3	7.3	0.1
10 SPW	-	82.1	5.7	7.1	0.3
3 SPW	400 ppm Ca^{2+}	74.8	1.2	7.8	0.1
	800 ppm Ca^{2+}	73.5	0.5	8.0	0.7
	350 ppm Mg^{2+}	71.1	1.5	9.6	0.3
	700 ppm Mg^{2+}	69.2	0.9	9.5	0.1

6.1 EC in 2-phase column studies upon spiking 3 SPW with Ca^{2+} and Mg^{2+}

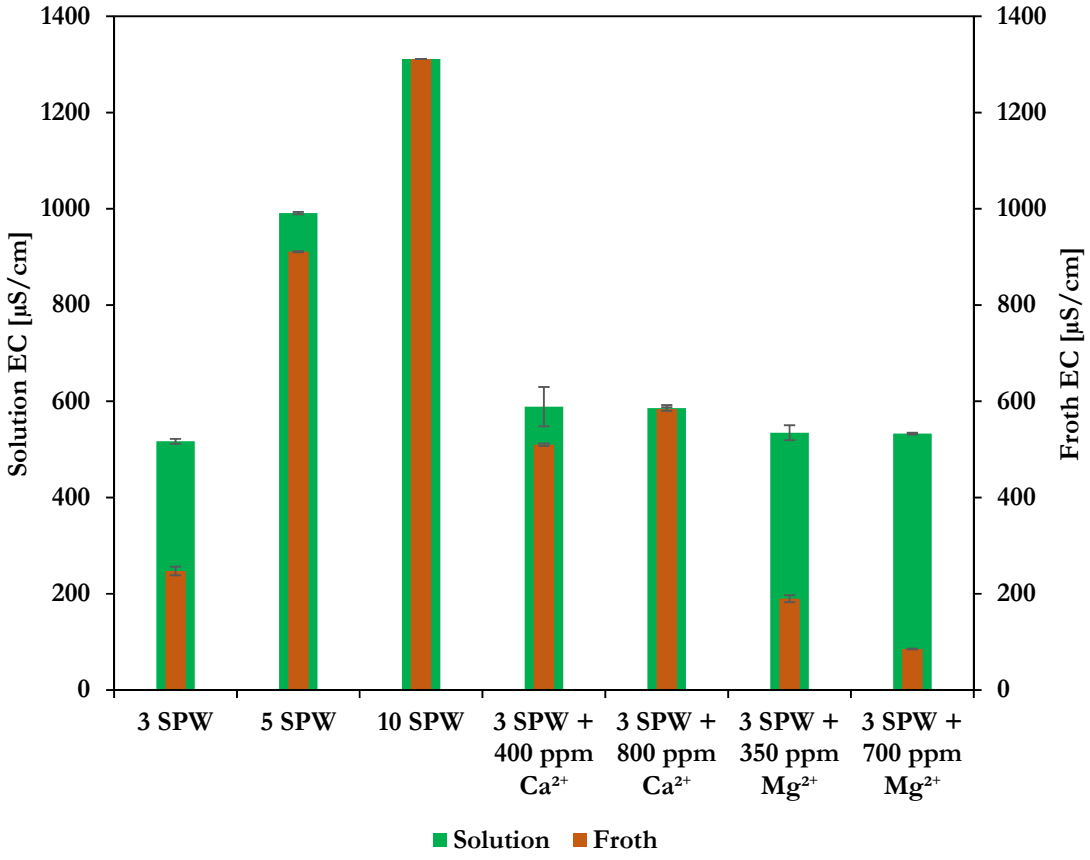

Figure 6-11 EC upon cation spiking in a 2-phase column study

Comparing the Ca^{2+} and Mg^{2+} ion spiking done on 3 SPW, it can be observed from **Figure 6-11** that spiking from 400 to 800 ppm Ca^{2+} ion concentration results in increased EC in the froth while the solution EC remains virtually the same. The Ca^{2+} and Mg^{2+} ion spiking shows lower EC compared to 5 and 10 SPW in solution and the froth. Spiking from 350 to 700 ppm with Mg^{2+} ion results in a significant decrease in froth EC compared to 3 SPW while the solution EC remains the same. The EC in the solution when spiking the Ca^{2+} and Mg^{2+} is the same as 3 SPW, the only variations is in the froth is seen.

6.2 EC in 3-phase column studies upon spiking 3 SPW with Ca^{2+} and Mg^{2+}

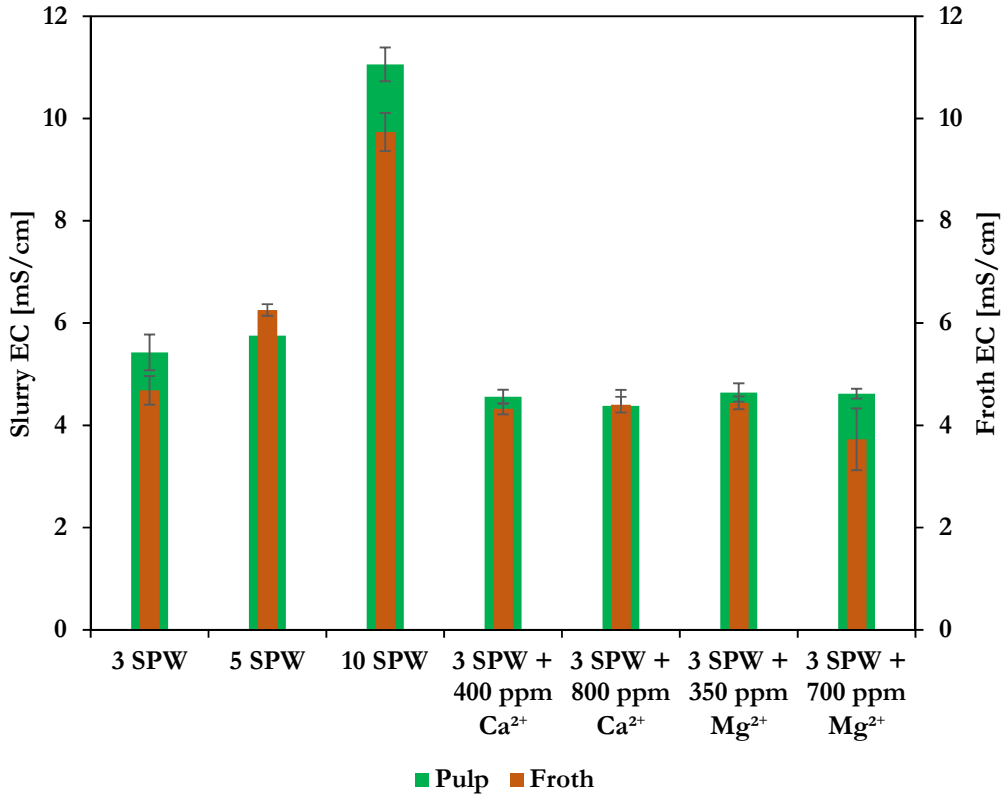

Figure 6-12 EC upon cation spiking in a 3-phase column study

Considering **Figure 6-12**, 400 and 800 ppm Ca^{2+}, and 350 ppm Mg^{2+}shows that the EC in the pulp phase is the same across the ion spiking. 700 ppm Mg^{2+}shows higher EC in the pulp phase than its froth phase.

6.3 Effect of EC on recovery upon spiking 3 SPW with Ca^{2+} and Mg^{2+}

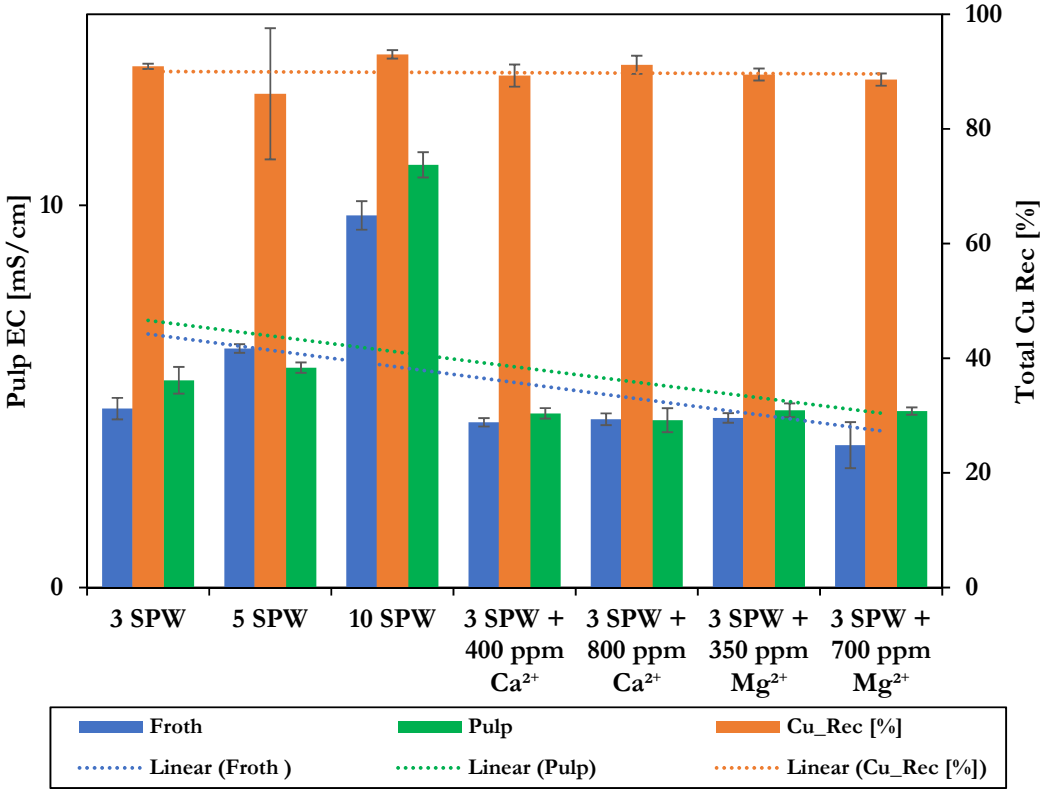

Figure 6-13 Copper recovery and EC relationship upon cationic concentration spiking

Copper recovery is almost constant throughout the flotation procedure, including when changing the water types. However, as the EC in the froth increases above the one in the pulp, copper recovery is impacted negatively as can be observed when using 5 SPW in **Figure 6-13**. When the EC between the froth and the pulp is similar, the recovery is not affected significantly. Spiking with 400 ppm Ca^{2+} results in a slightly high EC in the pulp phase and as such, the copper recovery at lower than 10 SPW and comparable to 3 SPW. At 800 ppm Ca^{2+} spiking, the EC between the froth and pulp phase is similar and the copper recovery increases above the 400 ppm Ca^{2+}. Spiking from 350 to 700 ppm Mg^{2+} results in decreased EC in the froth phase, much lower than 3, 5 and 10 SPW, however this doesn't seem to impact the copper recovery.

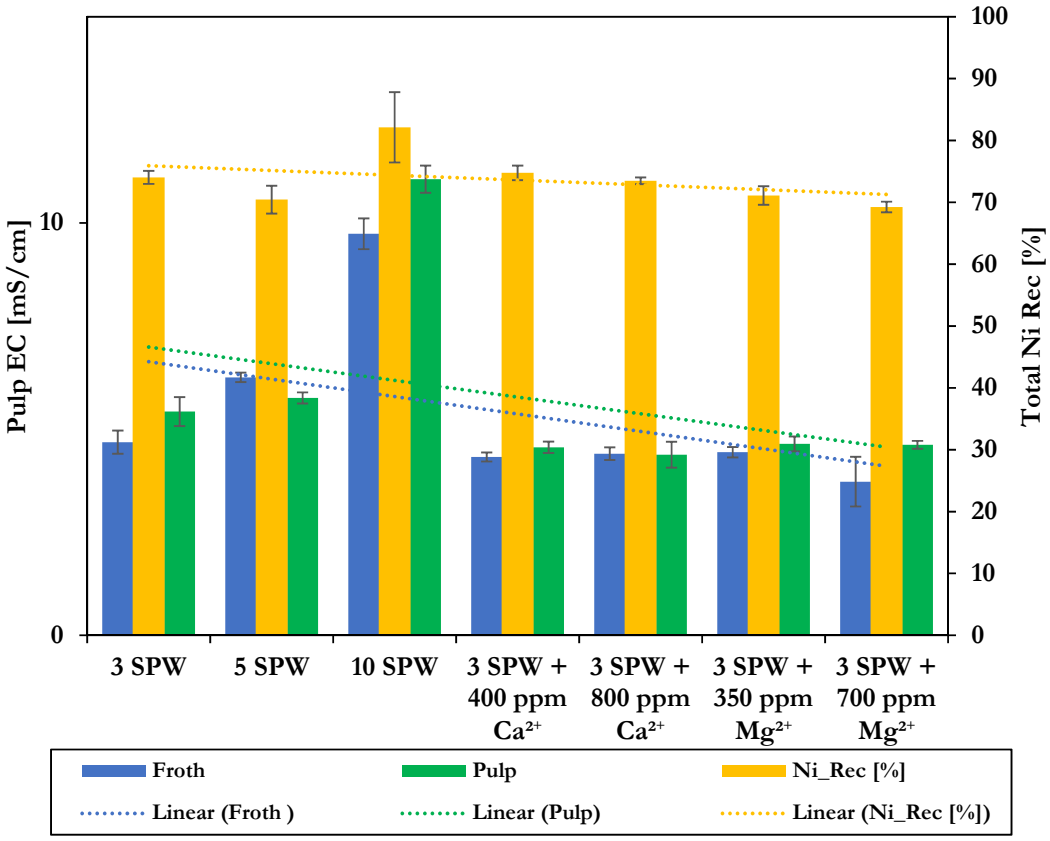

Figure 6-14 Nickel recovery and EC upon spiking with selected cations

Upon increasing the spiking concentration of the selected cations, there is a general decrease in nickel recovery as can be observed from **Figure 6-14**. Spiking from 400 to 800 ppm Ca^{2+} results in a slight increase in EC in the froth phase and at 800 ppm Ca^{2+} the EC in the froth phase is the same as in the pulp phase. This insignificantly reduces the nickel recovery. Increasing the ionic concentration of Mg^{2+} from 350 to 700 ppm results in decreased froth phase EC and this in turn shows reduced nickel recovery. At 700 ppm Mg^{2+} the difference in EC is more pronounces compared 350 ppm Mg^{2+}.

6.4 Statistical analysis on key variation on recovery and grade upon spiking 3 SPW with Ca^{2+} and Mg^{2+}

One-way Analysis of Means (ANOM) has a centre line referred to as the grand/overall mean (the average of the population parameters of interest) and two decision limits. From the graphs presented in this section, it is important to note that a statistical difference is significant if a point lies outside of the decision line (boundary-red lines). The confidence interval for this section is maintained at 95% meaning the grand mean is evaluated at $\alpha = 0.05$. α is defined as the likelihood of a true population parameter lying outside of the confidence interval, it is commonly expressed as a proportion.

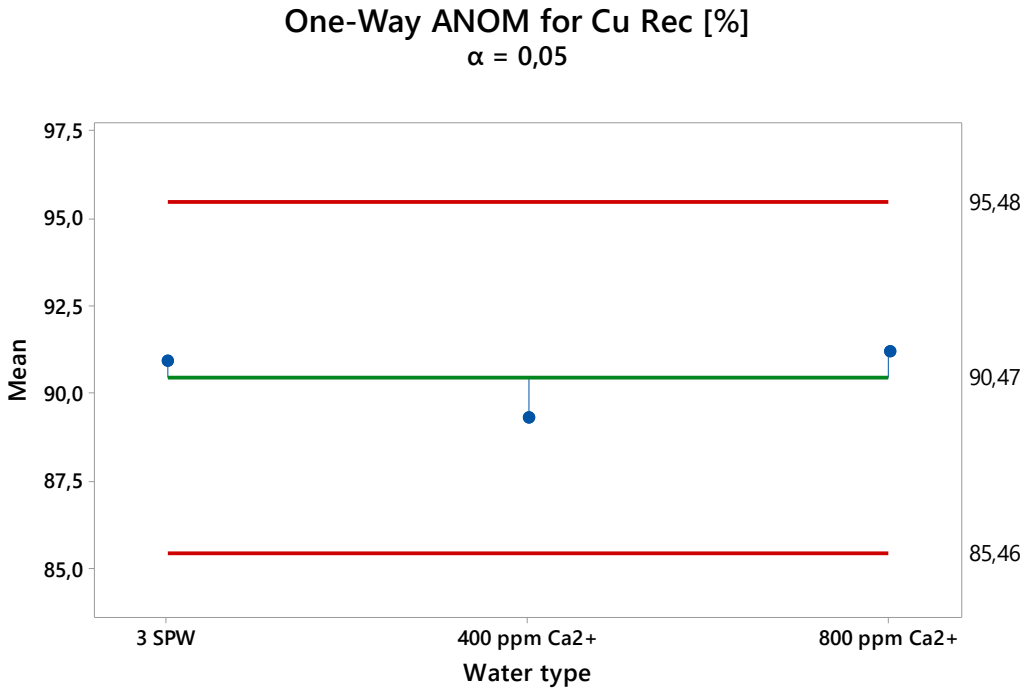

Figure 6-15 Statistical analysis on Ca^{2+} ion spiking on copper recovery

It can be observed from **Figure 6-15** that there is no statistical difference between 3 SPW, 400 and 800 ppm Ca^{2+} ion spiking on copper recovery as all the peak points are within the decision lines.

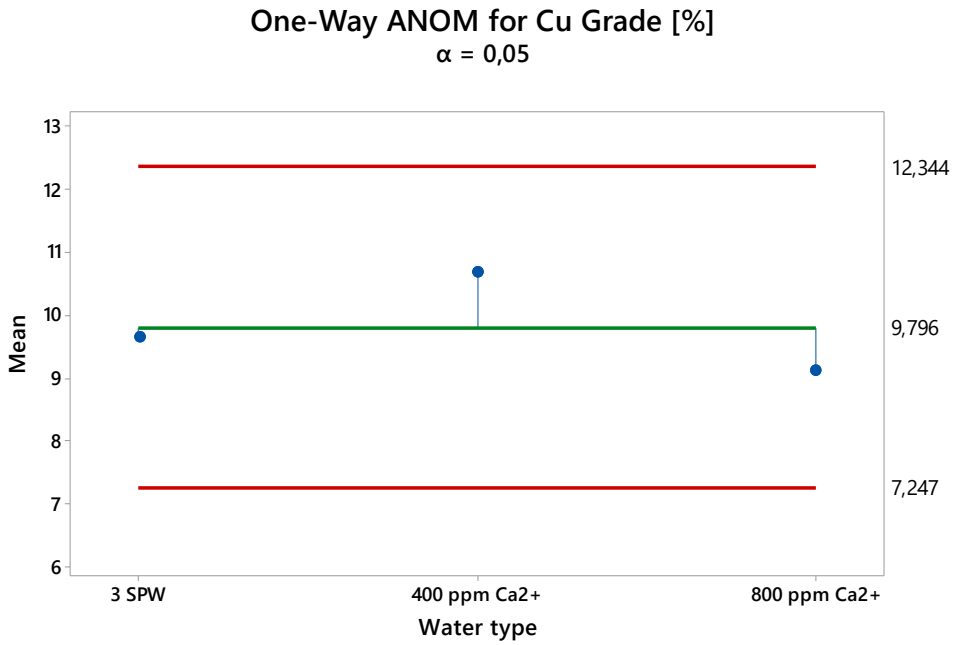

Figure 6-16 Statistical analysis on Ca^{2+} ion spiking on copper grade

Akin to copper recovery, copper grade at 3 SPW, 400 ppm Ca^{2+} and 800 ppm Ca^{2+} ion spiking shows no significant difference between each other as shown in **Figure 6-16**. The difference in recovery between 3 SPW, 400 ppm Ca^{2+} and 800 ppm Ca^{2+} shown in **Figure 6-5** is thus proved here to be insignificant.

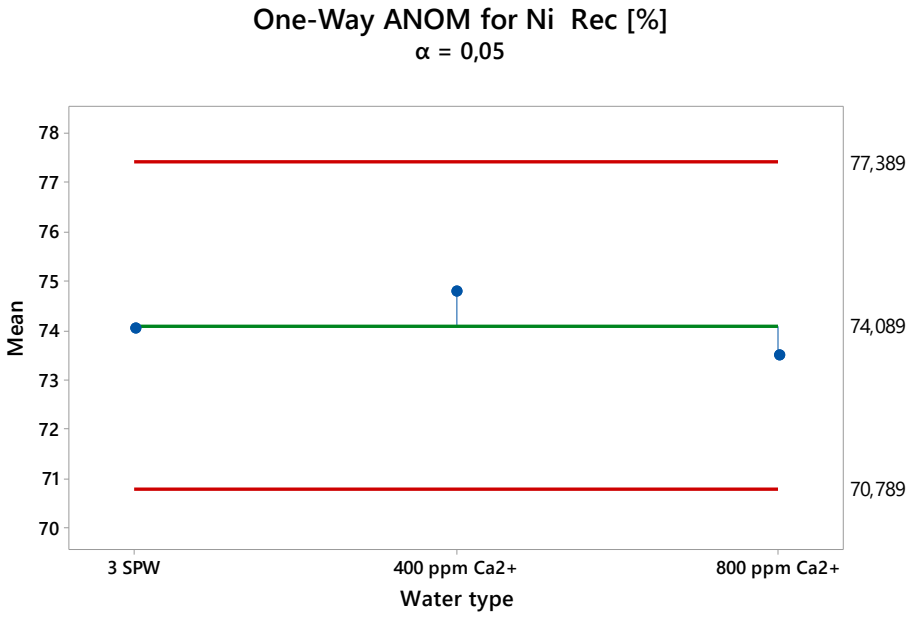

Figure 6-17 Statistical analysis on Ca^{2+} ion spiking on copper grade

As shown in **Figure 6-17,** Average 3 SPW nickel recovery is close to the grand mean however in comparison to the 400 ppm and 800 ppm Ca^{2+} ion spiking there is no considerable statistical difference on recovery upon Ca^{2+} spiking.

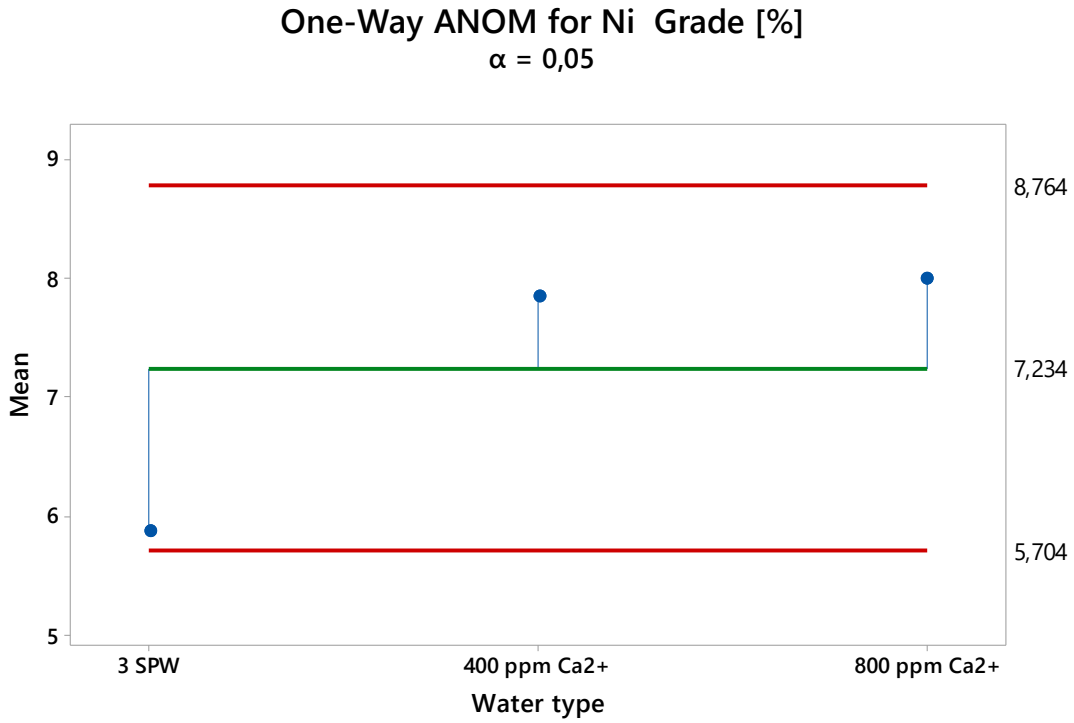

Figure 6-18 Statistical analysis on Ca^{2+} ion spiking on nickel grade

From **Figure 6-18**, the final nickel grade plots it shows that 3 SPW yields 5.9% while 400 ppm and 800 ppm Ca^{2+} yields 7.8% and 8.0% respectively. This however has been shown to be statistically insignificant; between the grades of 3 SPW, 400 ppm Ca^{2+} and 800 ppm Ca^{2+}, as all the means tested lie within the decision lines (95% confidence interval).

6.5 Key Findings upon spiking 3 SPW with Ca^{2+} and Mg^{2+}

- An increase from 350 to 700 ppm Mg^{2+} results in decreased water recovery
- 800 ppm Ca^{2+} spiking results in higher water recovery per solids recovery compared to 3 SPW, 5 SPW, 400 ppm Ca^{2+}, 350 ppm Mg^{2+}, 700 ppm Mg^{2+}
- Ca^{2+} spiking does not show any statistical difference with regards to recovery and grade of copper and nickel.
- In a 2-phase EC study, the EC of the solution is higher than that of the froth when 3 SPW is spiked with both Ca^{2+} and Mg^{2+}.
- In a 3-phase EC study, 400 ppm Ca^{2+}, 350 ppm Mg^{2+} and 700 ppm Mg^{2+}show higher EC in the pulp phase than the froth phase while 800 ppm Ca^{2+} shows that the EC in the pulp is equal to that of the froth.
- As the EC in the froth increases to levels higher than that in the pulp phase, copper and nickel recovery is negatively impacted; this is the case with 5 SPW.
- There is no statistical difference between recovery and grade; for copper and nickel comparing 3 SPW, 400 ppm Ca^{2+} and 800 ppm Ca^{2+}

7 FLOTATION RESPONSE UPON SPIKING 3 SPW WITH: SO_4^{2-}, NO_3^- AND $S_2O_3^{2-}$

The previous section (**Section 6**) dealt with assessing the effect cationic spiking on the flotation performance (Ca^{2+} and Mg^{2+}). This section (**Section 7**) deals with the effect of spiking 3 SPW with SO_4^{2-}, NO_3^- and $S_2O_3^{2-}$ to the levels of 5 and 10 SPW (as shown in **Table 7-1**). The spiked response is then compared to 3 SPW.

Table 7-1 Type of water quality used and its accompanying anionic spiking levels

	Water type	Ca^{2+} (ppm)	Mg^{2+} (ppm)	Na^+ (ppm)	Cl^- (ppm)	SO_4^{2-} (ppm)	$S_2O_3^{2-}$ (ppm)	NO_3^- (ppm)	NO_2^- (ppm)	CO_3^{2-} (ppm)	TDS (mg/L)	I.S [M]
	3 SPW	240	210	459	861	720	-	528	-	51	3069	0.073
	5 SPW	400	350	765	1435	1200	-	880	-	85	5115	0.121
	10 SPW	800	700	1530	2870	2400	-	1760	-	170	10230	0.242
5 SPW	Na_2SO_4	240	210	647.2	861	**1200**	-	528	-	51	3737	0.087
10 SPW	Na_2SO_4	240	210	1117.8	861	**2400**	-	528	-	51	5408	0.122
5 SPW	$NaNO_3$	240	210	772.3	861	720	-	**880**	-	51	3734	0.082
10 SPW	$NaNO_3$	240	210	1554.6	861	720	-	**1760**	-	51	5397	0.106
5 SPW	$Na_2S_2O_3$	240	210	479.3	861	720	**60**	528	-	51	3149	0.074
10 SPW	$Na_2S_2O_3$	240	210	485.4	861	720	**78**	528	-	51	3173	0.075

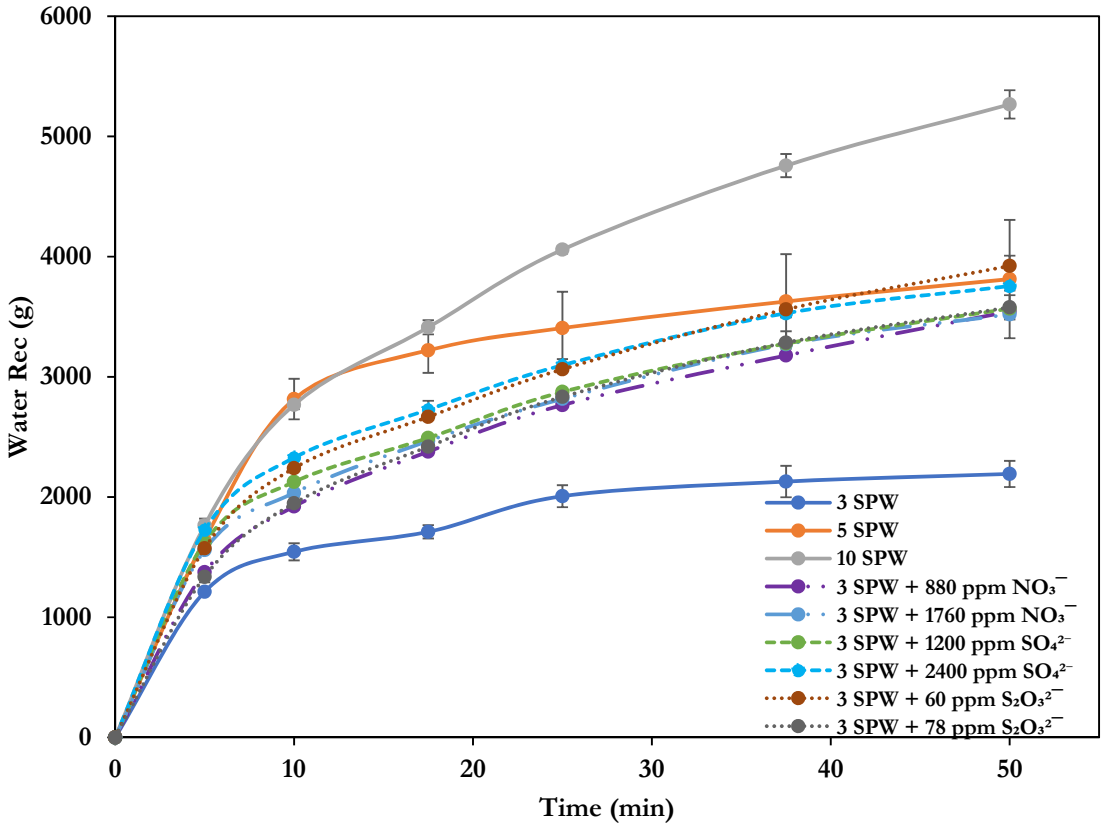

Figure 7-1 Water recovery per flotation time at different anionic concentration spiking

The water recovery upon spiking of selected anions is found to lie between 3 and 5 SPW, **Figure 7-1**. The spiked anions exhibit higher water recoveries compared to 3 SPW. 2400 ppm SO_4^{2-} and 60 ppm $S_2O_3^{2-}$ ion spiking have comparable water recoveries above and at the end of flotation, they have the same cumulative water recovery as 5 SPW. 880 ppm NO_3^-, 1760 ppm NO_3^-, 1200 ppm SO_4^{2-} and 78 ppm $S_2O_3^{2-}$ ion spiking recovers water in the same range by the end of flotation.

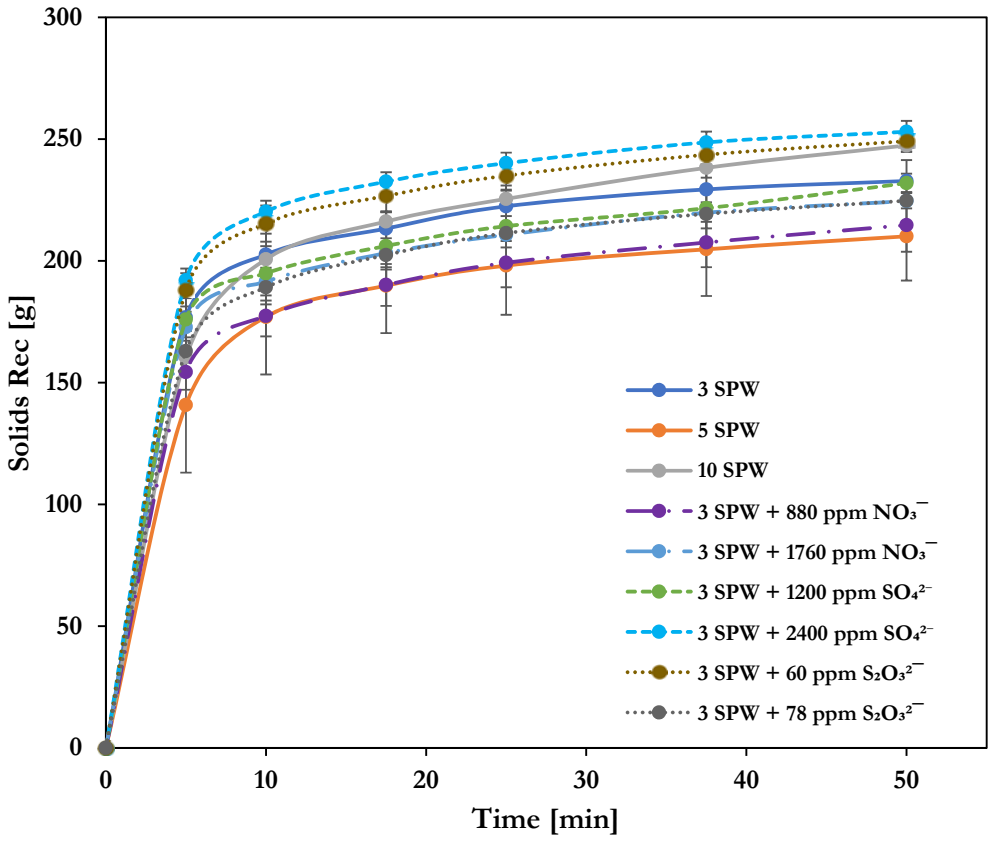

Figure 7-2 Solids recovered per unit flotation during anionic spiking

From **Figure 7-2**, the SO_4^{2-} ion spiked to 2400 ppm pulls more solids than 3, 5 and 10 SPW, while 5 SPW pulls the least solids. 880 ppm NO_3^- recovers solids comparable to 5 SPW while 1200 ppm SO_4^{2-}, 1760 ppm NO_3^- and 78 ppm $S_2O_3^{2-}$ recovers almost the same amount of solids by the end of flotation. 60 ppm $S_2O_3^{2-}$ ion spiking recovers more solids than 10 SPW despite having lower ionic strength than 10 SPW.

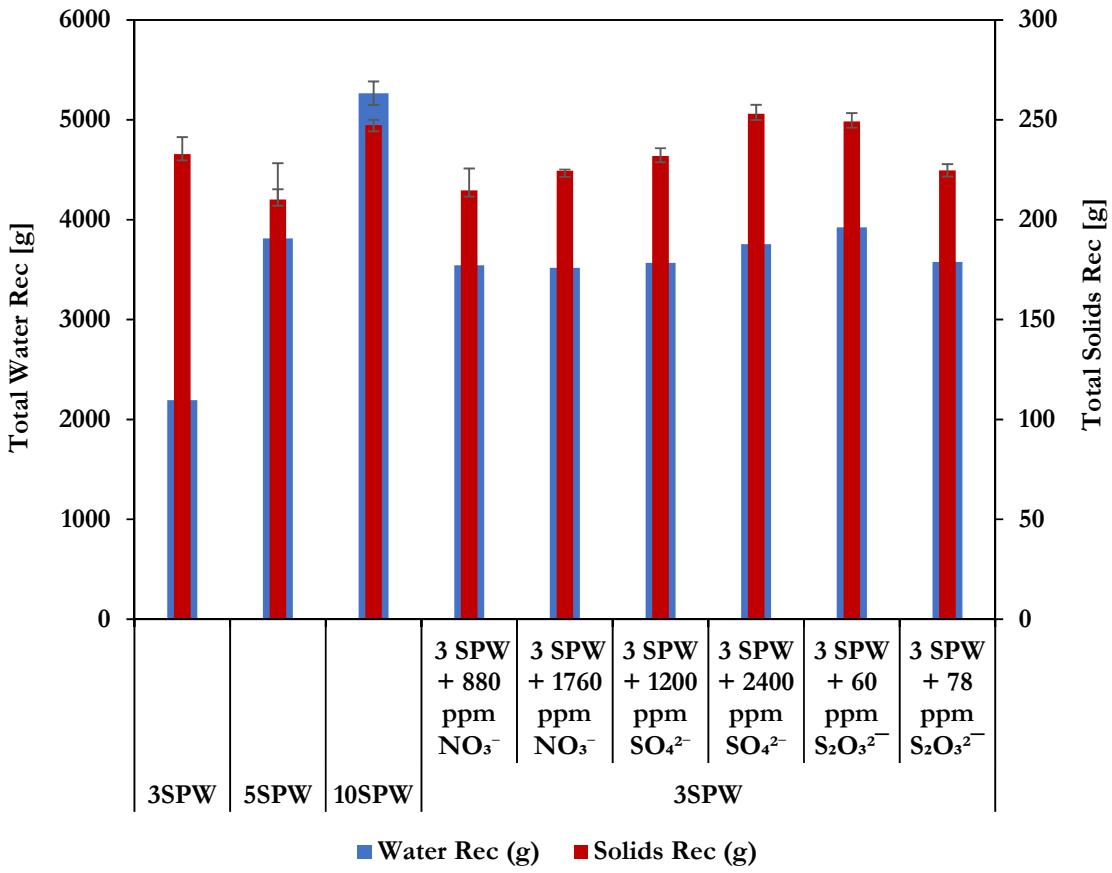

Figure 7-3 Final water recovery vs. solids recovery at different levels of anionic spiking.

Upon spiking of the selected anions, water recovery and mass pull varied. Spiking $S_2O_3^{2-}$ at 60 ppm pulls a lot more water than the other anions and it has higher mass pull compared to that recovered by spiking $S_2O_3^{2-}$ ion at 78 ppm. The variations are shown in **Table 7-2** including the standard error and depicted in **Figure 7-3.** 10 SPW recovers more water compared to the anions despite the anions being spiked to the levels of 5 and 10 SPW. 10 SPW, 2400 ppm SO_4^{2-} and 60 ppm $S_2O_3^{2-}$ pulls solids that are comparable to each other besides not having a correlation in terms of the water recovered. 880 ppm NO_3^-, 1760 ppm NO_3^- and 1200 ppm SO_4^{2-} recovers almost the same amount of water while of these ions' spiking 3 SPW with 1200 ppm SO_4^{2-} pulls more solids. NO_3^-, SO_4^{2-} and $S_2O_3^{2-}$ pulls a lot more water compared to 3 SPW; the baseline experiment. 5 SPW pulls almost the same amount of solids compared to 880 ppm NO_3^- besides having it recovering more water compared to 880 ppm NO_3^- ion spiking.

Table 7-2 Overall mass pull per water recovered at different levels of anionic concentration including the std. error values

Water [I.S]	Spiking	Solids Rec [g]	Solids Rec [Std_Error]	Water Rec [g]	Water Rec [Std_Error]
3 SPW	-	232.8	8.6	2192.0	109
5 SPW	-	210.1	18.2	3813.0	492
10 SPW	-	247.4	2.7	5266.4	117.7
3 SPW	880 ppm NO_3^-	214.7	11.0	3544.0	301.8
	1760 ppm NO_3^-	224.6	0.6	3520.0	125.2
	1200 ppm SO_4^{2-}	231.9	3.9	3567.5	0.8
	2400 ppm SO_4^{2-}	253.0	4.5	3755.1	37.3
	60 ppm $S_2O_3^{2-}$	249.2	4.2	3922.7	85.2
	78 ppm $S_2O_3^{2-}$	224.7	3.1	3578.1	100.9

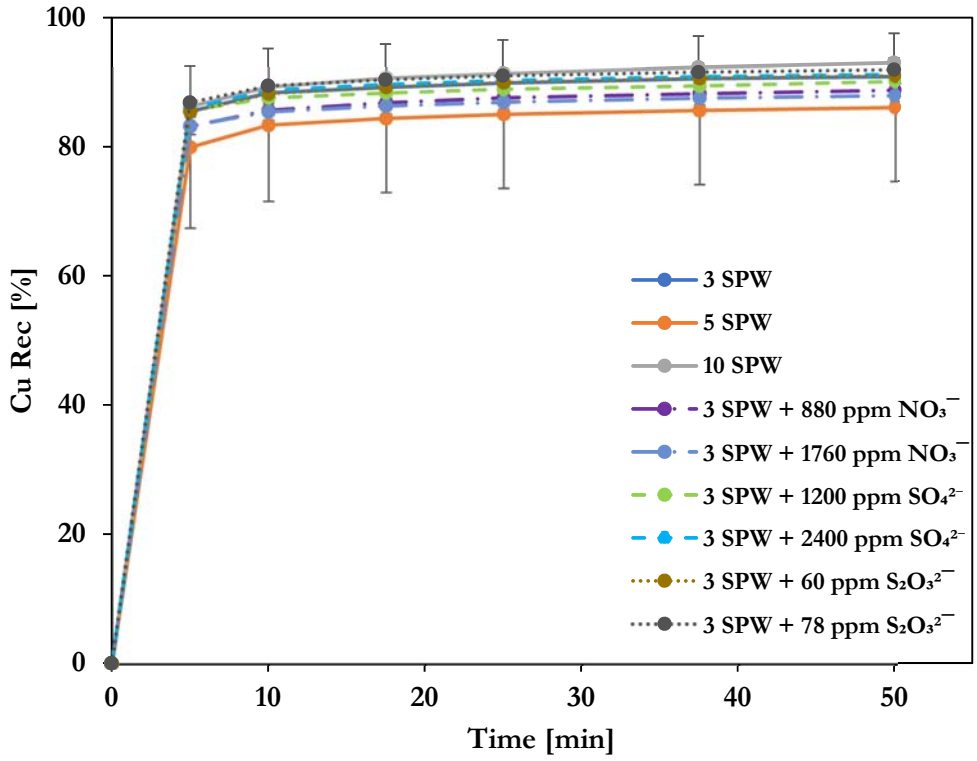

Figure 7-4 Copper recovery per unit flotation time

The copper recovery of the anions is highest at 10 SPW with 5 SPW recovering the lowest copper recovery and all other tests lying between them. As the concentration of NO_3^- increased from 880 to 1760 ppm, the recovery of copper increased slightly from 88% to 88.8% which is not a significant change. As can be seen from **Figure 7-2,** that; while spiking SO_4^{2-} from 1200 ppm to 2400 ppm results in increased recovery from 90.2 to 91.3%. Furthermore, spiking $S_2O_3^{2-}$ from 60 ppm to 78 ppm resulted in increased recovery slightly from 91% to 91.9%.

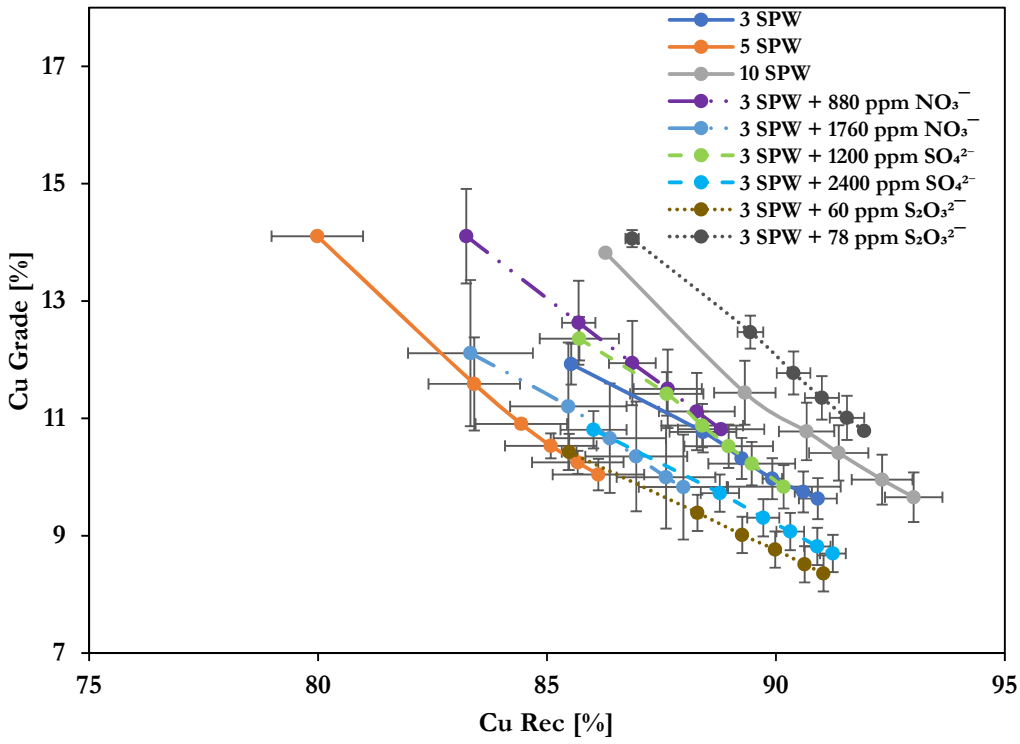

Figure 7-5 Copper grade per copper concentrate recovered at varying anionic concentration (note the axis range has been shortened for clarity the y-axis shows 7-18% Cu Grade while the x-axis shows 75-95% Cu Recovery)

From **Figure 7-5,** the general trend is that; as the copper recovery increases, the grade decreases. The NO_3^- at 880 ppm yields the same grade as 78 ppm $S_2O_3^{2-}$ at 10.8 %. Increasing the ionic concentration of SO_4^{2-} from 1200 ppm to 2400 ppm results in decreased copper grade.

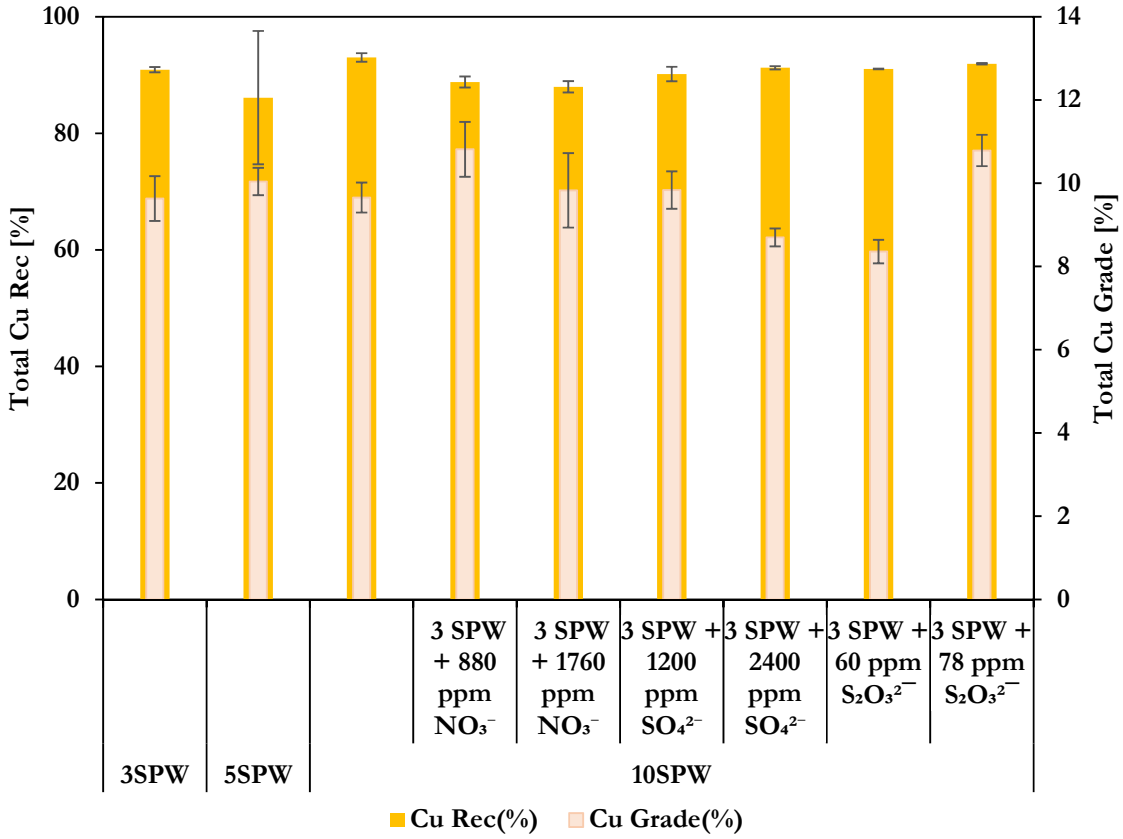

Figure 7-6 Final copper recovery vs. grade at different levels of anionic spiking concentration

As can be observed from **Figure 7-6**, spiking affects grade mostly, but the overall recovery is slightly affected but not significantly. 10 SPW returns the highest overall copper recovery at 93 %. The generalized effect of the anionic spiking is that; upon increasing the concentration, the recovery is virtually the same while grade is positively impacted especially in the case of $S_2O_3^{2-}$ ion. Spiking the $S_2O_3^{2-}$ ion from 60 ppm to 78 ppm results in increase in grade from 8.4 to 10.8 %.

Table 7-3 Overall copper recovery and grade at different anionic concentration levels including the std. error values

Water (I.S)	Spiking	Cu Rec [%]	Cu Rec [Std_Error]	Cu Grade [%]	Cu Grade [Std_Error]
3SPW	-	90.9	0.5	9.6	0.5
5SPW	-	86.1	11.4	10.0	0.3
10SPW	-	93.0	0.7	9.7	0.4
3 SPW	880 ppm NO_3^-	88.8	0.9	10.8	0.7
	1760 ppm NO_3^-	88.0	1.0	9.8	0.9
	1200 ppm SO_4^{2-}	90.2	1.2	9.8	0.5
	2400 ppm SO_4^{2-}	91.3	0.3	8.7	0.2
	60 ppm $S_2O_3^{2-}$	91.0	0.1	8.4	0.3
	78 ppm $S_2O_3^{2-}$	91.9	0.1	10.8	0.4

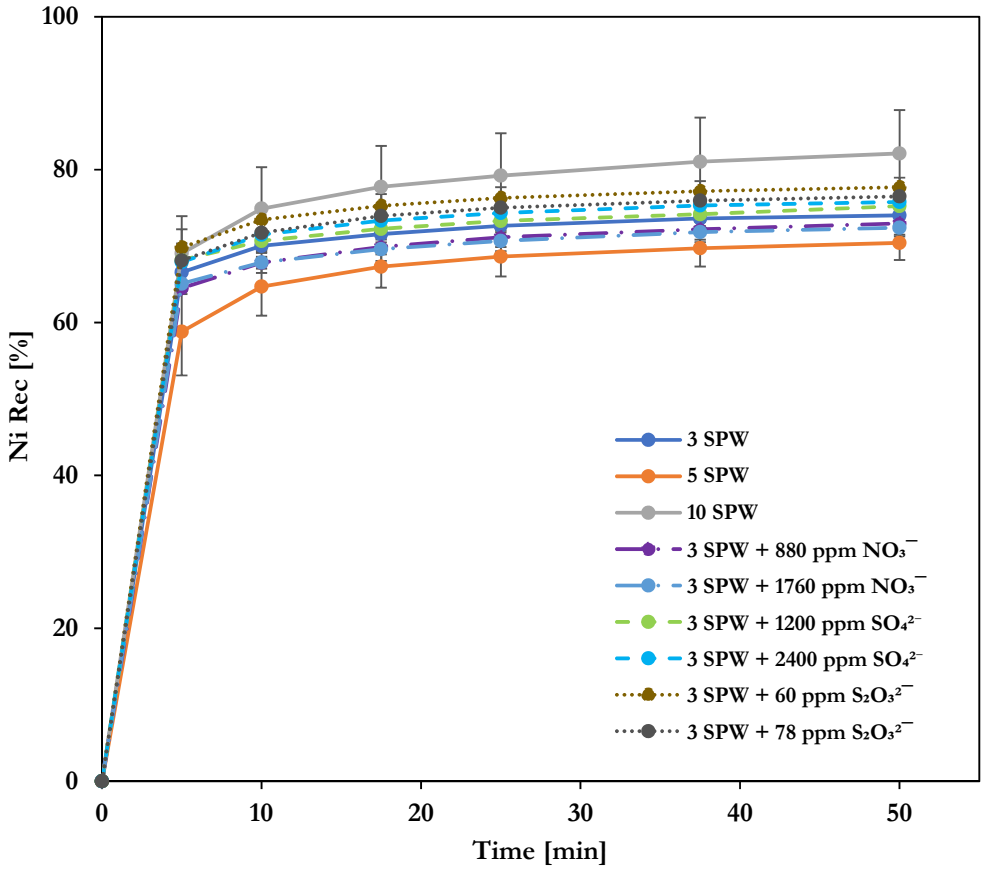

Figure 7-7 Nickel recovery per unit flotation time at different anionic concentrations

Nickel metal recovery kinetics is fast within the first 10 minutes of flotation as shown in **Figure 7-7**, however 5 SPW gives the lowest nickel cumulative recovery per unit flotation time at 70.43%. 10 SPW gives the highest recovery (82.12 %) per unit time. Spiking results in recoveries of nickel lying between 5 and 10 SPW.

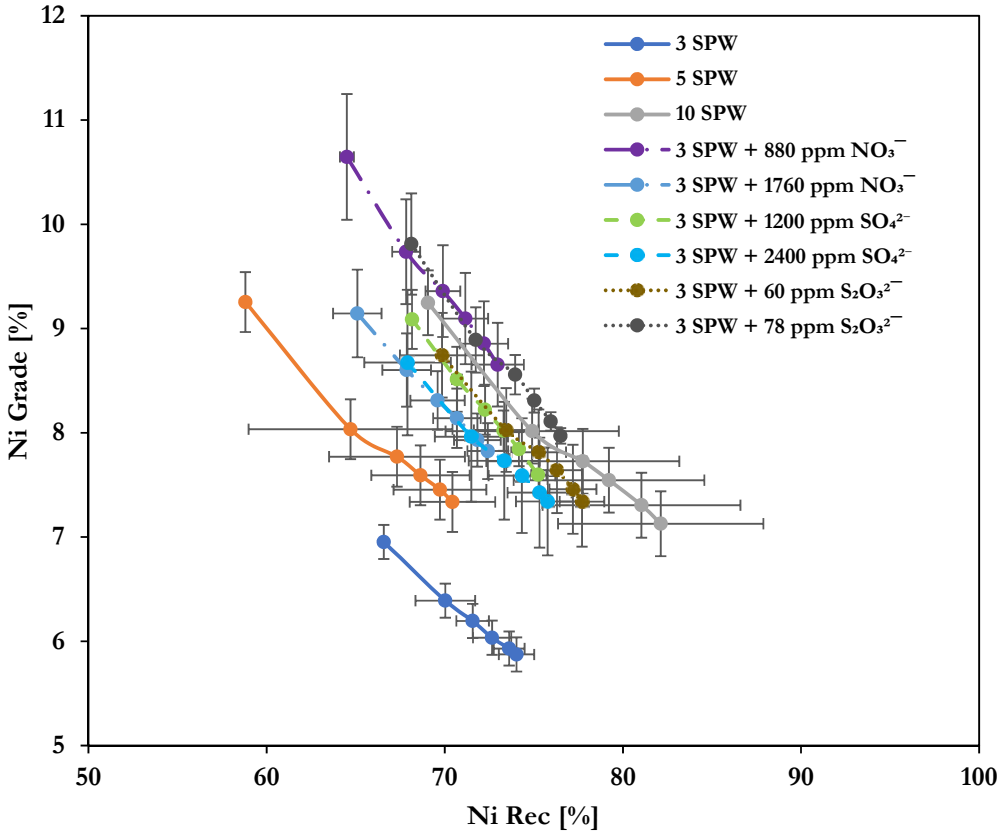

Figure 7-8 Nickel grade per concentrate recovered (note the axis range has been shortened for clarity the y-axis shows 5-12% Ni Grade while the x-axis shows 50-100% Ni Recovery)

Figure 7-8 shows that the NO_3^- concentration spiking at 880 ppm has the highest grade of 8.65% while 3 SPW has 5.87%. This means that the NO_3^- ion improves the flotation performance over that of 3 SPW with a marginal change in recovery (74.03%) in comparison to NO_3^- spiking at 880 ppm (72.97%).

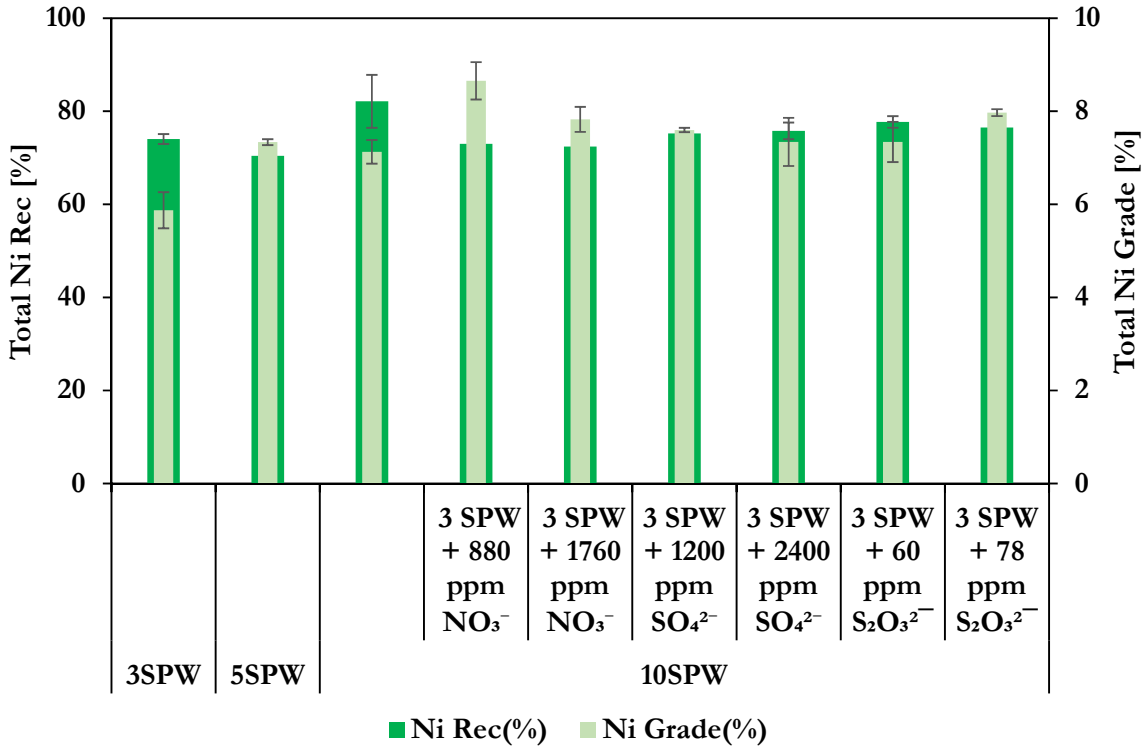

Figure 7-9 Final nickel recovery vs. grade at different anionic concentration

Figure 7-9 shows no significant effect with regards to recovery of nickel when SO_4^{2-} anionic concentration is spiked to 1200 ppm and 2400 ppm respectively. There is no much significant change in recovery when NO_3^- is spiked to 880 ppm and 1760 ppm NO_3^- respectively. However, 880 ppm NO_3^- spiking shows the highest grade. **Table 7-4** shows that 3 SPW gives recoveries higher than spiking at 880 ppm and 1760 ppm NO_3^-, despite their higher grade. $S_2O_3^{2-}$ spiking gives recoveries higher than 5 SPW but lower than 10 SPW.

Table 7-4 Overall effect of the anionic concentration spiking on nickel flotation performance including the std. error values

Water (I.S)	Spiking	Ni Rec [%]	Ni Rec [Std_Error]	Ni Grade [%]	Ni Grade [Std_Error]
3 SPW	-	74.03	1.1	5.87	0.4
5 SPW	-	70.43	2.3	7.34	0.1
10 SPW	-	82.12	5.7	7.13	0.3
3 SPW	880 ppm NO_3^-	72.97	1.5	8.65	0.4
	1760 ppm NO_3^-	72.41	1.1	7.82	0.3
	1200 ppm SO_4^{2-}	75.24	0.5	7.60	0.1
	2400 ppm SO_4^{2-}	75.78	1.8	7.34	0.5
	60 ppm $S_2O_3^{2-}$	77.70	1.3	7.34	0.4
	78 ppm $S_2O_3^{2-}$	76.50	0.2	7.97	0.1

7.1 EC in 2-phase column studies upon spiking 3 SPW with SO_4^{2-}, NO_3^- and $S_2O_3^{2-}$

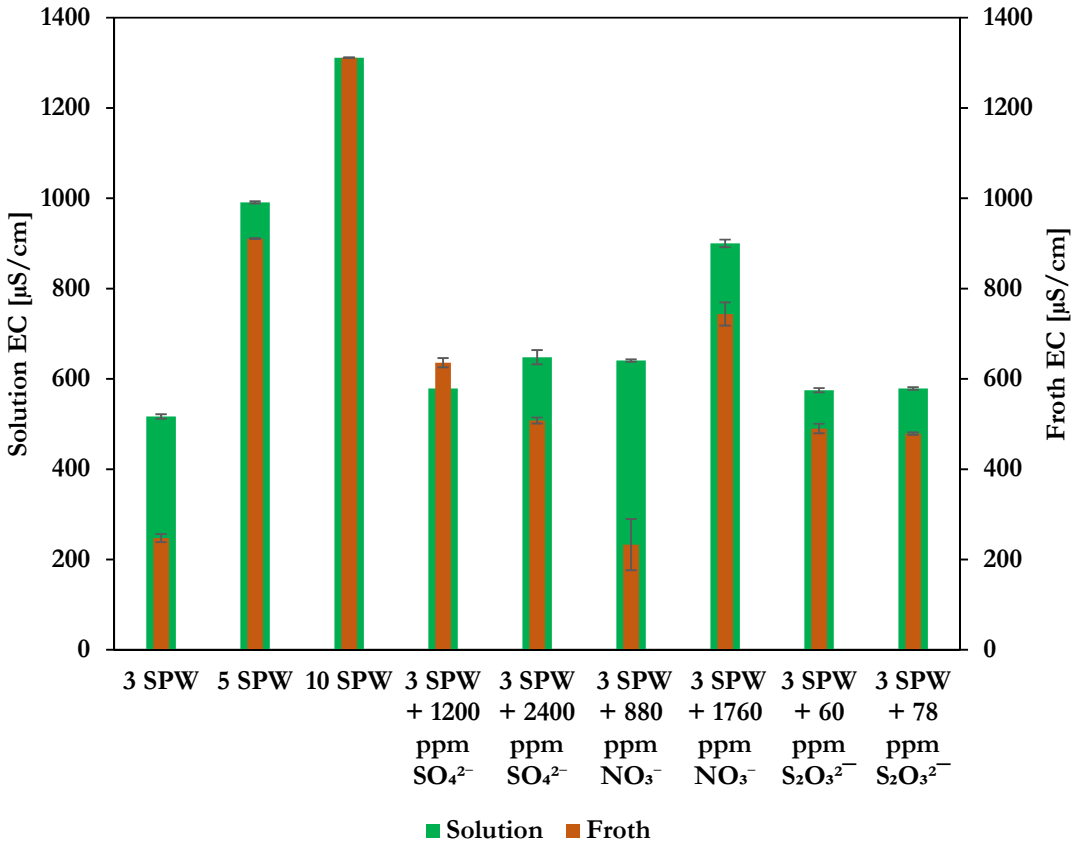

Figure 7-10 EC between the froth and solution upon anionic concentration spiking

Figure 7-10 shows that upon spiking with the selected anions, NO_3^- at 880 ppm gives the highest difference between the EC in solution and froth phase while spiking with 1200 ppm SO_4^{2-} results in a slightly higher EC in the froth than the solution. 60 and 78 ppm $S_2O_3^{2-}$ spiking result in the same EC between the froth and solution. Spiking from 880 to 1760 ppm NO_3^- concentration results in the highest difference between the EC in the froth. 3 SPW shows comparable EC with 880 ppm NO_3^- ion concentration in the froth.

7.2 EC in 3-phase column studies upon spiking 3 SPW with SO_4^{2-}, NO_3- and $S_2O_3^{2-}$

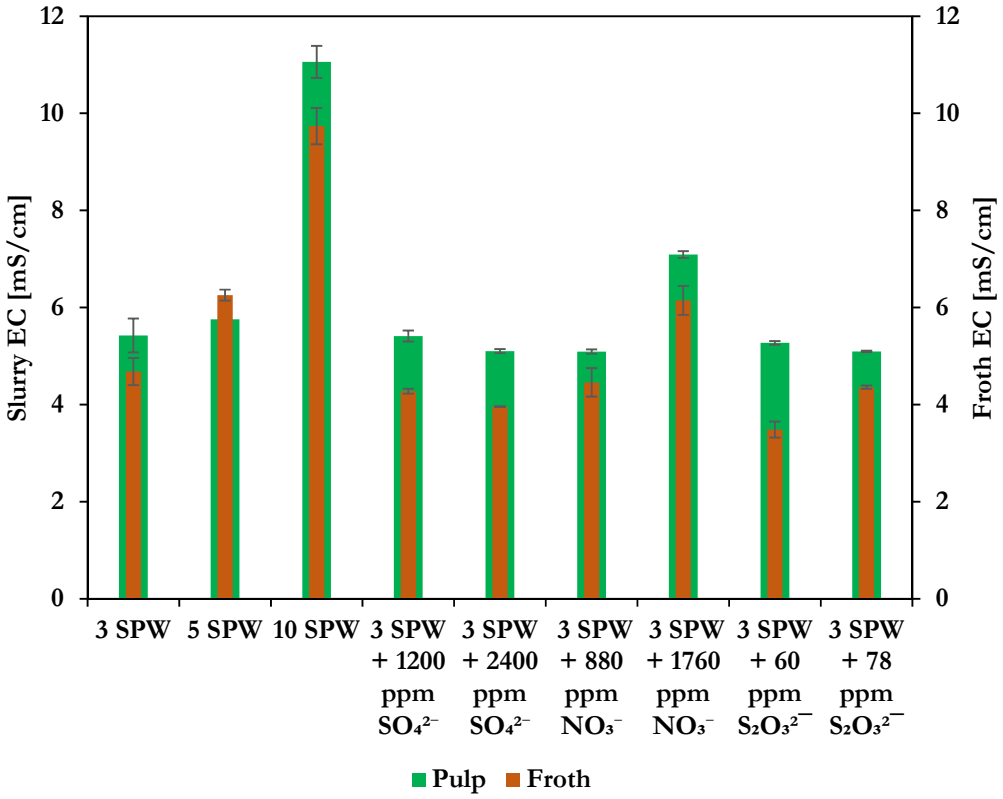

Figure 7-11 EC upon anionic spiking in a 3-phase column study

The general trend observed from **Figure 7-11**, the EC in the pulp phase is higher than the EC through all the anionic spiking concentrations. Spiking from 1200 ppm SO_4^{2-} to 2400 ppm SO_4^{2-} results in a decreased EC in the froth phase accompanied with a slight decrease in EC in the pulp phase. Spiking from 880 ppm NO_3^- to 1760 ppm NO_3^- results in a considerable difference in the EC in the pulp phase, a similar trend is observed for its EC in the pulp phase. From 60 ppm $S_2O_3^{2-}$ to 78 ppm $S_2O_3^{2-}$ the EC in the froth phase increases while that in the pulp phase remains almost the same.

7.3 Effect of EC on recovery upon spiking 3 SPW with SO_4^{2-}, NO_3^- and $S_2O_3^{2-}$

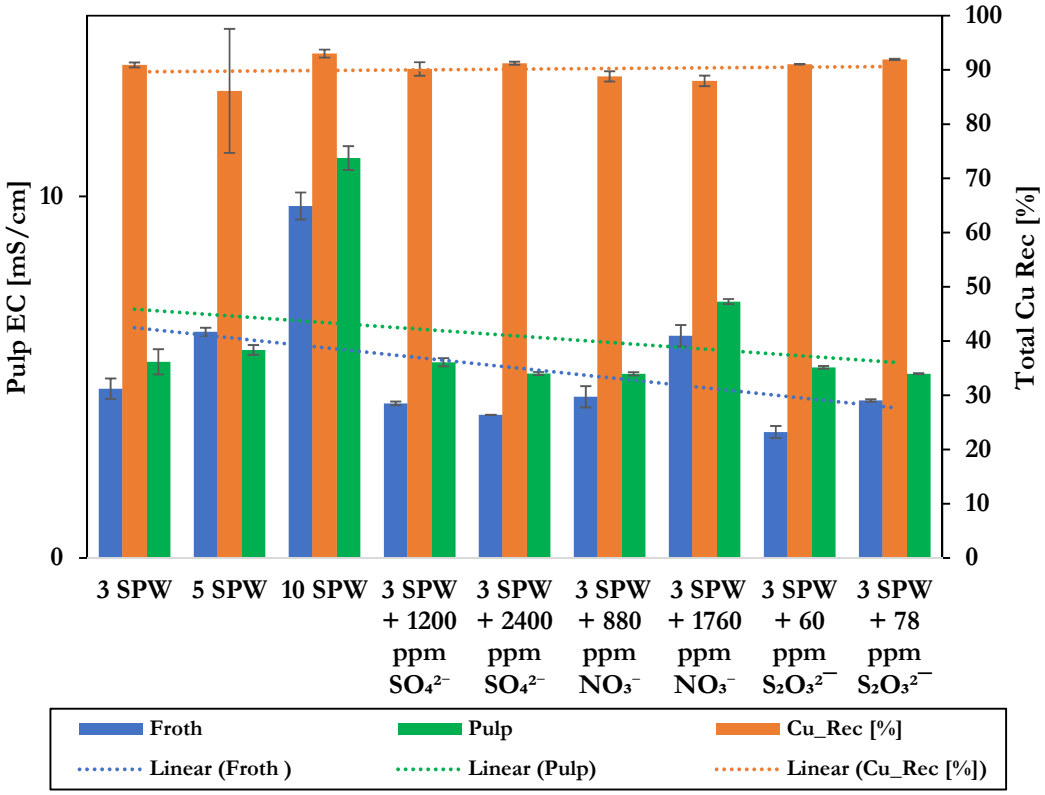

Figure 7-12 Copper recovery and EC relationship upon anionic concentration spiking

Throughout anionic spiking of the selected ions, the EC in the froth phase is shown to be lower than the pulp phase as shown in **Figure 7-12**. 1760 ppm NO_3^- shows copper recoveries similar to 5 SPW despite 5 SPW having a high EC in the froth phase. 60 ppm $S_2O_3^{2-}$ shows a big difference in EC between the froth phase and the pulp phase compared to 78 ppm but it exhibits slightly lower copper recovery. 2400 ppm SO_4^{2-} shows a copper recovery comparable to 78 ppm $S_2O_3^{2-}$ despite having a slightly higher difference in conductivity between the froth and pulp.

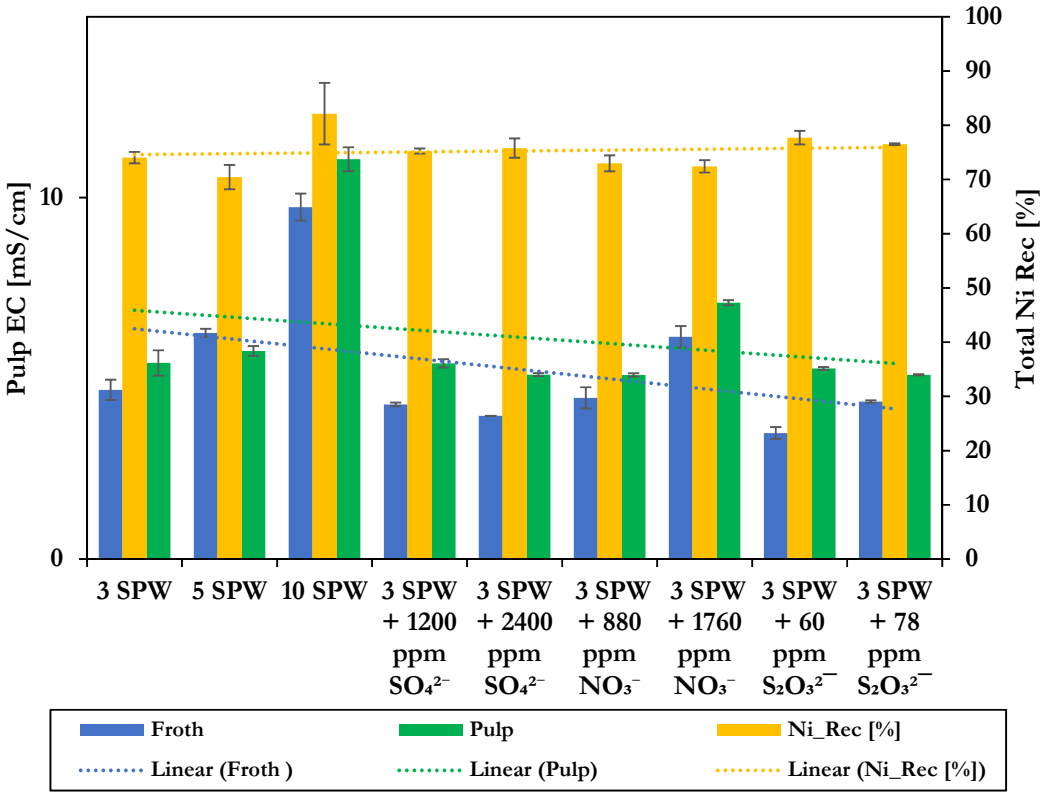

Figure 7-13 Nickel recovery and EC upon spiking with selected anions

Figure 7-13 shows the total recovery of copper and nickel upon selected ions concentration spiking. Upon spiking with the selected anions, the EC in the froth phase is lower than in the pulp phase across all the anions under investigation. Spiking from 1200 ppm to 2400 ppm SO_4^{2-} results in the same EC difference between the froth and pulp phase, and the nickel recovery is not significantly affected. Increasing the concentration from 880 ppm to 1760 ppm NO_3^- results in the same nickel recovery and exhibits the same difference between the pulp and froth phase. Spiking at 60 ppm $S_2O_3^{2-}$ results in better nickel recovery than 78 ppm $S_2O_3^{2-}$. The general trend with regards to EC is that the pulp EC is always higher than the froth EC for all the other conditions besides for 5 SPW. The increase in conductivity of the froth phase above that of the pulp phase in 5 SPW is followed by an anomalous behaviour in nickel recovery as it decreases.

7.4 Statistical analysis on key variation on recovery and grade upon spiking 3 SPW with SO_4^{2-}, NO_3^- and $S_2O_3^{2-}$

Only data that was considered worthy of further analysis is considered in this section.

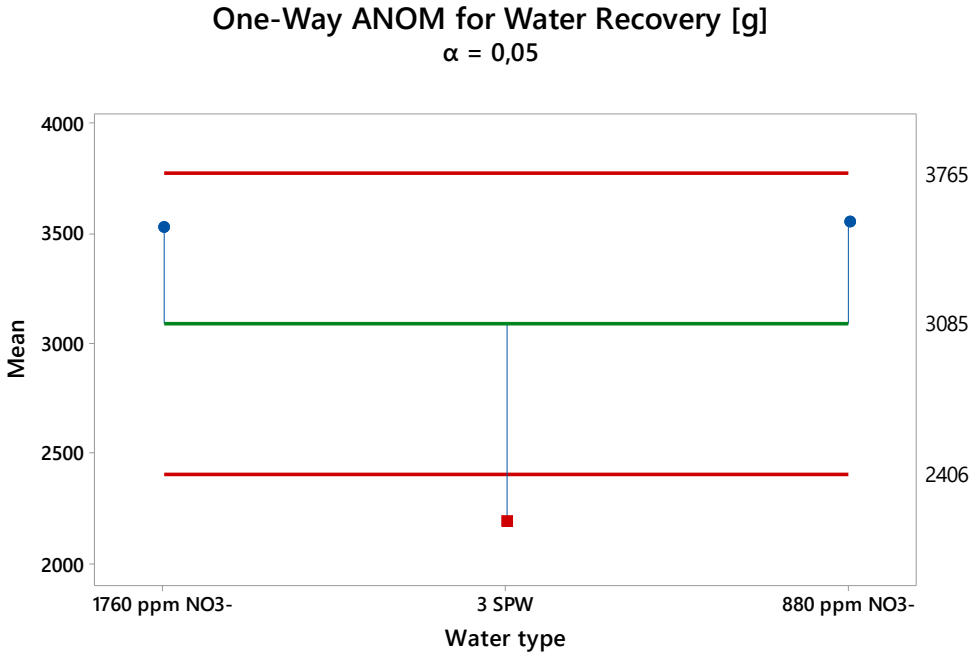

Figure 7-14 Statistical analysis on water recovery for NO_3^- spiking vs. 3 SPW

Figure 7-14 shows statistical analysis after spiking 3 SPW with 880 and 1760 ppm NO_3^- ion results in significant differences with regards to water recovery. The graph shows that 3 SPW lies outside the lower decision line and this proves **Figure 7-1** that there is a statistical difference between 3 SPW and the NO_3^- spiking. It can be noted however from the graph that there is no significant difference between the NO_3^- ion spiking at 880 ppm and 1760 ppm as they are within the boundary decision lines; however, the difference is apparent when compared to 3 SPW.

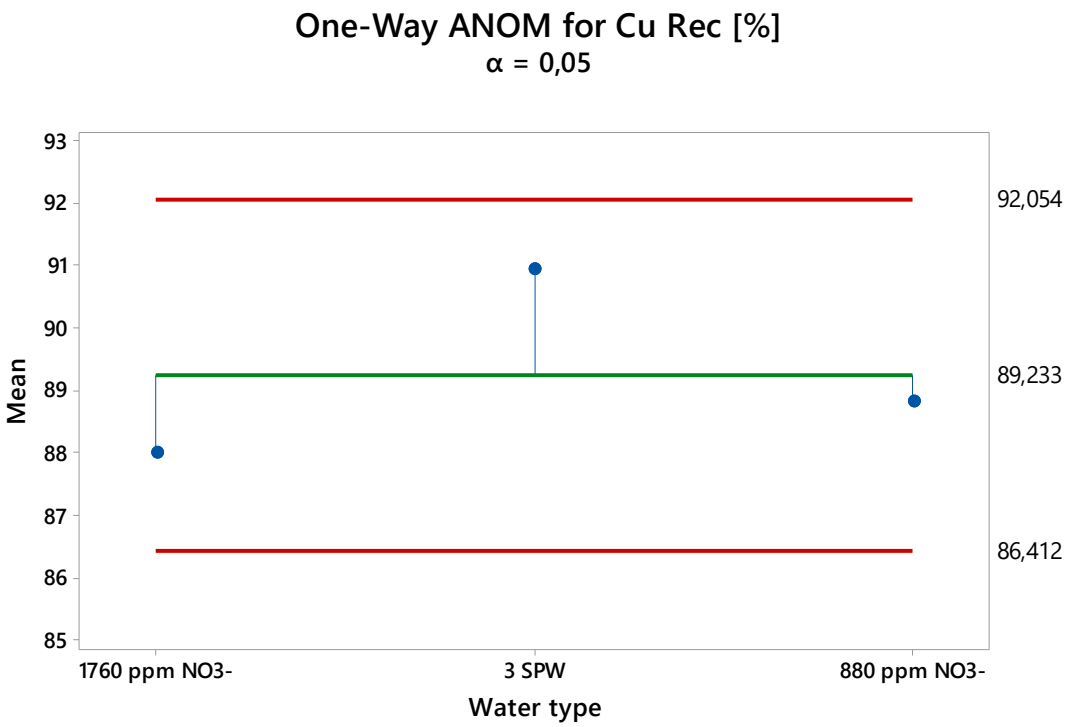

Figure 7-15 Statistical analysis on copper recovery for NO_3^- spiking vs. 3 SPW

Copper recovery when 3 SPW is spiked with the NO_3^- ion does not show any statistical difference within the 880 to 1760 ppm range as shown in **Figure 7-15**. The copper recovery at each concentration point is within the decision lines and this proves **Figure 7-6** that there is no difference between the performance of either ion concentration and the baseline 3 SPW.

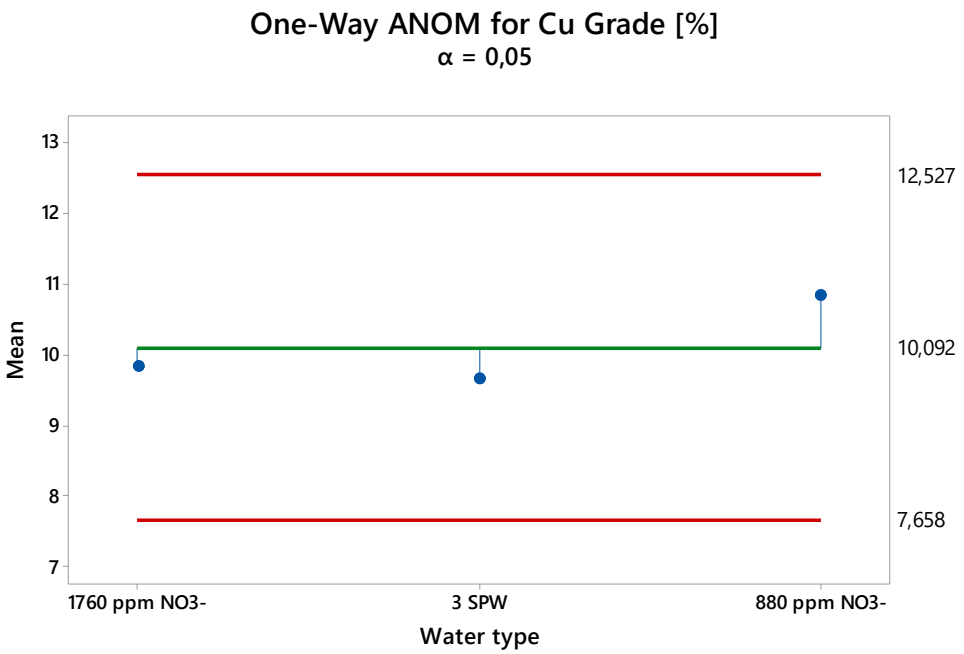

Figure 7-16 Statistical analysis on copper grade for NO_3^- spiking vs. 3 SPW

Figure 7-16 shows that upon spiking 3 SPW with 880 ppm and 1760 ppm NO_3^- respectively, proves that there is no considerable statistical difference in comparison to the control experiment; 3 SPW for copper grade based on **Figure 7-6**. The average means of the spiked ions are within the decision limits and hence are considered to have no significant statistical impact on grade in comparison with 3 SPW.

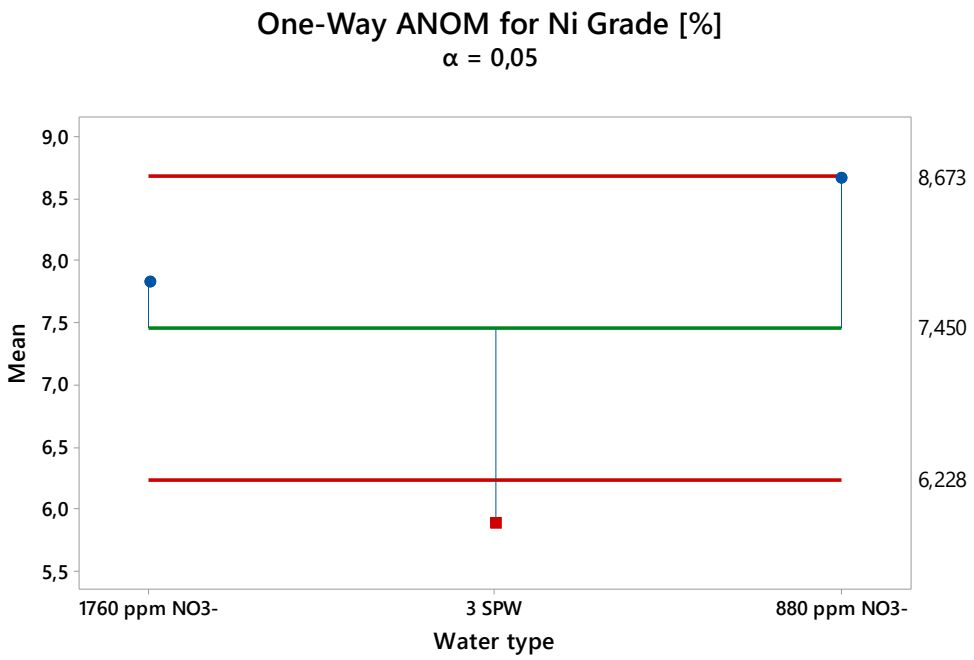

Figure 7-17 Statistical analysis on nickel grade for NO_3^- spiking vs. 3 SPW

From **Figure 7-17,** 880 ppm NO_3^- seems to be having an impact on nickel grade as illustrated by the decrease in nickel grade at 3 SPW. 1760 ppm NO_3^- exhibits nickel grade that is close to the grand while 880 ppm NO_3^- is close to the upper boundary decision line. This proves **Figure 7-9** that there is a statistical difference between 3 SPW and 880 ppm NO_3^-.

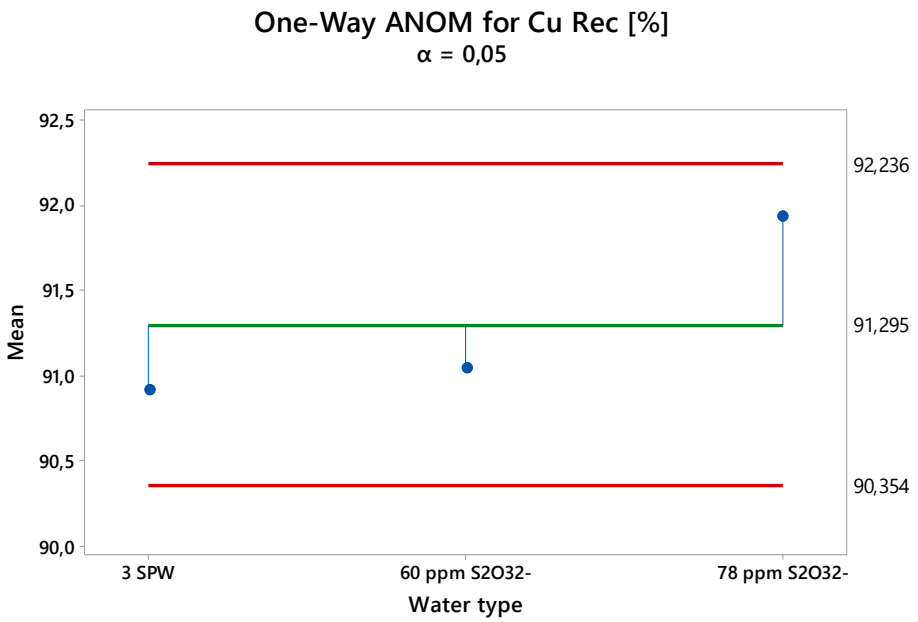

Figure 7-18 Statistical analysis on copper recovery for $S_2O_3^{2-}$ spiking vs. 3 SPW

Figure 7-18 proves **Figure 7-6** that spiking 3 SPW with $S_2O_3^{2-}$ has no statistical difference on copper recovery

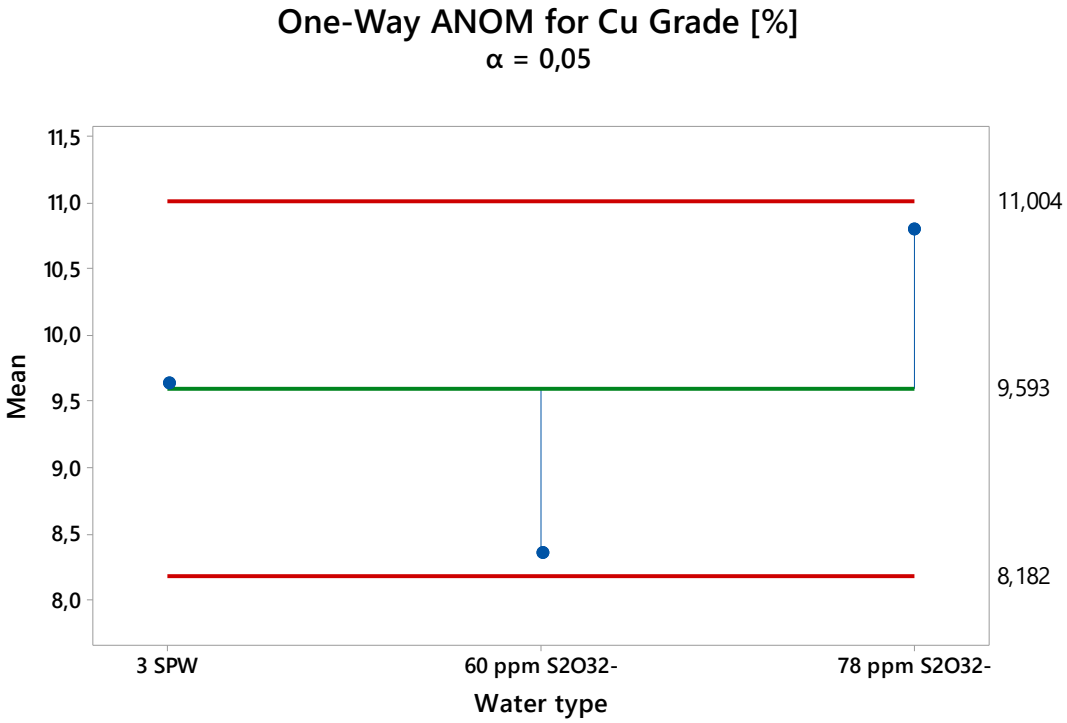

Figure 7-19 Statistical analysis on copper grade for $S_2O_3^{2-}$ spiking vs. 3 SPW

From the final nickel grade distribution; **Figure 7-9**, it shows that 3 SPW produces a nickel grade of 9.6% while spiking with 60 ppm $S_2O_3^{2-}$ ion results in 8.4% nickel grade and at 70 ppm $S_2O_3^{2-}$ yields 10.8% nickel grade. **Figure 7-19,** it is proved however that there is no statistical difference between these values as all the values lie within the upper and lower bound decision lines.

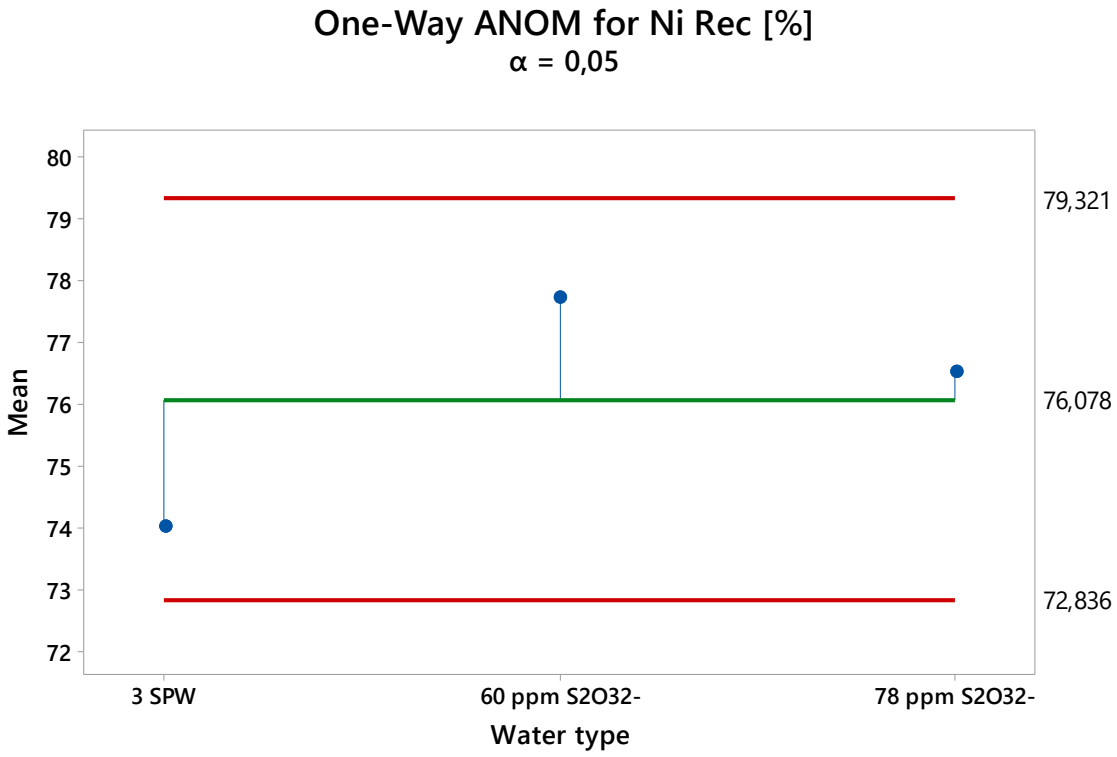

Figure 7-20 Statistical analysis on nickel recovery for $S_2O_3^{2-}$ spiking vs. 3 SPW

Figure 7-20 proves **Figure 7-9** that there is no statistical difference in nickel recovery with 3 SPW is spiked with 60 ppm $S_2O_3^{2-}$

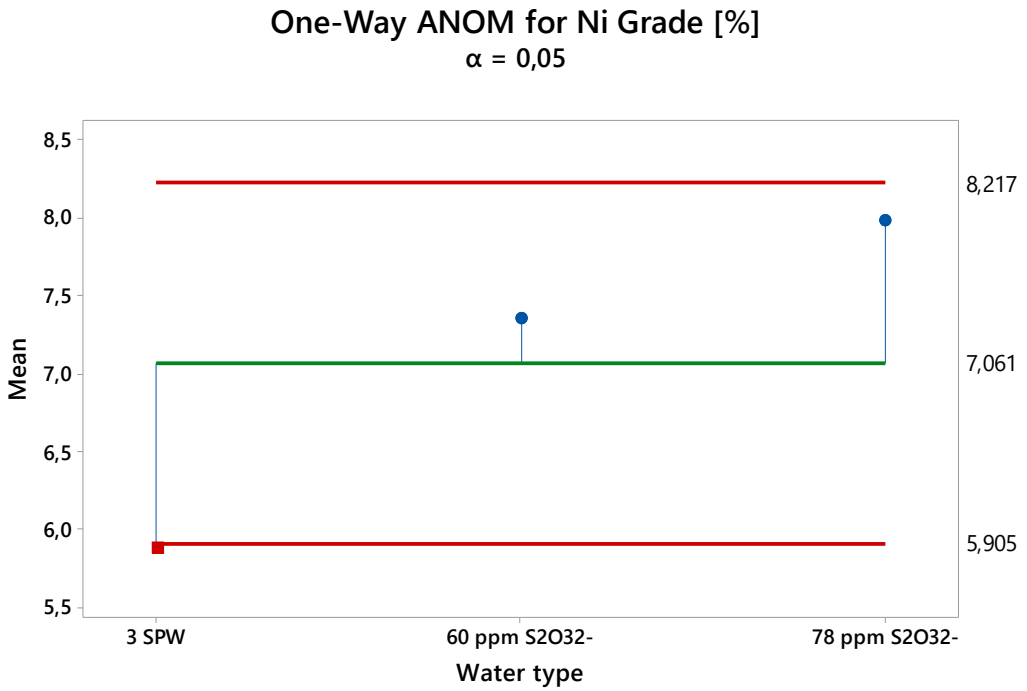

Figure 7-21 Statistical analysis on nickel grade for $S_2O_3^{2-}$ spiking vs. 3 SPW

Unlike nickel recovery upon spiking, nickel grade is shown to be impacted positively by spiking with $S_2O_3^{2-}$ ion, **Figure 7-21**. This proves **Figure 7-9** that grade increases considerably when compared to that of 3 SPW.

7.5 Key Findings upon spiking 3 SPW with: SO_4^{2-}, NO_3^- and $S_2O_3^{2-}$

- Increasing the anionic spiking concentrations result in no effect with regards to water recovery for NO_3^- and SO_4^{2-} while it results in decreased water recovery for $S_2O_3^{2-}$
- Spiking with SO_4^{2-} results in a considerable increase in solids recovery while $S_2O_3^{2-}$results in solids recovery.
- Spiking 3 SPW with $S_2O_3^{2-}$ statistically improves overall nickel grade
- In a 2-phase column study, spiking with NO_3^- and $S_2O_3^{2-}$results in the EC of the solution being higher than that of the froth phase while for 1200 ppm SO_4^{2-} the froth phase an insignificantly higher EC in the froth phase.
- In a 3-phase column study, upon anionic spiking; the pulp phase has higher EC than the froth phase.

8 SEQUENTIAL FLOTATION RESPONSE

Recalling that Kevitsa mine processes a low grade Cu-Ni-PGM ore and recoveries are managed and maintained predominantly by high throughput; approximately 25000 t/day. The copper circuit precedes the nickel circuit due to the fast floating properties of chalcopyrite. Lime is used at Kevitsa (another source of Ca^{2+} ions) so that the high pH environment will demote the floating tendency of pentlandite in the copper circuit. This means the nickel circuit feed will have high pH and require some acid to reduce the pH and make nickel floatable again. Aerophine 3418A is the collector for copper minerals and SIPX for nickel minerals while CMC is dosed to depress the associated gangue material for both chalcopyrite and pentlandite.

The sequential copper and nickel circuits are carefully arranged in-order to maximize the valuable material. The copper rougher concentrate is sent directly to copper cleaner cells while the final copper scavenger tails are sent as feed to the nickel circuit. Coming directly from the copper circuit, the nickel circuit feed contains reagents and pulp chemistry appropriate for the recovery of copper minerals. There is, therefore, need to carefully recondition this nickel feed by the addition of reagents intended for the recovery of nickel minerals. It should be noted that on site, the pulp chemistry of the nickel feed is adjusted using a versatile ethylenediaminetetraacetic acid EDTA chelating agent. EDTA is a hexadentate ligand mainly used to sequester metal ions such as Ca^{2+} by formation of sparingly soluble complexes (Kelebek et al., 1996).

pH adjustment is done using lime to ranges of 10-11, these conditions were not used at lab scale (Gray et al., 2016). This section does not include new data but it zeroes in on the recoveries and grades at circuit level and their contribution to the overall plant recovery values.

Figure 8-1 shows how the copper circuit is set up while **Figure 8-2** shows the nickel sequential cell set up. It is important to note that in this section, the flotation mass balance for the nickel circuit is made from the fresh copper circuit feed. Copper is recovered as chalcopyrite and nickel is recovered as pentlandite, both circuits were run at natural pH, as opposed to the on site pH of 10-11, and this causes pentlandite to float considerably faster and gets recovered together with the copper. The laboratory system was self-buffering between pH 8-9.5 and no chelating agent was added to improve nickel recoveries/grade.

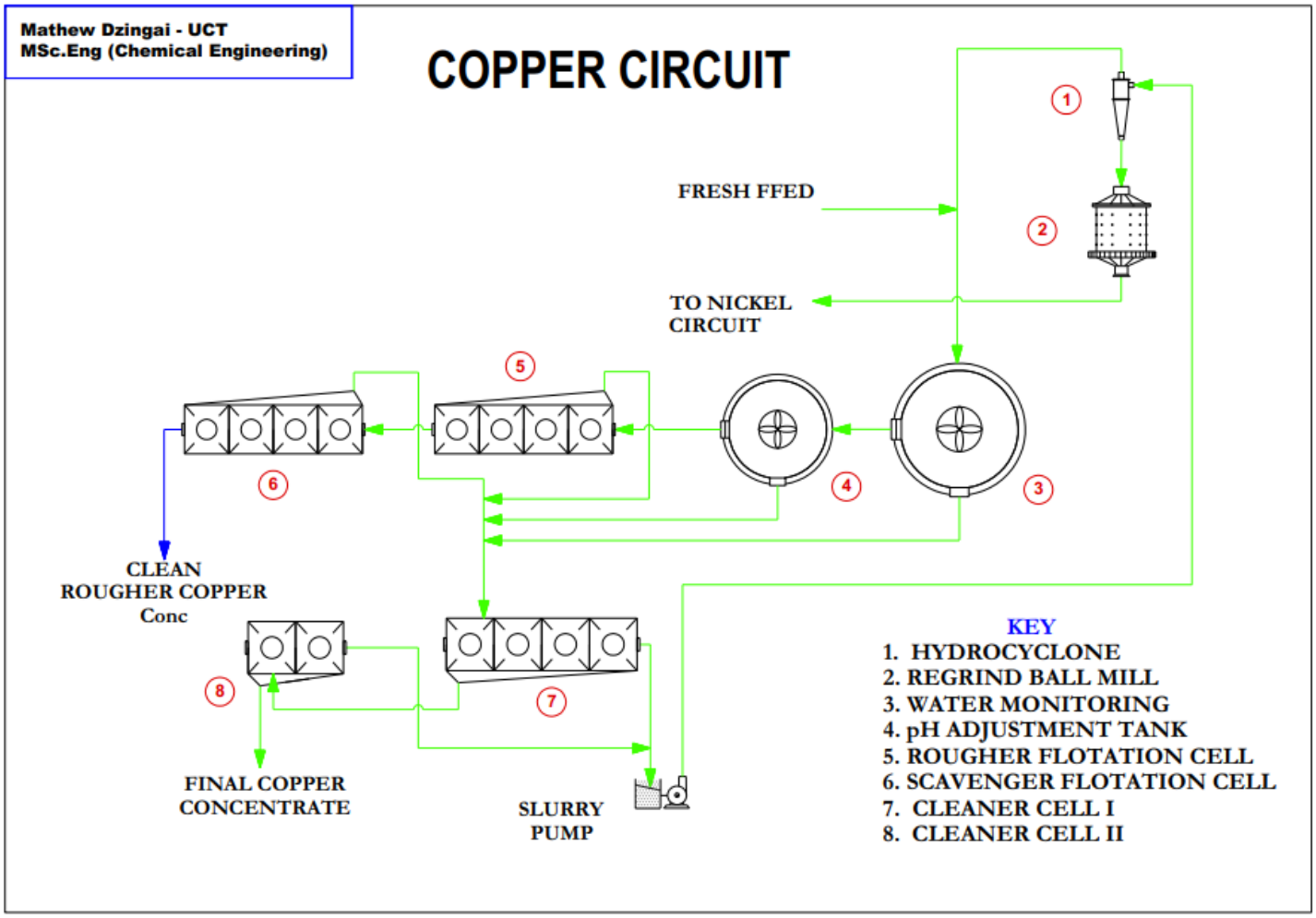

Figure 8-1 Sequential copper concentration circuit

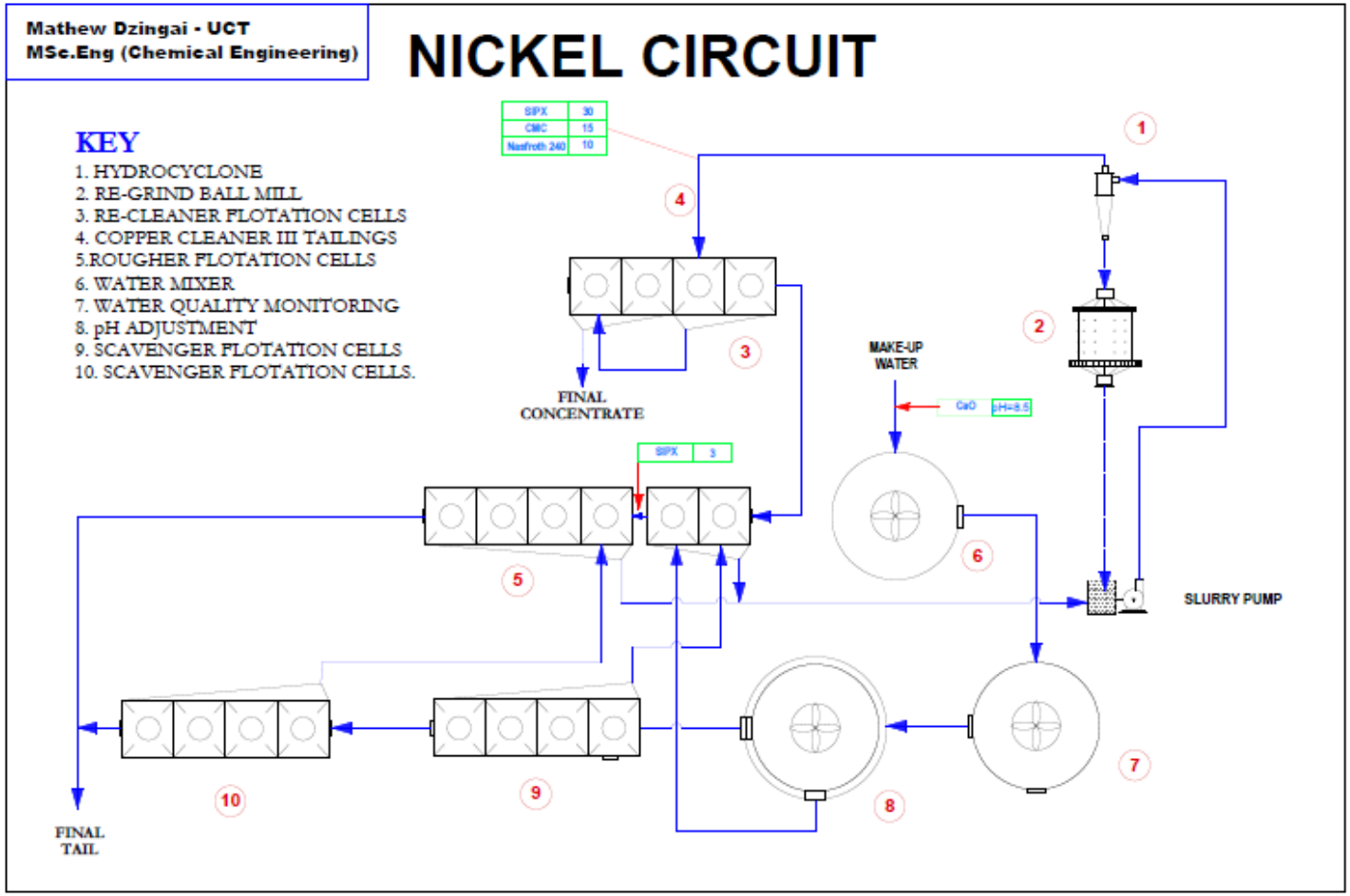

Figure 8-2 Sequential nickel concentration circuit

8.1 Copper-Nickel sequential flotation performance upon spiking 3 SPW with Ca^{2+} and Mg^{2+}

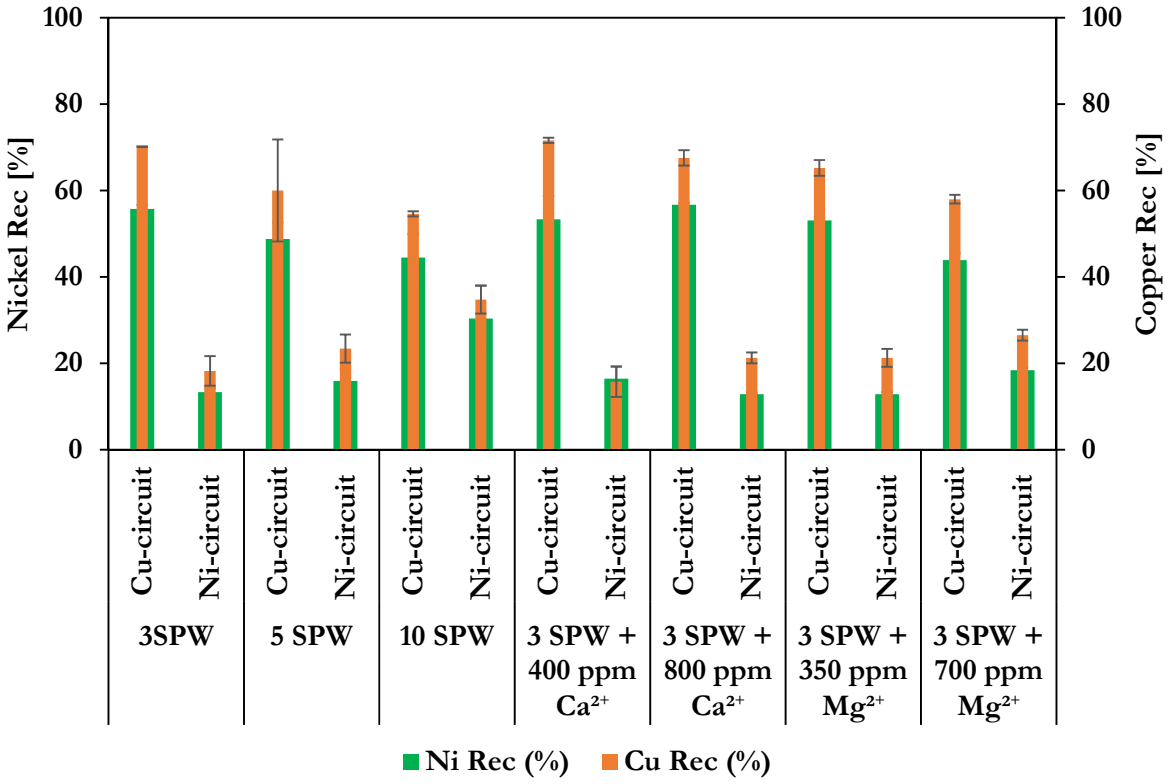

Figure 8-3 Nickel and copper recovery in the presence of selected cations per circuit

In this system nickel floats quite fast and most of it is recovered in the copper circuit. The copper circuit is run for 10 min split in half to recover C_1 and C_2. The nickel circuit is run for 40 minutes recovering C_3, C_4, C_5 and C_6. From **Figure 8-3** using 3 SPW, 70.16 % Cu and 55.75 % Ni is recovered in the copper circuit while akin to the copper circuit, the nickel circuit also recovers high amounts of copper, yielding 18.24 % Cu and 13.37 % Ni. Spiking with Ca^{2+} ion to 400 ppm in the copper circuit yields 71.61 % Cu and 53.34 % Ni while giving 15.76 % Cu and 16.46 % in the nickel circuit. The overall recovery is therefore calculated as the sum of the individual circuit per element.

Thus, the overall recovery for 3 SPW is 88.4 % Cu and 69.1 % Ni while at 400 ppm Ca^{2+} spiking, it yielded 87.4 % Cu and 69.8 % Ni. Spiking Mg^{2+} ion to 350 ppm significantly reduced recovery yielding 65.22 % Cu and 53.05 % Ni in the copper circuit and, 21.27 % Cu and 12.88 % Ni in the nickel circuit. At 700 ppm Mg^{2+}, the copper circuit recovered 57.99 % Cu and 43.90 % Ni while the nickel circuit yielded 26.52 % Cu and 18.41 % Ni.

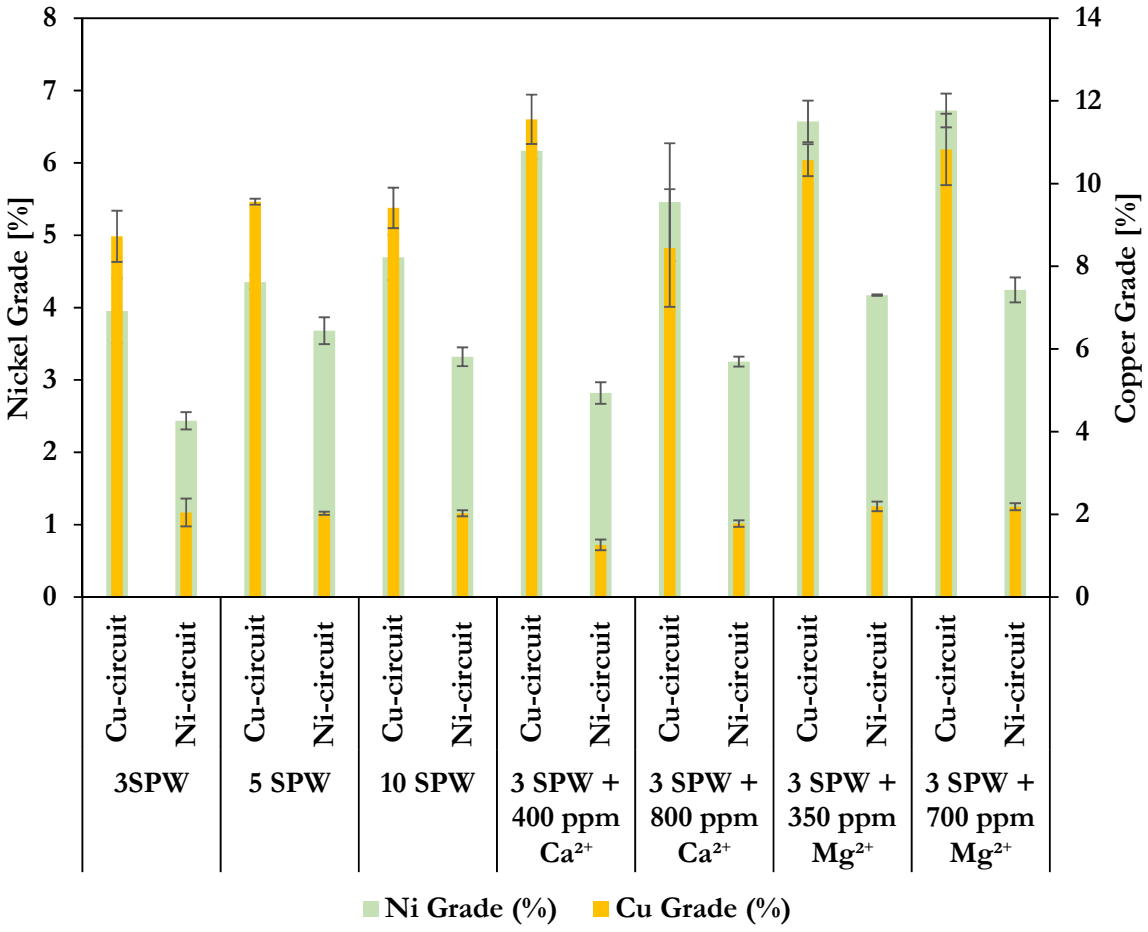

Figure 8-4 Nickel and copper grade in the presence of selected cations per circuit

Generally, as can be observed from **Figure 8-4**; copper grade is low in the nickel circuit at different water types and specific cation concentration. In the nickel circuit, the nickel grade is higher than copper grade. The general trend is that; there is a symbiotic decrease in copper and nickel grade per circuit. This means that copper grade is high in copper circuit and lower in the nickel circuit and the opposite is true for nickel recovery in the nickel circuit.

8.2 Copper-Nickel sequential flotation performance upon spiking 3 SPW with: SO_4^{2-}, NO_3^- and $S_2O_3^{2-}$

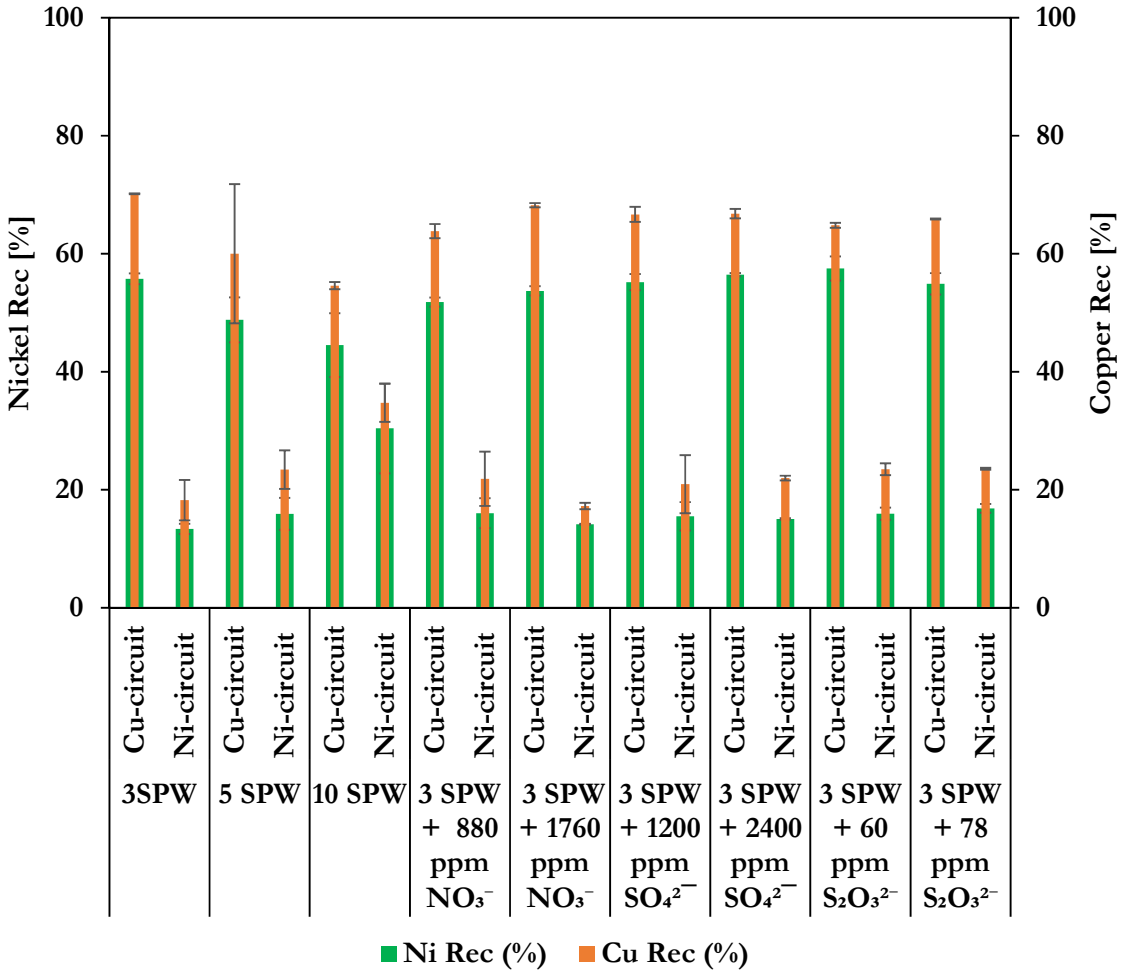

Figure 8-5 Nickel and copper recovery in the presence of anions per circuit

Figure 8-5 shows that upon anionic spiking, most of the nickel is recovered in then copper concentrate. In the copper circuit, spiking results with the same copper recovery for all the three anions in the copper circuit with no observable increase/decrease in recovery. There is a general decrease in nickel recovery as the water quality changes from 3, 5 and 10 SPW. In the nickel circuit, copper recovery is always higher than nickel recovery. The highest nickel recovery in the nickel circuit is observed at 10 SPW. SO_4^{2-}, NO_3^- and $S_2O_3^{2-}$ spiking show no significant difference in nickel recovery in the nickel circuit.

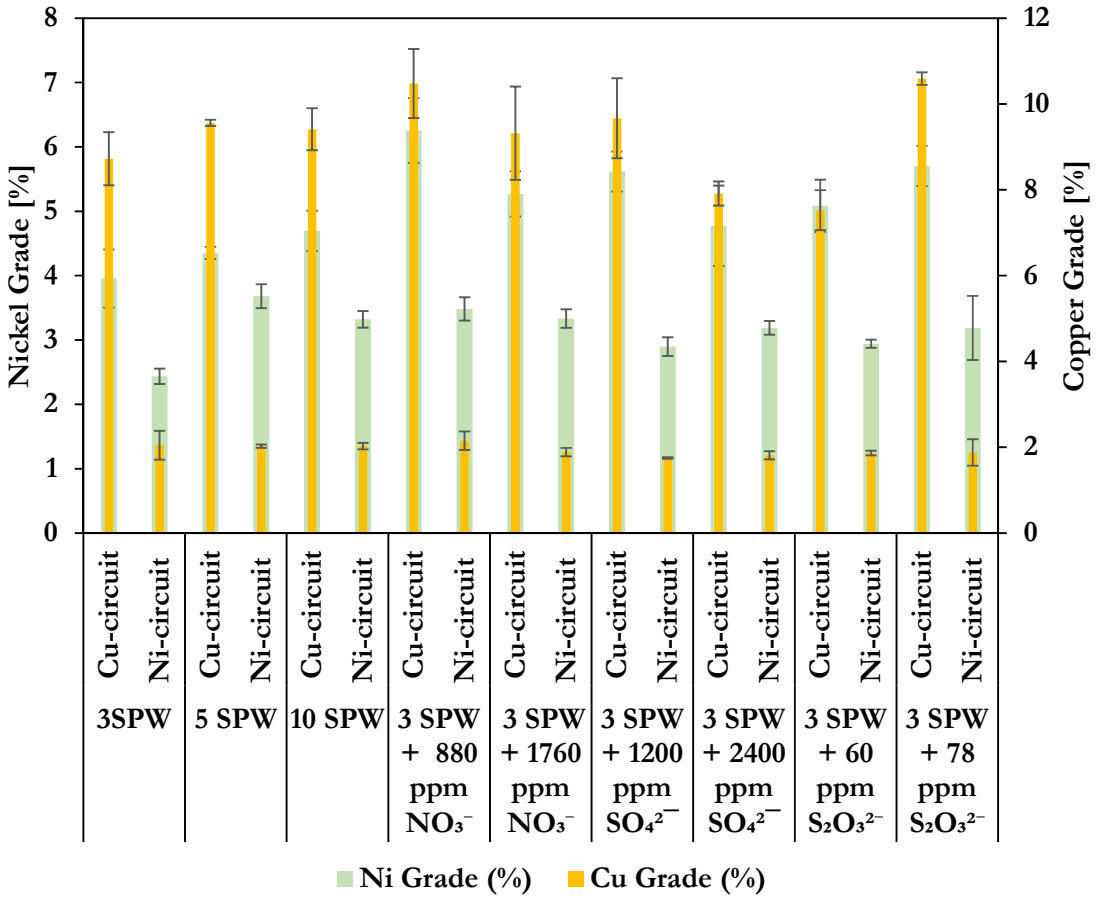

Figure 8-6 Nickel and copper grade in the presence of selected anions per circuit

As can be observed from **Figure 8-6**, spiking of specific anions may lead to improved copper grade in the copper circuit. Spiking the $S_2O_3^{2-}$ ion from 60 ppm to 78 ppm results in an improved copper grade from 7.53% to 10.59% respectively. Increasing the SO_4^{2-} ion concentration from 1200 ppm to 2400 ppm decreases the copper grade in the copper circuit this is a similar trend observed for spiking with 880 and 1760 ppm NO_3^-. Of the anions spiking, 880 ppm NO_3^- ion and 78 ppm $S_2O_3^{2-}$ ion spiking in the copper circuits exhibits the highest copper grade in the copper circuit while 60 ppm $S_2O_3^{2-}$ ion spiking exhibits considerably the lowest copper grade in the copper circuit. 5 SPW shows highest nickel grade in the nickel circuit.

The individual circuit performance is presented in **Table 8-1**, where the overall circuit recovery is the sum of the recovery in the copper and nickel circuit per each metal. The overall grade is the sum of the grade in the copper and nickel grade for each experimental condition.

Table 8-1 Overall nickel circuit performance in the presence of all the selected ions and synthetic pant water

	Cu-Ni Recovery			Cu-Ni Grade	
Water [I.S]	Circuit	Cu_rec	Ni_rec	Cu_grad	Ni_grad
3SPW	Cu-circuit	70.16	55.75	8.72	3.95
	Ni-circuit	18.24	13.37	2.05	2.44
5 SPW	Cu-circuit	60.00	48.79	9.56	4.35
	Ni-circuit	23.41	15.92	2.03	3.68
10 SPW	Cu-circuit	54.59	44.51	9.41	4.70
	Ni-circuit	34.73	30.40	2.03	3.32
400 ppm Ca^{2+}	Cu-circuit	71.61	53.34	11.55	6.17
	Ni-circuit	15.76	16.46	1.26	2.82
800ppm Ca^{2+}	Cu-circuit	67.55	56.68	8.44	5.46
	Ni-circuit	21.27	12.88	1.78	3.25
350 ppm Mg^{2+}	Cu-circuit	65.22	53.05	10.57	6.57
	Ni-circuit	21.27	12.88	2.19	4.17
700 ppm Mg^{2+}	Cu-circuit	57.99	43.90	10.83	6.72
	Ni-circuit	26.52	18.41	2.18	4.24
880 ppm NO_3^-	Cu-circuit	63.83	51.80	10.48	6.25
	Ni-circuit	21.86	16.03	2.15	3.48
1760 ppm NO_3^-	Cu-circuit	68.22	53.71	9.32	5.27
	Ni-circuit	17.25	14.16	1.89	3.33
1200 ppm SO_4^{2-}	Cu-circuit	66.67	55.18	9.67	5.62
	Ni-circuit	20.95	15.50	1.75	2.90
2400 ppm SO_4^{2-}	Cu-circuit	66.79	56.44	7.91	4.77
	Ni-circuit	21.98	15.05	1.81	3.19
60 ppm $S_2O_3^{2-}$	Cu-circuit	64.81	57.50	7.53	5.08
	Ni-circuit	23.48	15.95	1.87	2.94
78 ppm $S_2O_3^{2-}$	Cu-circuit	65.88	54.89	10.59	5.70
	Ni-circuit	23.57	16.85	1.88	3.19

8.3 Key Findings on copper-nickel sequential flotation upon spiking 3 SPW with: SO_4^{2-}, NO_3^- and $S_2O_3^{2-}$

- Copper recovery is high in the copper circuit as well as in the nickel circuit.
- Most of the nickel is recovered in the copper circuit
- For cationic spiking, 400 ppm Ca^{2+}, 350 ppm Mg^{2+} and 700 ppm Mg^{2+} have considerably the highest copper grades in the copper circuit per recovered concentrates.
- Spiking with SO_4^{2-}, NO_3^- and $S_2O_3^{2-}$ does not show any considerable impact on the recovery of nickel and copper in the sequential batch flotation test.

9 DISCUSSION

The main objective of this study was to investigate the effect of water quality and the impact of selected ions on the flotation performance of a low-grade Cu-Ni-PGM ore. The target metals for this investigation were copper which floats as chalcopyrite and nickel which floats as pentlandite. The key performance indicators used were: (a) water recovery, (b) solids recovery, (c) valuable metal recovery, (d) grade of the recovered concentrates and (e) electrical conductivity.

The ore was milled and floated in SPW of varying ionic strength as well as SPW in which selected ions were spiked to known ionic concentrations. The ion spiking was intended to mimic the recycling of water and the most prevalent ions which would likely be recycled and therefore accumulated, such ions as: Ca^{2+}, Mg^{2+}, NO_3^-, SO_4^{2-} and $S_2O_3^{2-}$. Three standard SPWs were used; 3, 5 and 10 SPW representing ionic strengths of 0.073, 0.121 and 0.242 M respectively. 3 SPW was used as the baseline for the spiking of selected ions to represent a complex water matrix as would be found on site. It is important to note that the original SPW did not contain $S_2O_3^{2-}$ and the spiking with 60 and 78 ppm $S_2O_3^{2-}$ was determined to be suitable by on-site measurement.

Batch flotation was used to determine the impact of increasing ionic strength on flotation and the effect of spiking Ca^{2+}, Mg^{2+}, NO_3^-, SO_4^{2-} and $S_2O_3^{2-}$ to levels of 5 and 10 SPW. Variations in water and solids recovery together with metal recoveries and grades where were noted. For all these conditions, batch flotation was done in a sequential manner for copper and nickel recovery respectively.

The same ionic strengths and spiking concentrations were used for froth (or foam) column studies with a focus on tracking the ion concentration distribution between the froth (or foam) and the slurry (or solution) by means of measuring the EC of each of the froth (foam) and the pulp (solution) phases. The differences implied whether the ions are selectively concentrated at the air-water or solids-water interphases in a 3-phase system or likewise at the bubble surface or within the solution for a 2-phase system.

Increasing ionic strength increased the water recovered to the concentrate in the order 3 SPW < 5 SPW < 10 SPW while the solids showed a minimum at 5 SPW in the order 5 SPW < 3 SPW < 10 SPW.

The collectors used throughout the investigation were: Aerophine 3418A (for the copper circuit) and SIPX (for the nickel circuit). These were added sequentially, and their selectivity was based on individual circuit recoveries and grades; as noted previously, not all pulp conditions, pH and EDTA addition in the nickel circuit, were replicated as would be on site.

CHAPTER 9

9.1 Effect of water quality on flotation performance: 3, 5 and 10 SPW

Figure 5-3 showed that as ionic strength increased the water recovery also increased. Corin et al. (2011) showed this same trend and suggested that the increase in ionic strength increased the NFG recovery by entrainment, increasing the froth stability and as a consequence resulted in increased water recovery. Cho and Laskowski (2002) showed that at high ionic strength there was possible inhibition of bubble coalescence. As bubble coalescence decreased, the gas hold-up in the froth phase increased and this led to higher water recovery due to increased bubble interfacial area and increased water-gas bonding forces resulting in more water being recovered to the concentrate. In line with these findings, Manono et al. (2013) showed that bubble size diameter decreased in the order $d_{10SPW} < d_{5SW} < d_{3SPW}$. Bubble coalescence inhibition may also presumably be due to the concentration of the ions at the bubble surface. While using MIBC in developing a novel technique to investigate the bubble coalescence in the presence of salts, such as NaCl and $CaCl_2$, Gungoren et al. (2018) suggested that even though bubble coalescence is controlled by frothers, dissolved ions have a great tendency of inhibiting bubble coalescence. **Figure 5-14** corroborated these findings; as the ionic strength increased and water recovery increased the EC of the froth increased implying that ions that make up the SPW matrix are concentrated more at the bubble surface compared to the mineral surface.

The increase in water recovery had a bearing on the solids recovery as illustrated in **Figure 5-4**. As the ionic strength increased; 3 and 5 SPW recovered solids in the same range while 10 SPW exhibited the highest solids recovery. This is in agreement with previous fundamental studies carried out by Corin et al. (2011), Manono et al. (2012), and Corin and Wiese, (2014) without decoupling the effect of ion type. The increase in solids with increasing ionic strength suggests that the overall increase in ionic strength may have resulted in the modification of the pulp and surface chemistry of mineral particles which could have led to the activation of gangue and hence dilution of the concentrate; lower grade, as copper recoveries did not seem to have been affected.

The increase in ionic strength was shown to have no apparent effect on copper recovery but a slight decrease in copper grade was seen in **Figure 5-9**. A notable increase in nickel recovery and accompanying decrease in grade as the ionic strength of water increased was illustrated in **Figure 5-10**. This increase in recovery of nickel could be as a result of the increase in froth stability, owing to possible gangue activation and/or increased entrainment.

This means that while recycling of water on site will not have a large impact on the valuable mineral recoveries, there is need to manage the quality of the water, in order to maintain a suitable grade, particularly for the nickel circuit which may be operated at moderate ionic strength; 5 SPW, in cases where no EDTA chelating agent or pH control is used to modify the pulp properties.

9.2 Effect of $Ca^{2+}$and Mg^{2+} ionic spiking on flotation performance

Ikumapayi and Makitalo (2013) suggested that Ca^{2+} ions adsorb on the mineral surface during the flotation process and may partially precipitate as $CaOH^{+}$ on the mineral surface. The presence of Ca^{2+} may compete with xanthate for adsorption onto the sulphide minerals, including pyrrhotite, which is considered as gangue in the ore used in this study (Musuku et al., 2016). Clarke and Fornasiero (1995) conducted a study on the removal of oxidation products from sulphide mineral surfaces and found that the surface oxidation products consisted mainly of metal hydroxides and sulphur-oxy species which in turn reduced the mineral hydrophobicity and made collector adsorption less selective.

It was shown by Levay et al. (2001) that $CaOH^{+}$, $CaCO_3$, $MgCO_3$ and $MgOH^{+}$ which are considered colloidal species, possibly attach to the mineral surface forming a hydrophilic coating. Ralston (1999) stated that the presence of such coating on the mineral surface hindered mineral-collector interaction and inevitably the mineral hydrophobicity as the particle-bubble attachment efficiency is compromised.

Figure 6-7 showed that 400 ppm Ca^{2+} was the maximum concentration beyond which the flotation performance was negatively impacted. Beyond 400 ppm Ca^{2+} the grade decreased, and it is assumed that if the concentration of the cation increased further, the grade would continue to decrease. From **Figure 6-10**, unlike copper recovery and its grade, nickel was insignificantly affected by spiking with Ca^{2+} from 400 to 800 ppm. Most of the nickel was recovered in the copper circuit owing to lack of pH control, as is done on site, hence there was no obvious impact of the Ca^{2+} ions in the nickel circuit and little impact on the nickel recovery.

From **Figure 6-13**, it was illustrated that at 800 ppm Ca^{2+} the pulp and froth EC were almost the same which suggested that the amount of Ca^{2+} carried into the froth was the same as that remaining in solution, the Ca^{2+} was evenly distributed between the pulp and the froth. This resulted in a decrease in the copper and nickel grade. The correlation of ion distribution between the pulp and the froth phase with recoveries and grades is ion-type dependent as some observations showed that at high pulp EC the grade of copper and nickel decreased, as was the case for Ca^{2+} at 800 ppm the grade started decreasing.

There was no significant nickel recovery difference when the system was spiked with Mg^{2+} however, the nickel grade was significantly impacted as it showed an increase of approximately 3.65% from 3 SPW to 350 ppm Mg^{2+}. This suggested that Mg^{2+} may have enhanced gangue depression for the ore type used in this investigation. Laskowski and Castro, (2017) investigated the hydrolysis of metallic ions in mineral processing circuits and its effect on flotation and found out that Mg^{2+} forms hydrolysis products that strongly depresses molybdenite (a sulphide mineral) over typical plant pH ranges. Mg^{2+} is a divalent and its effects on this ore are quite similar to that of Ca^{2+} as it also leads to the formation of hydrophilic sites on chalcopyrite resulting in lower flotation of the chalcopyrite (Levay et al., 2001)

For the conditions used in this study, spiking Mg^{2+} resulted in increased grade of copper and nickel and this suggested that the threshold may lie outside of the boundary concentrations used. Ca^{2+} showed that 400 ppm was the threshold beyond which the copper and nickel grade started decreasing.

Keeping in mind that the outcomes of this study are ore-dependent, when the recycled water is being monitored for the amount of Ca^{2+} and Mg^{2+} present, it is imperative to operate at a maximum concentration of 400 ppm Ca^{2+} beyond this concentration point the grades for copper and nickel will decrease. The presence of Mg^{2+} up to 700 ppm may be considered to have no negative impacts on nickel circuits as its efficacy was only showing improvements in grade of nickel while further increase in Mg^{2+} concentration may result in decreases in copper grade in the copper circuits.

9.3 Effect of spiking 3 SPW with NO_3^- on flotation performance

For **Figure 7-3** looking at the solids recovery it was shown that though 3 SPW had higher solids recovery than NO_3^- at 880 and 1760 ppm NO_3^-, 3 SPW recovered far less water than either 880 or 1760 ppm NO_3^-. This showed that the NO_3^- caused the froth to be significantly more stable; Corin et al. (2011); Manono et al. (2016); Corin and Wiese, (2014). It is important to note that these references investigated the effects in increasing overall ionic strength without decoupling the effects of individual ions however remain relevant as the overall ionic strength of all of the spiked 3 SPW solutions is of course higher than 3 SPW without spiking.

NO_3^- may have an impact on gangue depression, as the grade increased above that of 3 SPW when NO_3^- was spiked showing a contrasting trend to literature on increasing overall ionic strength (Manono et al., 2016). The water recovery was in the order 3 SPW < 880 ppm <= 1760 ppm <5 SPW < 10 SPW while the solids showed a minimum at 5 SPW and followed the order 5 SPW < 880 ppm < 1760 < 3 SPW < 10 SPW. The copper and nickel recoveries were not impacted while the copper grade was higher for the spiked samples and followed the order 10 SPW <= 3 SPW < 5 SPW < 1760 ppm < 880 ppm and the nickel grade order was 3 SPW < 10 SPW < 5 SPW < 1760 ppm < 880 ppm. According to Corin et al. (2011) and Manono et al. (2018b) an increase in overall ionic strength will result in increased froth stability (derived from increased water recovery, **Table 4-4**) and a decrease in sulphide grade. The increase in nickel grade upon spiking 3 SPW with NO_3^- could be due to some degree of increased collector selectivity at 880 ppm NO_3^- owing to pulp chemical species with may be present.

However, beyond 880 ppm NO_3^- , it was speculated that, for this ore, the gangue material surface became saturated with the ion such that it became difficult for CMC to attach and as a result at 1760 ppm NO_3^- this gangue material was not depressed and reported to the concentrate, diluting the purity of the nickel recovered, as shown by the sharp decrease in the grade of nickel.

The EC as observed from **Figure 7-11**suggested that for a 3-phase the NO_3^- ions are more concentrated around the mineral surface as compared to the froth phase at 1760 ppm, as exemplified by higher ECs in the pulp phase. While a huge difference between the froth and solution at 880 ppm shown in **Figure 7-10** could indicate the reagent action with the NO_3^- ion before the introduction of the ore and as such results in a marked high grade of copper and nickel compared to the 1760 ppm. The NO_3^- could be enhancing the mineral-ion-reagent interaction but

beyond the 880 ppm point, there could be over saturation of the ion resulting in the activation of the gangue hence the grade starts to decrease.

Maintaining that the outcomes of this study are ore-dependent, the peak NO_3^- concentration which exhibited high copper and nickel grade was 880 ppm and beyond this concentration, the grade decreased sharply. This means that in plant operations when monitoring recycled concentrator water, it is important to consider concentrations of NO_3^- to be around 880 ppm since beyond this point the grade of copper and nickel will start to decrease.

9.4 Effect of spiking 3 SPW with SO_4^{2-} on flotation performance

Corin et al. (2011) observed that increasing ionic strength for a Merensky reef ore did not have an effect on the recovery of the sulphide mineral as measured by copper and nickel recovery however the grade was impacted negatively due to the increase in ionic strength which resulted in high solids and water recovery, and introduced more naturally floatable gangue (NFG) to the final concentrate. The increase in solids and /or NFG recovery is a result of the gangue activating nature of SO_4^{2-}. This is akin to the observation made in this research as the ionic strength was increased by spiking of the SO_4^{2-}.

As the concentration of SO_4^{2-} ions increased, the overall ionic strength of water also increased, recovering more water compared to 3 SPW and stabilizing the froth as shown in **Figure 7-3**. Furthermore, it is important to note, upon increasing the concentration of the SO_4^{2-} from 1200 to 2400 ppm, overall copper and nickel recovery remained practically the same with only a slight decrease in grade owing to higher solids recovery, which can be attributed to gangue material recovery.

The relationship between recovery and EC(upon spiking with SO_4^{2-}) for copper and nickel is depicted in **Figure 7-12** and **Figure 7-13** respectively. The EC showed that most of the ions remained in the pulp phase. The presence of a high concentration of SO_4^{2-} in the pulp phase, implied that ions are concentrated at the mineral surface. This could have led to gangue activation as the gangue gets coated by the SO_4^{2-}. 1200 ppm SO_4^{2-} was the maximum concentration beyond which the copper and nickel grades started decreasing.

Maintaining that the outcomes of this study are ore-dependant, 1200 ppm SO_4^{2-} was the peak concentration beyond which the copper and nickel indicated decreases. This implies that for recycling streams using concentrator water, it is imperative to maintain the concentration of the SO_4^{2-} ions around 1200 ppm and counter measure should be taken when this concentration has been exceeded since the copper and nickel grades will decrease.

9.5 Effect of spiking 3 SPW with $S_2O_3^{2-}$ on flotation performance

Figure 7-1 shows that; though 3 SPW was spiked with $S_2O_3^{2-}$ to the levels of 5 and 10 SPW, it was shown in this study that water recovered was sandwiched between 3 and 10 SPW meaning that 10 SPW presented the most stable froth compared to the other conditions. As $S_2O_3^{2-}$ increased from 60 to 78 ppm, water recovery slightly decreased presumably increasing bubble coalescence (Kirjavainen et al., 2002).

The response of solids recovered was shown in **Figure 7-2**. The descending order of solids recovery is 60 ppm $S_2O_3^{2-}$ > 10 SPW> 3 SPW> 78 ppm $S_2O_3^{2-}$ > 5 SPW, showing a maximum at 5 SPW.

Spiking 3 SPW with $S_2O_3^{2-}$ from 60 to 78 ppm showed that the copper and nickel grades increased, with a slight increase in copper recovery. From **Figure 7-9**, $S_2O_3^{2-}$ improved the gangue depression associated within the nickel sulphide flotation as there is a statistically significant nickel grade increase between 3 SPW, 60 ppm $S_2O_3^{2-}$ and 78 ppm $S_2O_3^{2-}$ as shown in **Figure 7-21**. Copper was less affected showing preferential nickel recovery over copper.

Agar (1989) conducted electrochemical studies to determine the interaction of $S_2O_3^{2-}$ on pentlandite and pyrrhotite surfaces and concluded that $S_2O_3^{2-}$ competes with xanthate for adsorption on the mineral thereby controlling the onset of the induced mineral hydrophobicity of the sulphide mineral. It is important to note that even though the $S_2O_3^{2-}$ competed for surface adsorption with the xanthate, it did not consume the xanthate. Xanthate chemisorption takes place at the active nickel sites, this xanthate can be oxidised to form dixanthogen which then enhances hydrophobicity (Agar, 1989). Akin to Kirjavainen et al. (2002) who claimed that the $S_2O_3^{2-}$ improves sulphide floatability by decreasing the likelihood of adsorption of hydrophilic compounds, such as hydroxides formed through redox processes. This is also confirmed in **Figure 7-11** as it shows that the $S_2O_3^{2-}$ is concentrated in the pulp phase compared to its froth phase, as such there was a statistically significant increase in grade of copper and nickel shown in this study for the ore type used.

Figure 7-11 also shows that ions are more concentrated in the pulp phase compared to the froth phase as shown by higher EC in the pulp phase, further suggesting that there is possible improvement of xanthate attachment to the target sulphide mineral enhanced by the presence of

$S_2O_3^{2-}$ in the pulp. The $S_2O_3^{2-}$ tests showed that the threshold concentration was not yet reached within the range considered in this study.

The findings of this study suggested that the increase in $S_2O_3^{2-}$ concentration is good for flotation, at least within the range considered in this investigation. This was exemplified by increases in copper and nickel grade upon increase in $S_2O_3^{2-}$concentration. It could be assumed that plant operations can operate using recycled water at $S_2O_3^{2-}$ concentrations higher than 60 and 78 ppm as the threshold seemed to lie outside the range considered in this study.

CHAPTER 11

10 CONCLUSIONS

Assessing the effect of increased ionic strength and the accumulation of selected ions on flotation response of a Cu-Ni-PGM ore was the objective of this study. **Chapter 3** outlined six key performance-based questions that this investigation sought to address and formulated the relationship between key performance indicators and the factors that affect them. In answering these questions, the validity of the postulated hypothesis was examined.

1. **How does the increase in ionic strength (3, 5 and 10 SPW) affect flotation performance?**

Thus, the froth stability increases with an increase in ionic strength. The copper and nickel recovery were not impacted while the grade decreased as the ionic strength increased. An increase in ionic strength led to gangue activation hence the decrease in grade.

2. **How does spiking Ca^{2+} and Mg^{2+} affect flotation performance of a Cu-Ni-PGM ore?**

Ca^{2+}: Copper and nickel recovery where insignificantly impacted while the copper grade decreased in the order 800 ppm < 10 SPW <= 3 SPW <5 SPW <400 ppm while nickel grade followed the order 3 SPW < 10 SPW < 5 SPW <400 ppm < 800 ppm. This showed that elevated concentrations of Ca^{2+} above 400 ppm decreased the grades of copper and nickel.

Mg^{2+}: Water recovery was in the order 3 SPW < 350 ppm < 700 ppm <= 5 SPW < 10 SPW while solids recovery followed the order 700 ppm < 350 ppm <= 5 SPW < 3 SPW < 10 SPW. Copper and nickel recovery were insignificantly affected. Copper grade was in the decreasing order of 3 SPW < 10 SPW < 5 SPW < 700 ppm < 350 ppm while nickel grade followed the trend 3 SPW < 10 SPW < 5 SPW < 700 ppm < 350 ppm. The threshold for Mg^{2+} was deemed to be outside the spiking boundaries for this study.

Spiking with Ca^{2+} and Mg^{2+} had little impact on copper and nickel recovery however the grade was impacted hence it is important to maintain a level of ions below the threshold concentrations for better flotation performance.

3. **How does spiking, NO_3^-, SO_4^{2-} and $S_2O_3^{2-}$ affect the flotation performance of a Cu-Ni-PGM ore?**

NO_3^-: 880 ppm NO_3^- showed a higher nickel grade and recovery however further increase to 1760 ppm NO_3^- resulted in a decrease in nickel grade. The pulp phase shows an increase in the ions at 1760 ppm.

SO_4^{2-}: 1200 ppm SO_4^{2-} resulted in the similar copper recoveries and grades as 3 SPW while spiking it to 2400 ppm SO_4^{2-} resulted in a decrease in copper grade. The 1200 ppm SO_4^{2-} showed a positive impact on nickel grade more so than 2400 ppm SO_4^{2-} when compared to 3 SPW which had lower nickel grade. This suggested that 1200 ppm SO_4^{2-} (in comparison to 3 SPW) was the threshold concentration beyond which the nickel grade was impacted.

$S_2O_3^{2-}$: Spiking 3 SPW with 60 and 78 ppm $S_2O_3^{2-}$ resulted in improved floatability of the valuable nickel mineral. Nickel recovery and grade showed an improvement; when spiked from 60 to 78 ppm $S_2O_3^{2-}$ while there was a decrease in copper grade noted as 3 SPW was spiked from 60 to 78 ppm $S_2O_3^{2}$.

4. **Is there a concentration of the selected divalent cations and the selected anions (between 3 and 10 SPW) beyond which the flotation performance is adversely impacted?**

Ca^{2+}: Ca^{2+} showed that 400 ppm gave improved copper grade and at 800 ppm copper grade decreased, this suggests that 400 ppm Ca^{2+} is the maximum concentration beyond which there is a negative impact on the copper flotation circuit.

Mg^{2+}: Mg^{2+} spiking did not show a maximum concentration point as the copper and nickel grade increased as the spiking increased from 350 ppm to 700 ppm.

NO_3^-: 880 ppm NO_3^- was the maximum concentration beyond which the copper and nickel grade begin to get negatively impacted.

SO_4^{2-}: 1200 ppm was the maximum concentration beyond which the copper grade was affected.

$S_2O_3^{2-}$: 60 ppm was the threshold with regards to copper grade.

5. **What is the ions distribution across the pulp and the froth phase?**

Ions distribution were measured based on the EC values from the 2 and 3 phase column studies. The phase (either pulp or froth) which possessed the highest EC values was deemed to have more ionic concentration compared to the phase with less EC. As such, the differences in EC was

directly linked to the recovery and it was a general observation that for a 3-phase system, the pulp possessed higher EC compared to its froth phase except for the case of 5 SPW which had higher EC in the froth phase compared to its pulp phase.

2-Phase:

It was shown that for a 2-phase column study; as the ionic strength of water increased from 3 to 10 SPW, the descending order of the difference in EC between the foam and solution phase was 3 SPW> 5 SPW> 10 SPW with higher EC in the solution phase; with an equal distribution of the ions at 10 SPW (foam EC= solution EC).

The 2-phase column studies showed the response of the water to the accumulation of ions before the ore was introduced, this can assist in considering recycling as the effect of the ions at the air-water interface can be decoupled from the effect of the ions at the mineral-solution interface in a 3-phase column system.

3-Phase:

5 SPW and 800 ppm Ca^{2+} showed higher froth EC than pulp EC and this can be related back to the nickel grade which showed higher values at 800 ppm. The remaining conditions of Mg^{2+} and 400 ppm Ca^{2+} showed a higher EC in the pulp phase. For all the anions spiking, the pulp phase showed higher EC than the froth phase.

Ions distribution did not seem to impact recovery of copper or nickel. Notably, the ion distribution between the froth and the pulp and the correlation to the grade is ion dependent. In some instances when the EC in the pulp phase was higher compared to the froth phase, the grade decreased while with the same ion and grade increased for example the contrast between 880 ppm NO_3^- and 78 ppm $S_2O_3^{2-}$.

10.1 Concluding Remarks

In conclusion, this study has shown that as ionic strength increased there was a corresponding increase in water recovery while solids recovery did not always follow the same trend. The presence of ions at different concentrations was used to decouple the deleterious ions from the ones that are beneficial to the flotation process. The ions which are deemed deleterious were beneficial until a certain concentration point referred to as the threshold concentration beyond which flotation was negatively affected and such ions are Ca^{2+}, SO_4^{2-}, and NO_3^-. However, Mg^{2+} and $S_2O_3^{2-}$ ions were beneficial to the process as they resulted in increases in grade for copper and nickel without

any marked threshold concentration. The ionic concentration of the pulp was shown to be higher compared to the froth phase for all the ions under investigation except for moderate concentrations such as 5 SPW. This study has shown that the electrical conductivity is a good indicator of pulp water chemistry and may be used as a precursor to inform decisions on water recycling for any low-grade Cu-Ni-PGM that exhibits the same geomorphological properties as the Kevitsa ore. This work proved the hypothesis suggested in **Chapter 3.**

11 RECOMMENDATIONS

After considering the results and conclusions drawn, the following recommendations are made:

- Use 2 different ore type for the same procedure and assess if the same observations can be extended to other ores.
- A method should be developed to monitor the ion-collector-frother-bubble-particle mechanism of interaction.
- Spiking should also be done on pure minerals to fundamentally decipher the batch flotation results.
- Reagent variation on spiked data could also help to understand the extent of spiking on flotation reagent impacts.
- Use a soluble chelating agent to depress nickel flotation in the copper circuit.

12 REFERENCES

Agar, M. H. and G. E. (1989) Eilectrochemical Investigations into the Flotation Chemistry of Pentlandite and Pyrrhotite: Process Water and Xanthate Interactions, *The Canadian Journal of Metallurgy and Materials Science*, 28(3), pp. 189–198.

Ambrose, R. . D. and P. . (1944) Development and use of certain flotation reagents.

Bradshaw, D. J. (1997) Synergistic effects between thiol collectors used in flotation of pyrite.

Bradshaw, D. J., Harris, P. J. and Connor, C. T. O. (1998a) Synergistic interactions between reagents in sulphide flotation, (august), pp. 189–194.

Bradshaw, D. J., Harris, P. J. and Connor, C. T. O. (1998b) Synergistic interactions between reagents in sulphide flotation, *The Journal of The South African Institute of Mining and Metallurgy*, 98(4), pp. 189–194.

Buckley, A. N. and Woods, R. (1997) Chemisorption—the thermodynamically favoured process in the interaction of thiol collectors with sulphide minerals, *International Journal of Mineral Processing*, 51(1–4), pp. 15–26. doi: 10.1016/s0301-7516(97)00016-1.

Bulatovic, S. M. (2007) Handbook of flotation reagents, pp. 1–6. doi: 10.1016/B978-0-444 53029-5.50027-7.

E. Burdukova, G.C. Van Leerdam, F.E. Prins, R.G. Smeink, D.J. Bradshaw and J.S. Laskowski (2008) Effect of calcium ions on the adsorption of CMC onto the basal planes of New York - a TOF_SIMS studu, *Chemical Engineering*.

Celik, M. and Somasundaran, P. (1980) Minerals by flotation and correlation with surfactant, in *American Institute of Mining, Metallurgy and Petroleum Engineers, Inc.*

Chau, T. (2009) A review of techniques for measurement of contact angles and their applicability on mineral surfaces, *Minerals Engineering*, 22, pp. 213–219.

Cho, Y. S. and Laskowski, J. S. (2002) Effect of flotation frothers on bubble size and foam stability, *International Journal of Mineral Processing*, 64(2–3), pp. 69–80. doi: 10.1016/S0301-7516(01)00064-3.

Corin, K. C., Reddy, A., Miyen, L., Wiese, J. G., Harris, P. J. (2011) The effect of ionic strength of plant water on valuable mineral and gangue recovery in a platinum bearing ore from the Merensky reef, *Minerals Engineering*. Elsevier Ltd, 24(2), pp. 131–137. doi: 10.1016/j.mineng.2010.10.015

Corin, K. C. and Wiese, J. G. (2014) Investigating froth stability: A comparative study of ionic strength and frother dosage *Minerals Engineering*. Elsevier Ltd, pp. 1–5. doi: 10.1016/j.mineng.2014.03.001.

Craig, V. ., Ninham, B. . and Pashley, R. (1993) The effect of electrolytes on bubble coalescence in water, *Jornal of Physical Chemistry*, 39(97), pp. 10192–10197.

Davis, F., Hyatt, D. and Cox, C. (1975) Environmental problems of flotation reagents in mineral processing plant tailings water.

Finkelstein, N. P. and Lovell, V. M. (1972) Fundamental studies of the flotation process: the work of the National Institute for Metallurgy, *Journal of the South African Institute of Mining and Metallurgy*, (July), p. 15.

Gray, D., Cameron, T. and Briggs, A. (2016) Kevitsa Nickel Copper Mine, Lapland, Finland, *NI 43-101 Technical Report 30th March*, (March), p. 146.

Gu, T., Gao, Y. and He, L. (1988) Hemimicelle formation of cationic surfactants at the silica gelwater interface, *Journal of the Chemical Society, Faraday Transactions : Physical Chemistry in Condensed Phases*, 84(12), pp. 4471–4473. doi: 10.1039/F19888404471.

Gungoren, Can, Islek, Elif, Baktarhan, Yasin, Unver, Ilgin Kursun, Ozdemir, Orhan (2018) A novel technique to investigate the bubble coalescence in the presence of surfactant (MIBC) and electrolytes (NaCl and $CaCl_2$), *Physicochemical Problems of Mineral Processing*, 54(4), pp. 1215–1222. doi: 10.5277/ppmp18158.

Gunn, G. and Benham, A. (2009) Minerals profile: Platinum, *British Geological Survey - Natutal enviroment research council*, Platinum(September), pp. 1–32.

Haggard, E. L., Sheridan, C. M. and Harding, K. G. (2015) Quantification of water usage at a South African platinum processing plant, *Water SA*, 41(2), pp. 279–286. doi: 10.4314/wsa.v41i2.14.

Hearn, S., , Muchon, H. And , Boskovic, S. (2015) A new approach to designing flotation frothers

Hirajima, Tsuyoshi, Suyantara, Gde Pandhe Wisnu, Ichikawa, Osamu, Elmahdy, Ahmed Mohamed, Miki, Hajime, Sasaki, Keiko (2016) Effect of Mg^{2+} and Ca^{2+} as divalent seawater cations on the floatability of molybdenite and chalcopyrite', *Minerals Engineering*. Elsevier Ltd, 96–97, pp. 83–93. doi: 10.1016/j.mineng.2016.06.023.

Hu, W. (2014) Flotation Circuit Optimisation and Design, (September). Available at: http://spiral.imperial.ac.uk/handle/10044/1/24805.

Ikumapayi, Fatai, Makitalo, Maria, Johansson, Bjorn, Hanumantha, Kota (2012) Recycling of process water in sulphide flotation : Effect of calcium and sulphate ions on flotation of galena, *Minerals Engineering*. Elsevier Ltd, 39, pp. 77–88. doi: 10.1016/j.mineng.2012.07.016.

Ikumapayi, F. and Makitalo, M. (2013) Recycling process water in sulphide flotation , Part A : Effect of calcium and sulphate on sphalerite recovery, 29(4), pp. 183–192.

Katko, T., Luonsi, A. and Juuti, P. (2006) Water pollution control and strategies in Finnish pulp and paper industries in the 20th century, *International Journal of Environment and Pollution*, 23(4), p. 368. doi: 10.1504/ijep.2005.007600.

Kawatra (2009) Froth Flotation – Fundamental Principles Flotation System, pp. 1–30.

Kelebek, S., Wells, P. F. and Fekete, S (1996) Differential flotation of chalcopyrite, pentlandite and pyrrhotite in Ni-Cu sulphide ores, *Metallurgical Technology Centre*, 35(4), pp. 329–336. doi: doi.org/10.1016/S0008-4433(96)00017-1.

Khoshdast, H. (2011) Flotation Frothers: Review of Their Classifications, Properties and Preparation,*The Open Mineral Processing Journal*, 4(1), pp. 25–44. doi: 10.2174/1874841401104010025.

Kirjavainen, V. (1996) Review and analysis of factors controlling the mechnical flotation of gangue minerals, *Minerals Engineering*, 46, pp. 21–34.

Kirjavainen, V. and Heiskanen, K. (2007) Some factors that affect beneficiation of sulphide nickel – copper ores, 20, pp. 629–633. doi: 10.1016/j.mineng.2007.01.001.

Kirjavainen, V., Schreithofer, N. and Heiskanen, K. (2002) Effect of calcium and thiosulfate ions on flotation selectivity of nickel-copper ores, *Minerals Engineering*, 15(1–2), pp. 1–5. doi: 10.1016/S0892-6875(01)00213-8.

Klimpel (1996) The effect of water chemistry, reagent type, and other environmental factors on the performance of industrial grinding and flotation processes involving sulphide minerals, *Society for mining, metallurgy and exploration,* 5002.

Konopacka, Z. and Drzymala, J. (2010) Types of particles recovery-water recovery entrainment plots useful in flotation research, *Adsorption*, 16(4–5), pp. 313–320. doi: 10.1007/s10450-010-9246.

Laskowski, J. S. (2004) Testing flotation frothers, *Physical Review B*, 38, pp. 13–22.

Laskowski, J. S. and Castro, S. (2017) Hydrolysis of metallic ions in mineral processing circuits and its effect on flotation, *COM Conference of Metallurgists*. doi: 10.14288/1.0347200.

Levay, G., Smart, R. and Skinner, W. (2001) The impact of water quality on flotation performance, *Journal of The South African Institute of Mining and Metallurgy*, 1, pp. 69–76. doi: 10.1007/978-3-319-

17446-4.

Li, Yubiao, Li, Wanqing, Xiao, Qing, He, Nan, Ren, Zijie, Lartey, Clement, Gerson, Andrea (2017) The Influence of Common Monovalent and Divalent Chlorides on Chalcopyrite Flotation, *Minerals Engineering*. doi:10.3390/min7070111.

Lotter, N. O. and Bradshaw, D. J. (2010) The formulation and use of mixed collectors in sulphide flotation, *Minerals Engineering*. Elsevier Ltd, 23(11–13), pp. 945–951. doi: 10.1016/j.mineng.2010.03.011.

Manono, M., Corin, K. and Wiese, J. (2018) Water quality effects on a sulfidic PGM ore : Implications for froth stability and gangue management, 54(4), pp. 1253–1265. doi: 10.5277/ppmp18181.

Manono, M S, Matibidi, K, Thubakgale, C K, Corin, K C, Wiese, J G (2017) Water Quality in PGM Ore Flotation : The effect of Ionic Strength and pH, pp. 777–784.

Manono, M. S., Corin, K. C. and Wiese, J. G. (2012) An investigation into the effect of various ions and their ionic strength on the flotation performance of a platinum bearing ore from the Merensky reef, *Minerals Engineering*. doi: 10.1016/j.mineng.2012.03.035.

Manono, M. S., Corin, K. C. and Wiese, J. G. (2013) The effect of ionic strength of plant water on foam stability: A 2-phase flotation study, *Minerals Engineering*. doi: 10.1016/j.mineng.2012.09.009.

Manono, M. S., Corin, K. C. and Wiese, J. G. (2016) The influence of electrolytes present in process water on the flotation behaviour of a Cu-Ni containing ore, *Minerals Engineering*. Elsevier Ltd, 96–97,pp.99–107.doi:10.1016/j.mineng.2016.06.015.

Melo, F. and Laskowski, J. S. (2006) Fundamental properties of flotation frothers and their effect on flotation, *Minerals Engineering*, 19(6–8), pp. 766–773. doi: 10.1016/j.mineng.2005.09.031.

Musuku, B., Muzinda, I. and Lumsden, B. (2016) Cu-Ni processing improvements at First Quantum's Kevitsa mine, *Minerals Engineering*. Elsevier Ltd, 88, pp. 9–17. doi: 10.1016/j.mineng.2015.08.005.

Muzenda, E. (2010) An Investigation into the Effect of Water Quality on Flotation Performance, 4(9),pp.562–566.

Muzinda, I. and Schreithofer, N. (2018) Water quality e ff ects on fl otation : Impacts and control of residual xanthates, 125(March), pp. 34–41. doi: 10.1016/j.mineng.2018.03.032.

P. Clarke, D. Fornasiero, J. R. And R. S. C. S. (1995) A study of the removal of oxidation products from sulphide mineral surfaces, *Minerals Engineering*, 8, pp. 1347–1357.

Qiu, Xuemin, Yang, Hongying, Chen, Guobao, Luo, Wenjie (2018) An Alternative Depressant of Chalcopyrite in Cu–Mo Differential Flotation and Its Interaction Mechanism, *Minerals*, 9(1), p. 1. doi:10.3390/min9010001.

Ralston, J. (1999) Controlled flotation processes : Prediction and manipulation of bubble- particle capture, *The Journal of The South African Institute of Mining and Metallurgy*, (February), pp. 27–34.

Runpeng Liao, Jiushuai Deng, Hao Lai, Jiaozhong Cai, Xi Zhang, Shuming Wen, Hua Yang, Jianying Deng, J. and Sun, F. and X. (2018) An Overview of Technologies and Selective Depressing Agents for Separating Chalcopyrite and Talc, *International Journal of Metallurgical & Materials Engineering* ,4.

Savassi, O. N, Alexander, D. J, Franzidis, J. P, Manlapig, E.V (1998) An emperical model for entraimnet in industrial flotation plants, *Minerals Engineering*, 11(3), pp. 243–256.

Schreithofer, N. (2018) Overview of historical plant data analysis work performed at Aalto Motivation of the work.

Schreithofer, N., Muzinda, I. and Kevitsa, B. (2017) *Boliden Kevitsa Mine*. Slatter K.A.;Vaux ; N.D. Plint; M. COLE; V. Dilsook ; D. De oostendorp, N. P. and B. (2009) Water management in anglo platinum process operations : effects of water quality on process operations, (October), pp. 46–55.

Usaini, M. N. S., Ali, M. and Usman, H. A. (2014) Determination of liberation size of akiri copper ore, Nasarawa State, North-Central Nigeria, *Int. J. Eng. Dev. Res*, 2(2), pp. 1444–1452.

Wang, L., Peng, Y. and Runge, K. (2016) Entrainment in froth flotation: The degree of entrainment and its contributing factors, *Powder Technology*. Elsevier B.V., 288, pp. 202–211. doi: 10.1016/j.powtec.2015.10.049.

Wiese, J. (2009) Investigating depressant behaviour in the flotation of selected Merensky ores, (November), p. 140.

Wiese, J, Harris, P. and Bradshaw, D. (2005) Investigation of the role and interactions of a dithiophosphate collector in the flotation of sulphides from the Merensky reef, 18, pp. 791–800.

doi:10.1016/j.mineng.2005.01.032.

Wiese, J., Harris, P. and Bradshaw, D. (2005) The influence of the reagent suite on the flotation of ores from the Merensky reef, *Minerals Engineering*, 18(2 SPEC. ISS.), pp. 189–198. doi: 10.1016/j.mineng.2004.09.013.

Wills, B. A. and Napier-Munn, T. (2006) An introduction to the practical aspects of ore treatment and mineral recovery, *Mineral processing technology*. doi: 10.1016/b978-075064450-1/50003-5.

APPENDICES

Appendix A-1: Water and Solids recovery for 3, 5 and 10 SPW

Where: C (C1, C2……C6) = weight of concentrate (g)
F = Feed (g)
T1 and T2 = Tailings (g) for assaying
T = Overall tailings (g)

Water type	Sample	Time, min	Mass Pull, g	Water Rec, g	Cum Mass, g	Cum Water, g	Ave cum Mass, g	Std dev	Std error	Ave cum w Rec, g	Std dev	Std error
Run-01		0				0.00	0.00		0.00	0.00		0.00
3 SPW	C1	5	181.30	1219.70	181.30	1219.70	176.79	6.38	4.51	1211.35	11.81	8.35
	C2	10	29.86	396.00	211.16	1615.70	202.57	12.16	8.59	1544.40	100.83	71.30
	C3	17.5	8.81	150.50	219.97	1766.20	213.28	9.46	6.69	1710.55	78.70	55.65
	C4	25	10.97	332.40	230.94	2098.60	222.44	12.03	8.50	2006.95	129.61	91.65
	C5	37.5	7.52	160.90	238.46	2259.50	229.37	12.86	9.09	2128.75	184.91	130.75
	C6	50	2.92	41.50	241.38	2301.00	232.83	12.10	8.55	2192.00	154.15	109.00
	F		970.54									
	T		724.38									
	T2		3.72									
	T3		1.06									
	Cc+Tt											
	Mass Bal											
Run-02		0				0.00						
3 SPW	C1	5	172.28	1203.00	172.28	1203.00						
	C2	10	21.69	270.10	193.97	1473.10						
	C3	17.5	12.62	181.80	206.59	1654.90						
	C4	25	7.34	260.40	213.93	1915.30						
	C5	37.5	6.34	82.70	220.27	1998.00						
	C6	50	4.00	85.00	224.27	2083.00						
	F		966.97									
	T		731.44									
	T2		5.26									
	T3		6.00									
	Cc+Tt											
	Mass Bal											

Water type	Sample	Time, min	Mass Pull, g	Water Rec, g	Cum Mass, g	Cum Water, g	Ave cum Mass, g	Std dev	Std error	Ave cum w Rec, g	Std dev	Std error
Run-01		0				0.00	0.00		0.00	0.00		0.00
5 SPW	C1	5	168.62	1628.90	168.62	1628.90	140.84	39.29	27.78	1643.08	20.05	14.18
	C2	10	32.03	1017.23	200.65	2646.13	177.00	33.45	23.66	2814.81	238.55	168.68
	C3	17.5	8.65	386.60	209.30	3032.73	189.83	27.54	19.48	3220.45	265.48	187.72
	C4	25	9.08	70.66	218.38	3103.39	198.12	28.66	20.27	3405.39	427.09	302.00
	C5	37.5	5.71	130.40	224.09	3233.79	204.84	27.22	19.25	3627.10	556.22	393.30
	C6	50	4.19	87.20	228.28	3320.99	210.11	25.70	18.18	3812.97	695.76	491.98
	F		981.27									
	T		730.82									
	T2		11.70									
	T3		10.47									
	Cc+Tt											
	Mass Bal											
Run-02		0				0.00						
5 SPW	C1	5	113.06	1657.26	113.06	1657.26						
	C2	10	40.28	1326.23	153.34	2983.49						
	C3	17.5	17.01	424.68	170.35	3408.17						
	C4	25	7.50	299.22	177.85	3707.39						
	C5	37.5	7.74	313.01	185.59	4020.40						
	C6	50	6.34	284.55	191.93	4304.95						
	F		889.60									
	T		673.02									
	T2		12.18									
	T3		12.47									
	Cc+Tt											
	Mass Bal											

Water type	Sample	Time, min	Mass Pull, g	Water Rec, g	Cum Mass, g	Cum Water, g	Ave cum Mass, g	Std dev	Std error	Ave cum w Rec, g	Std dev	Std error
Run-01		0					0.00		0.00	0.00		0.00
10 SPW	C1	5	162.44	1769.85	162.44	1769.85	160.35	2.96	2.09	1764.59	7.44	5.26
	C2	10	41.70	1035.64	204.14	2805.49	200.65	4.94	3.49	2767.77	53.34	37.72
	C3	17.5	15.90	665.45	220.04	3470.94	216.16	5.49	3.88	3411.88	83.53	59.06
	C4	25	8.78	554.21	228.82	4025.15	225.46	4.76	3.36	4057.82	46.20	32.67
	C5	37.5	13.46	828.64	242.28	4853.79	238.24	5.72	4.05	4757.37	136.37	96.42
	C6	50	7.77	530.29	250.05	5384.08	247.40	3.75	2.66	5266.36	166.48	117.72
	F		865.06									
	T		592.26									
	T2		11.02									
	T3		11.73									
	Cc+Tt											
	Mass Bal											
Run-02		0										
10 SPW	C1	5	158.26	1759.33	158.26	1759.33						
	C2	10	38.90	970.72	197.16	2730.05						
	C3	17.5	15.12	622.76	212.28	3352.81						
	C4	25	9.81	737.67	222.09	4090.48						
	C5	37.5	12.10	570.46	234.19	4660.94						
	C6	50	10.55	487.70	244.74	5148.64						
	F		902.75									
	T		638.21									
	T2		10.37									
	T3		9.43									
	Cc+Tt											
	Mass Bal											

Appendix A-2: Water and Solids recovery for 3 SPW spiked with Ca^{2+} and Mg^{2+}

Water type	Sample	Time, min	Mass Pull, g	Water Rec, g	Cum Mass, g	Cum Water, g	Ave cum Mass, g	Std dev	Std error	Ave cum w Rec, g	Std dev	Std error
		0					0.00		0.00	0.00		0.00
Run-01	C1	5	158.14	1566.51	158.14	1566.51	158.80	0.93	0.65	1570.63	5.82	4.12
3SPW	C2	10	28.07	669.18	186.21	2235.69	189.56	4.73	3.34	2272.99	52.74	37.30
3 SPW + 400 ppm Ca^{2+}	C3	17.5	14.49	495.25	200.70	2730.94	203.24	3.59	2.53	2790.63	84.41	59.69
	C4	25	12.44	541.26	213.14	3272.20	213.37	0.32	0.22	3255.83	23.16	16.38
	C5	37.5	20.72	611.51	233.86	3883.71	228.12	8.12	5.75	3807.03	108.45	76.68
	C6	50	4.18	233.53	238.04	4117.24	232.89	7.28	5.15	4069.99	66.83	47.26
	F		872.79									
	T		616.70									
	T2		10.48									
	T3		7.57									
	Cc+Tt											
	Mass Bal											
		0										
Run-02	C1	5	159.45	1574.74	159.45	1574.74						
3SPW	C2	10	33.45	735.54	192.90	2310.28						
3 SPW + 400 ppm Ca^{2+}	C3	17.5	12.87	540.03	205.77	2850.31						
	C4	25	7.82	389.14	213.59	3239.45						
	C5	37.5	8.78	490.89	222.37	3730.34						
	C6	50	5.37	292.39	227.74	4022.73						
	F		889.82									
	T		634.88									
	T2		12.96									
	T3		14.24									
	Cc+Tt											
	Mass Bal											

Water type	Sample	Time, min	Mass Pull, g	Water Rec, g	Cum Mass, g	Cum Water, g	Ave cum Mass, g	Std dev	Std error	Ave cum w Rec, g	Std dev	Std error
		0					0.00		0.00	0.00		0.00
Run-01	C1	5	203.31	2006.07	203.31	2006.07	198.79	6.39	4.52	1943.99	87.80	62.09
3SPW	C2	10	31.49	670.94	234.80	2677.01	231.15	5.17	3.66	2663.90	18.55	13.12
3 SPW + 800 ppm Ca^{2+}	C3	17.5	12.21	647.13	247.01	3324.14	243.99	4.28	3.03	3283.93	56.87	40.21
	C4	25	7.66	515.02	254.67	3839.16	251.85	3.99	2.82	3782.75	79.78	56.42
	C5	37.5	9.66	631.15	264.33	4470.31	261.59	3.88	2.75	4364.22	150.04	106.10
	C6	50	3.74	247.06	268.07	4717.37	265.89	3.08	2.18	4626.58	128.40	90.79
	F		918.87									
	T		630.57									
	T2		5.25									
	T3		14.98									
	Cc+Tt											
	Mass Bal											
		0										
Run-02	C1	5	194.27	1881.90	194.27	1881.90						
3SPW	C2	10	33.22	768.88	227.49	2650.78						
3 SPW + 800 ppm Ca^{2+}	C3	17.5	13.47	592.94	240.96	3243.72						
	C4	25	8.07	482.61	249.03	3726.33						
	C5	37.5	9.81	531.79	258.84	4258.12						
	C6	50	4.87	277.67	263.71	4535.79						
	F		940.02									
	T		669.64									
	T2		9.51									
	T3		11.84									
	Cc+Tt											
	Mass Bal											

Water type	Sample	Time, min	Mass Pull, g	Water Rec, g	Cum Mass, g	Cum Water, g	Ave cum Mass, g	Std dev	Std error	Ave cum w Rec, g	Std dev	Std error
		0					0.00		0.00	0.00		0.00
Run-01	C1	5	143.23	1435.80	143.23	1435.80	146.77	5.00	3.54	1410.03	36.45	25.78
3SPW	C2	10	26.74	606.97	169.97	2042.77	174.53	6.45	4.56	2058.68	22.50	15.91
3 SPW + 350 ppm Mg^{2+}	C3	17.5	11.80	414.09	181.77	2456.86	186.29	6.39	4.52	2482.31	35.98	25.45
	C4	25	8.20	305.55	189.97	2762.41	194.64	6.60	4.67	2830.95	96.93	68.54
	C5	37.5	10.64	390.77	200.61	3153.18	204.79	5.90	4.18	3273.02	169.47	119.84
	C6	50	4.24	239.67	204.85	3392.85	209.80	6.99	4.94	3568.43	248.31	175.58
	F		913.21									
	T		686.29									
	T2		11.44									
	T3		10.63									
	Cc+Tt											
	Mass Bal											
		0										
Run-02	C1	5	150.30	1384.25	150.30	1384.25						
3SPW	C2	10	28.79	690.34	179.09	2074.59						
3 SPW + 350 ppm Mg^{2+}	C3	17.5	11.71	433.16	190.80	2507.75						
	C4	25	8.50	391.74	199.30	2899.49						
	C5		9.66	493.36	208.96	3392.85						
	C6		5.78	351.16	214.74	3744.01						
	F	37.5	904.77									
	T	50	665.76									
	T2		10.21									
	T3		14.06									
	Cc+Tt											
	Mass Bal											

Water type	Sample	Time, min	Mass Pull, g	Water Rec, g	Cum Mass, g	Cum Water, g	Ave cum Mass, g	Std dev	Std error	Ave cum w Rec, g	Std dev	Std error
		0					0.00		0.00	0.00		0.00
Run-01	C1	5	126.71	1342.57	126.71	1342.57	128.04	1.88	1.33	1365.61	32.58	23.04
3SPW	C2	10	30.32	647.16	157.03	1989.73	156.87	0.23	0.16	1999.48	13.79	9.75
3 SPW + 700 ppm Mg^{2+}	C3	17.5	17.93	605.27	174.96	2595.00	172.36	3.68	2.60	2513.20	115.69	81.81
	C4	25	11.13	510.42	186.09	3105.42	183.00	4.37	3.09	2977.93	180.31	127.50
	C5	37.5	10.99	529.92	197.08	3635.34	194.67	3.41	2.41	3519.20	164.25	116.15
	C6	50	8.00	393.95	205.08	4029.29	202.11	4.21	2.97	3889.42	197.81	139.88
	F		911.23									
	T		683.97									
	T2		9.84									
	T3		12.34									
	Cc+Tt											
	Mass Bal											
Run-02		0										
3SPW	C1	5	129.37	1388.64	129.37	1388.64						
3 SPW + 700 ppm Mg^{2+}	C2	10	27.34	620.59	156.71	2009.23						
	C3	17.5	13.05	422.16	169.76	2431.39						
	C4	25	10.15	419.04	179.91	2850.43						
	C5	37.5	12.35	552.62	192.26	3403.05						
	C6	50	6.87	346.49	199.13	3749.54						
	F		921.95									
	T		685.09									
	T2		26.33									
	T3		11.40									
	Cc+Tt											
	Mass Bal											

Appendix A-3: Water and Solids recovery for 3 SPW spiked with: NO_3^-, SO_4^{2-} and $S_2O_3^{2-}$

Water type	Sample	Time, min	Mass Pull, g	Water Rec, g	Cum Mass, g	Cum Water, g	Ave cum Mass, g	Std dev	Std error	Ave cum w Rec, g	Std dev	Std error
		0					0.00		0.00	0.00		0.00
Run-01	C1	5	161.60	1421.60	161.60	1421.60	154.35	10.26	7.25	1374.15	67.10	47.45
3SPW	C2	10	24.24	590.60	185.84	2012.20	177.42	11.91	8.43	1921.44	128.36	90.76
3 SPW + 880 ppm NO_3^-	C3	17.5	12.89	486.81	198.73	2499.01	190.13	12.17	8.61	2377.62	171.67	121.39
	C4	25	10.52	480.03	209.25	2979.04	199.21	14.20	10.04	2764.98	302.73	214.07
	C5	37.5	8.49	438.58	217.74	3417.62	207.58	14.38	10.17	3177.31	339.85	240.31
	C6	50	7.89	428.17	225.63	3845.79	214.70	15.46	10.94	3543.96	426.85	301.83
	F		923.42									
	T		672.59									
	T2		14.49									
	T3		10.71									
	Cc+Tt											
	Mass Bal											
		0										
Run-02	C1	5	147.09	1326.70	147.09	1326.70						
3SPW	C2	10	21.90	503.97	168.99	1830.67						
3 SPW + 880 ppm NO_3^-	C3	17.5	12.53	425.56	181.52	2256.23						
	C4	25	7.65	294.68	189.17	2550.91						
	C5	37.5	8.24	386.09	197.41	2937.00						
	C6	50	6.35	305.13	203.76	3242.13						
	F		919.38									
	T		687.82									
	T2		14.15									
	T3		13.65									
	Cc+Tt											
	Mass Bal											

Water type	Sample	Time, min	Mass Pull, g	Water Rec, g	Cum Mass, g	Cum Water, g	Ave cum Mass, g	Std dev	Std error	Ave cum w Rec, g	Std dev	Std error
		0					0.00		0.00	0.00	0.00	0.00
Run-01	C1	5	174.37	1577.70	174.37	1577.70	172.80	2.22	1.57	1558.73	26.83	18.98
3SPW	C2	10	18.00	521.19	192.37	2098.89	191.47	1.28	0.91	2034.63	90.88	64.26
3 SPW + 1760 ppm NO_3^-	C3	17.5	9.96	387.23	202.33	2486.12	203.19	1.22	0.86	2466.86	27.24	19.26
	C4	25	8.42	408.35	210.75	2894.47	210.72	0.04	0.03	2816.99	109.58	77.48
	C5	37.5	8.56	435.16	219.31	3329.63	219.78	0.66	0.47	3270.01	84.32	59.62
	C6	50	5.82	315.30	225.13	3644.93	224.57	0.79	0.56	3519.69	177.12	125.24
	F		924.84									
	T		671.78									
	T2		13.32									
	T3		14.61									
	Cc+Tt											
	Mass Bal											
		0										
Run-02	C1	5	171.23	1539.75	171.23	1539.75						
3SPW	C2	10	19.33	430.62	190.56	1970.37						
3 SPW + 1760 ppm NO_3^-	C3	17.5	13.49	477.22	204.05	2447.59						
	C4	25	6.64	291.91	210.69	2739.50						
	C5	37.5	9.55	470.89	220.24	3210.39						
	C6	50	3.77	184.06	224.01	3394.45						
	F		919.44									
	T		670.31									
	T2		11.82									
	T3		13.30									
	Cc+Tt											
	Mass Bal											

Water type	Sample	Time, min	Mass Pull, g	Water Rec, g	Cum Mass, g	Cum Water, g	Ave cum Mass, g	Std dev	Std error	Ave cum w Rec, g	Std dev	Std error
		0					0.00		0.00	0.00		0.00
Run-01	C1	5	184.67	1644.58	184.67	1644.58	175.95	12.34	8.72	1620.45	34.13	24.14
3SPW	C2	10	21.36	555.85	206.03	2200.43	194.88	15.78	11.16	2125.66	105.75	74.78
3 SPW + 1200 ppm SO_4^{2-}	C3	17.5	9.77	369.98	215.80	2570.41	206.12	13.69	9.68	2491.88	111.07	78.54
	C4	25	7.17	343.74	222.97	2914.15	214.25	12.34	8.72	2874.52	56.05	39.63
	C5	37.5	6.99	348.43	229.96	3262.58	221.64	11.77	8.32	3276.54	19.74	13.95
	C6	50	5.83	305.68	235.79	3568.26	231.94	5.45	3.85	3567.51	1.06	0.75
	F		909.23									
	T		646.76									
	T2		12.64									
	T3		14.04									
	Cc+Tt											
	Mass Bal											
		0										
Run-02	C1	5	167.22	1596.31	167.22	1596.31						
3SPW	C2	10	16.50	454.57	183.72	2050.88						
3 SPW + 1200 ppm SO_4^{2-}	C3	17.5	12.72	362.46	196.44	2413.34						
	C4	25	9.08	421.55	205.52	2834.89						
	C5	37.5	7.80	455.60	213.32	3290.49						
	C6	50	14.76	276.27	228.08	3566.76						
	F		911.24									
	T		658.82									
	T2		12.42									
	T3		11.92									
	Cc+Tt											
	Mass Bal											

Water type	Sample	Time, min	Mass Pull, g	Water Rec, g	Cum Mass, g	Cum Water, g	Ave cum Mass, g	Std dev	Std error	Ave cum w Rec, g	Std dev	Std error
Run-01		0					0.00		0.00	0.00		0.00
3SPW	C1	5	189.03	1631.90	189.03	1631.90	192.00	4.20	2.97	1726.12	133.25	94.22
3 SPW + 2400 ppm SO_4^{2-}	C2	10	26.67	677.33	215.70	2309.23	220.20	6.36	4.50	2327.13	25.31	17.90
	C3	17.5	12.96	491.31	228.66	2800.54	232.54	5.49	3.88	2727.00	104.01	73.55
	C4	25	7.14	346.54	235.80	3147.08	240.13	6.12	4.33	3096.65	71.33	50.43
	C5	37.5	8.39	416.58	244.19	3563.66	248.65	6.31	4.46	3529.08	48.90	34.58
	C6	50	4.37	228.69	248.56	3792.35	253.04	6.33	4.47	3755.08	52.71	37.27
	F		916.68									
	T		646.65									
	T2		12.76									
	T3		8.71									
	Cc+Tt											
	Mass Bal											
		0										
Run-02	C1	5	194.97	1820.34	194.97	1820.34						
3SPW	C2	10	29.73	524.68	224.70	2345.02						
3 SPW + 2400 ppm SO_4^{2-}	C3	17.5	11.72	308.43	236.42	2653.45						
	C4	25	8.04	392.76	244.46	3046.21						
	C5	37.5	8.65	448.29	253.11	3494.50						
	C6	50	4.40	223.31	257.51	3717.81						
	F		916.54									
	T		634.60									
	T2		11.73									
	T3		12.70									
	Cc+Tt											
	Mass Bal											

Water type	Sample	Time, min	Mass Pull, g	Water Rec, g	Cum Mass, g	Cum Water, g	Ave cum Mass, g	Std dev	Std error	Ave cum w Rec, g	Std dev	Std error
		0					0.00		0.00	0.00		0.00
Run-01	C1	5	179.11	1589.97	179.11	1589.97	187.97	12.53	8.86	1573.65	23.08	16.32
3SPW	C2	10	28.80	664.18	207.91	2254.15	215.33	10.49	7.41	2240.40	19.45	13.75
3 SPW + 60 ppm $S_2O_3^{2-}$	C3	17.5	12.48	417.26	220.39	2671.41	226.68	8.89	6.29	2666.87	6.42	4.54
	C4	25	8.87	418.29	229.26	3089.70	234.98	8.09	5.72	3062.98	37.79	26.72
	C5	37.5	9.54	532.83	238.80	3622.53	243.58	6.75	4.78	3561.16	86.79	61.37
	C6	50	6.15	385.29	244.95	4007.82	249.17	5.96	4.22	3922.66	120.44	85.16
	F		918.06									
	T		648.28									
	T2		12.64									
	T3		12.19									
	Cc+Tt											
	Mass Bal											
Run-02		0										
3SPW	C1	5	196.83	1557.33	196.83	1557.33						
3 SPW + 60 ppm $S_2O_3^{2-}$	C2	10	25.91	669.32	222.74	2226.65						
	C3	17.5	10.22	435.68	232.96	2662.33						
	C4	25	7.74	373.93	240.70	3036.26						
	C5	37.5	7.65	463.53	248.35	3499.79						
	C6	50	5.03	337.70	253.38	3837.49						
	F		915.60									
	T		641.55									
	T2		11.49									
	T3		9.18									
	Cc+Tt											
	Mass Bal											

Water type	Sample	Time, min	Mass Pull, g	Water Rec, g	Cum Mass, g	Cum Water, g	Ave cum Mass, g	Std dev	Std error	Ave cum w Rec, g	Std dev	Std error
		0					0.00		0.00	0.00		0.00
Run-01	C1	5	171.33	1382.99	171.33	1382.99	162.96	11.84	8.38	1336.41	65.87	46.58
3SPW	C2	10	24.78	617.65	196.11	2000.64	189.13	9.87	6.98	1948.02	74.42	52.62
3 SPW + 78 ppm $S_2O_3^{2-}$	C3	17.5	11.30	436.16	207.41	2436.80	202.41	7.07	5.00	2419.32	24.73	17.48
	C4	25	7.27	335.17	214.68	2771.97	211.41	4.63	3.28	2833.55	87.08	61.58
	C5	37.5	7.86	419.31	222.54	3191.28	219.29	4.60	3.26	3284.86	132.34	93.58
	C6	50	5.30	285.97	227.84	3477.25	224.71	4.43	3.13	3578.13	142.67	100.88
	F		910.16									
	T		658.47									
	T2		11.05									
	T3		12.80									
	Cc+Tt											
	Mass Bal											
Run-02		0										
3SPW	C1	5	154.58	1289.83	154.58	1289.83						
3 SPW + 78 ppm $S_2O_3^{2-}$	C2	10	27.57	605.57	182.15	1895.40						
	C3	17.5	15.26	506.43	197.41	2401.83						
	C4	25	10.72	493.29	208.13	2895.12						
	C5	37.5	7.90	483.32	216.03	3378.44						
	C6	50	5.55	300.57	221.58	3679.01						
	F		902.79									
	T		658.49									
	T2		12.83									
	T3		9.89									
	Cc+Tt											
	Mass Bal											

Appendix A-4: Copper and Nickel's recovery and grade for 3, 5 and 10 SPW

	Sample	Time, min	Copper %	Copper Grade %	Copper Rec %	Ave Copper grade %	Std dev	Std error	Ave Copper rec %	Std dev	Std error	Nickel %	Nickel Grade 10%	Nickel Rec %	Ave Nickel grade %	Std dev	Std error	Ave Nickel rec %	Std dev	Std error
				10									10							
Run-01		0		0.00	0.00	0.00		0.00	0.00		0.00	0.00		0.00			0.00	0.00		0.00
3 SPW	C1	5	1.14	11.35	84.80	11.93	0.81	0.57	85.53	1.03	0.73	0.65	6.50	64.90	6.95	0.65	0.46	66.58	2.37	1.68
	C2	10	0.29	10.15	88.33	10.77	0.88	0.62	88.41	0.11	0.08	0.26	5.94	69.12	6.39	0.64	0.45	70.03	1.29	0.91
	C3	17.5	0.20	9.82	89.04	10.32	0.70	0.49	89.25	0.30	0.21	0.28	5.81	70.49	6.20	0.54	0.38	71.56	1.52	1.07
	C4	25	0.15	9.43	89.73	9.97	0.77	0.54	89.92	0.26	0.19	0.21	5.64	71.79	6.03	0.56	0.39	72.66	1.23	0.87
	C5	37.5	0.15	9.18	90.19	9.75	0.80	0.57	90.60	0.58	0.41	0.20	5.53	72.62	5.93	0.57	0.40	73.61	1.41	1.00
	C6	50	0.23	9.09	90.46	9.63	0.76	0.54	90.92	0.65	0.46	0.22	5.49	72.97	5.87	0.55	0.39	74.03	1.49	1.05
	F		0.28									0.20								
	T																			
	T2		0.03		0.06							0.08								
	T3		0.04									0.06								
	Cc+Tt																			
	Mass Bal																			
Run-02		0										0.00								
3 SPW	C1	5	1.25	12.50	86.26							0.74	7.41	68.25						
	C2	10	0.26	11.39	88.48							0.23	6.84	70.94						
	C3	17.5	0.19	10.81	89.47							0.25	6.58	72.64						
	C4	25	0.22	10.52	90.11							0.23	6.43	73.53						
	C5	37.5	0.36	10.32	91.01							0.32	6.34	74.61						
	C6	50	0.22	10.17	91.37							0.22	6.26	75.08						
	F		0.28									0.19								
	T																			
	T2		0.03									0.06								
	T3		0.04									0.06								
	Cc+Tt																			
	Mass Bal																			

	Sample	Time, min	Copper %	Copper Grade %	Copper Rec %	Ave Copper grade %	Std dev	Std error	Ave Copper rec %	Std dev	Std error	Nickel %	Nickel Grade 10%	Nickel Rec %	Ave Nickel grade %	Std dev	Std error	Ave Nickel rec %	Std dev	Std error
Run-01		0			0.00			0.00	0.00		0.00	0.00		0.00			0.00	0.00		0.00
5 SPW	C1	5	1.33	13.31	92.50	14.10	1.12	0.79	79.98	17.70	12.51	0.89	8.90	64.53	9.25	0.51	0.36	58.81	8.09	5.72
	C2	10	0.21	11.51	95.21	11.59	0.10	0.07	83.41	16.69	11.80	0.29	7.94	68.52	8.03	0.14	0.10	64.71	5.39	3.81
	C3	17.5	0.19	11.12	95.90	10.91	0.30	0.21	84.44	16.21	11.46	0.42	7.78	70.08	7.77	0.02	0.01	67.32	3.90	2.76
	C4	25	0.17	10.73	96.54	10.53	0.28	0.20	85.08	16.20	11.46	0.30	7.58	71.25	7.59	0.01	0.01	68.64	3.69	2.61
	C5	37.5	0.25	10.52	97.14	10.25	0.38	0.27	85.67	16.22	11.47	0.36	7.48	72.13	7.45	0.04	0.03	69.73	3.40	2.40
	C6	50	0.25	10.37	97.56	10.04	0.46	0.33	86.12	16.18	11.44	0.30	7.40	72.68	7.34	0.09	0.06	70.43	3.18	2.25
	F		0.26									0.25								
	T																			
	T2		0.03									0.09								
	T3		0.04									0.08								
	Cc+Tt																			
	Mass Bal																			
Run-02		0																		
5 SPW	C1	5	1.49	14.90	67.47							0.96	9.61	53.09						
	C2	10	0.26	11.66	71.61							0.40	8.13	60.90						
	C3	17.5	0.20	10.69	72.98							0.44	7.76	64.56						
	C4	25	0.22	10.34	73.63							0.40	7.60	66.03						
	C5	37.5	0.19	9.98	74.21							0.34	7.43	67.33						
	C6	50	0.19	9.71	74.68							0.28	7.27	68.19						
	F		0.26									0.24								
	T																			
	T2		0.03									0.08								
	T3		0.05									0.10								
	Cc+Tt																			
	Mass Bal																			

APPENDICES

	Sample	Time, min	Copper %	Copper Grade %	Copper Rec %	Ave Copper grade %	Std dev	Std error	Ave Copper rec %	Std dev	Std error	Nickel %	Nickel Grade 10%	Nickel Rec %	Ave Nickel grade %	Std dev	Std error	Ave Nickel rec %	Std dev	Std error
Run-01		0						0.00	0.00		0.00							0.00		0.00
10 SPW	C1	5	1.33	13.28	85.61	13.82	0.77	0.55	86.28	0.95	0.67	0.89	8.91	73.92	9.25	0.48	0.34	69.06	6.88	4.87
	C2	10	0.19	10.95	88.72	11.44	0.69	0.49	89.32	0.86	0.60	0.30	7.70	80.32	8.02	0.44	0.31	74.91	7.65	5.41
	C3	17.5	0.21	10.31	90.02	10.78	0.67	0.47	90.67	0.91	0.65	0.34	7.39	83.10	7.73	0.47	0.33	77.75	7.57	5.35
	C4	25	0.20	9.99	90.71	10.41	0.60	0.43	91.37	0.94	0.66	0.37	7.25	84.77	7.55	0.42	0.29	79.22	7.85	5.55
	C5	37.5	0.18	9.53	91.69	9.96	0.60	0.42	92.32	0.89	0.63	0.30	7.01	86.81	7.31	0.41	0.29	81.04	8.15	5.76
	C6	50	0.19	9.30	92.27	9.66	0.51	0.36	93.01	1.04	0.74	0.25	6.87	87.80	7.13	0.36	0.25	82.12	8.03	5.68
	F		0.29									0.26								
	T																			
	T2		0.03									0.04								
	T3		0.03									0.03								
	Cc+Tt																			
	Mass Bal																			
Run-02		0																		
10 SPW	C1	5	1.44	14.37	86.95							0.96	9.59	64.19						
	C2	10	0.20	11.93	89.93							0.32	8.33	69.49						
	C3	17.5	0.24	11.25	91.32							0.45	8.06	72.40						
	C4	25	0.19	10.84	92.03							0.31	7.84	73.67						
	C5	37.5	0.20	10.38	92.95							0.32	7.60	75.28						
	C6	50	0.20	10.02	93.75							0.26	7.38	76.44						
	F		0.26									0.24								
	T																			
	T2		0.03									0.08								
	T3		0.03									0.09								
	Cc+Tt																			
	Mass Bal																			

Appendix A-5: Copper and Nickel's recovery and grade for 3 SPW spiked with Ca^{2+} and Mg^{2+}

	Sample	Time, min	Copper %	Copper Grade %	Copper Rec %	Ave Copper grade %	Std dev	Std error	Ave Copper rec %	Std dev	Std error	Nickel %	Nickel Grade 10%	Nickel Rec %	Ave Nickel grade %	Std dev	Std error	Ave Nickel rec %	Std dev	Std error
		0			0.00			0.00	0.00		0.00							0.00		0.00
Run-01	C1	5	1.54	15.37	86.73	14.85	0.73	0.52	84.86	2.63	1.86	1.01	10.12	66.13	10.10	0.03	0.02	65.71	0.60	0.42
3SPW	C2	10	0.24	13.41	89.14	12.82	0.84	0.60	87.37	2.50	1.77	0.35	9.13	70.23	8.99	0.19	0.14	69.80	0.60	0.42
3 SPW + 400 ppm Ca^{2+}	C3	17.5	0.19	12.58	90.13	12.07	0.72	0.51	88.28	2.62	1.85	0.38	8.74	72.53	8.62	0.17	0.12	71.79	1.05	0.74
	C4	25	0.19	11.96	90.96	11.59	0.53	0.37	88.98	2.81	1.98	0.30	8.41	74.08	8.36	0.08	0.05	73.07	1.43	1.01
	C5	37.5	0.00	10.90	90.96	10.83	0.09	0.06	88.98	2.81	1.98	0.17	7.81	75.50	7.95	0.19	0.14	74.26	1.75	1.24
	C6	50	0.19	10.74	91.24	10.65	0.13	0.09	89.30	2.74	1.94	0.26	7.72	75.94	7.84	0.16	0.12	74.76	1.67	1.18
	F		0.26									0.25								
	T																			
	T2		0.03									0.09								
	T3		0.05									0.10								
	Cc+Tt																			
	Mass Bal																			
		0																		
Run-02	C1	5	1.43	14.33	83.00							1.01	10.08	65.29						
3SPW	C2	10	0.21	12.22	85.61							0.30	8.85	69.38						
3 SPW + 400 ppm Ca^{2+}	C3	17.5	0.17	11.56	86.42							0.32	8.50	71.05						
	C4	25	0.20	11.21	86.99							0.32	8.30	72.05						
	C5	37.5	0.00	10.77	86.99							0.27	8.08	73.02						
	C6	50	0.19	10.56	87.36							0.25	7.95	73.58						
	F		0.28									0.26								
	T																			
	T2		0.03									0.08								
	T3		0.07									0.11								
	Cc+Tt																			
	Mass Bal																			

	Sample	Time, min	Copper %	Copper Grade %	Copper Rec %	Ave Copper grade %	Std dev	Std error	Ave Copper rec %	Std dev	Std error	Nickel %	Nickel Grade 10%	Nickel Rec %	Ave Nickel grade %	Std dev	Std error	Ave Nickel rec %	Std dev	Std error
		0							0.00		0.00						0.00	0.00		0.00
Run-01	C1	5	0.98	9.78	83.81	11.54	2.48	1.75	86.10	3.23	2.29	0.86	8.61	64.97	9.63	1.44	1.01	66.00	1.46	1.03
3SPW	C2	10	0.24	8.79	87.00	10.22	2.01	1.42	88.82	2.59	1.83	0.33	7.90	68.84	8.71	1.15	0.81	69.56	1.02	0.72
3 SPW + 800 ppm Ca^{2+}	C3	17.5	0.18	8.45	87.92	9.77	1.86	1.32	89.67	2.48	1.75	0.37	7.69	70.51	8.44	1.06	0.75	71.17	0.95	0.67
	C4	25	0.20	8.25	88.56	9.52	1.79	1.26	90.24	2.38	1.68	0.33	7.56	71.44	8.28	1.02	0.72	72.06	0.87	0.62
	C5	37.5	0.17	8.01	89.24	9.23	1.71	1.21	90.86	2.29	1.62	0.31	7.40	72.56	8.08	0.97	0.69	73.10	0.76	0.54
	C6	50	0.23	7.93	89.60	9.10	1.66	1.17	91.18	2.23	1.58	0.27	7.33	72.94	7.99	0.94	0.66	73.48	0.76	0.54
	F		0.26									0.27								
	T																			
	T2		0.03									0.11								
	T3		0.04									0.11								
	Cc+Tt																			
	Mass Bal																			
		0																		
Run-02	C1	5	1.33	13.29	88.38							1.06	10.64	67.04						
3SPW	C2	10	0.20	11.64	90.65							0.30	9.53	70.27						
3 SPW + 800 ppm Ca^{2+}	C3	17.5	0.17	11.08	91.42							0.36	9.19	71.84						
	C4	25	0.18	10.78	91.92							0.32	9.00	72.67						
	C5	37.5	0.17	10.44	92.48							0.30	8.77	73.63						
	C6	50	0.17	10.28	92.76							0.24	8.65	74.02						
	F		0.25									0.26								
	T																			
	T2		0.03									0.11								
	T3		0.03									0.12								
	Cc+Tt																			
	Mass Bal																			

	Sample	Time, min	Copper %	Copper Grade %	Copper Rec %	Ave Copper grade %	Std dev	Std error	Ave Copper rec %	Std dev	Std error	Nickel %	Nickel Grade 10%	Nickel Rec %	Ave Nickel grade %	Std dev	Std error	Ave Nickel rec %	Std dev	Std error
		0			0.00			0.00	0.00		0.00						0.00	0.00		0.00
Run-01	C1	5	1.42	14.21	82.73	14.68	0.67	0.47	83.68	1.34	0.95	1.17	11.66	60.45	12.01	0.49	0.35	61.95	2.13	1.51
3SPW	C2	10	0.25	12.37	85.49	12.76	0.55	0.39	86.49	1.41	1.00	0.40	10.46	64.35	10.75	0.41	0.29	65.93	2.24	1.58
3 SPW + 350 ppm Mg^{2+}	C3	17.5	0.22	11.71	86.54	12.10	0.55	0.39	87.56	1.44	1.02	0.51	10.11	66.53	10.39	0.40	0.28	68.04	2.14	1.52
	C4	25	0.21	11.29	87.23	11.68	0.54	0.38	88.28	1.49	1.05	0.41	9.85	67.73	10.12	0.38	0.27	69.26	2.15	1.52
	C5	37.5	0.19	10.80	88.06	11.20	0.57	0.40	89.08	1.44	1.02	0.36	9.52	69.10	9.80	0.40	0.29	70.56	2.06	1.45
	C6	50	0.22	10.62	88.44	10.98	0.51	0.36	89.49	1.49	1.05	0.33	9.39	69.60	9.64	0.36	0.25	71.11	2.12	1.50
	F		0.25									0.27								
	T																			
	T2		0.03									0.11								
	T3		0.05									0.13								
	Cc+Tt																			
	Mass Bal																			
		0																		
Run-02	C1	5	1.51	15.15	84.62							1.24	12.36	63.46						
3SPW	C2	10	0.27	13.14	87.48							0.41	11.03	67.51						
3 SPW + 350 ppm Mg^{2+}	C3	17.5	0.25	12.49	88.57							0.51	10.67	69.56						
	C4	25	0.24	12.06	89.33							0.42	10.39	70.78						
	C5		0.21	11.60	90.10							0.38	10.09	72.01						
	C6		0.21	11.34	90.54							0.30	9.90	72.61						
	F	37.5	0.27									0.27								
	T	50																		
	T2		0.04									0.12								
	T3		0.04									0.12								
	Cc+Tt																			
	Mass Bal																			

	Sample	Time, min	Copper %	Copper Grade %	Copper Rec %	Ave Copper grade %	Std dev	Std error	Ave Copper rec %	Std dev	Std error	Nickel %	Nickel Grade 10%	Nickel Rec %	Ave Nickel grade %	Std dev	Std error	Ave Nickel rec %	Std dev	Std error
		0						0.00	0.00		0.00						0.00	0.00		0.00
Run-01	C1	5	1.65	16.50	82.28	15.28	1.73	1.22	80.96	1.86	1.32	1.27	12.74	57.91	12.33	0.58	0.41	57.16	1.06	0.75
3SPW	C2	10	0.29	13.87	85.71	13.01	1.22	0.86	84.52	1.69	1.20	0.48	11.20	63.09	10.97	0.33	0.23	62.30	1.10	0.78
3 SPW + 700 ppm Mg^{2+}	C3	17.5	0.22	12.68	87.28	12.04	0.90	0.64	86.03	1.77	1.25	0.51	10.58	66.40	10.47	0.16	0.11	65.34	1.50	1.06
	C4	25	0.23	12.06	88.28	11.48	0.82	0.58	87.04	1.75	1.24	0.39	10.18	67.95	10.10	0.12	0.09	66.91	1.48	1.05
	C5	37.5	0.19	11.49	89.09	10.91	0.82	0.58	87.99	1.55	1.10	0.34	9.80	69.30	9.71	0.14	0.10	68.43	1.22	0.86
	C6	50	0.19	11.11	89.68	10.58	0.76	0.54	88.61	1.52	1.07	0.28	9.53	70.10	9.46	0.10	0.07	69.24	1.22	0.86
	F		0.26									0.27								
	T																			
	T2		0.04									0.12								
	T3		0.03									0.12								
	Cc+Tt																			
	Mass Bal																			
Run-02		0																		
3SPW	C1	5	1.41	14.06	79.64							1.19	11.93	56.42						
3 SPW + 700 ppm Mg^{2+}	C2	10	0.31	12.15	83.32							0.51	10.74	61.52						
	C3	17.5	0.26	11.41	84.78							0.58	10.35	64.28						
	C4	25	0.23	10.90	85.80							0.43	10.01	65.86						
	C5	37.5	0.20	10.33	86.89							0.38	9.61	67.57						
	C6	50	0.21	10.04	87.53							0.32	9.39	68.38						
	F		0.22									0.23								
	T																			
	T2		0.04									0.11								
	T3		0.04									0.13								
	Cc+Tt																			
	Mass Bal																			

Appendix A-6: Copper and Nickel's recovery and grade for 3 SPW spiked with: NO_3^-, SO_4^{2-} and $S_2O_3^{2-}$

	Sample	Time, min	Copper %	Copper Grade %	Copper Rec %	Ave Copper grade %	Std dev	Std error	Ave Copper rec %	Std dev	Std error	Nickel %	Nickel Grade 10%	Nickel Rec %	Ave Nickel grade %	Std dev	Std error	Ave Nickel rec %	Std dev	Std error
		0							0.00		0.00							0.00		0.00
Run-01	C1	5	1.31	13.14	83.16	14.11	1.37	0.97	83.24	0.12	0.08	1.00	10.04	64.89	10.65	0.85	0.60	64.51	0.55	0.39
3SPW	C2	10	0.31	11.82	86.06	12.63	1.14	0.81	85.69	0.51	0.36	0.38	9.23	68.61	9.74	0.71	0.50	67.83	1.11	0.78
3 SPW + 880 ppm NO_3^-	C3	17.5	0.26	11.23	87.37	11.94	1.01	0.72	86.86	0.72	0.51	0.44	8.92	70.87	9.36	0.62	0.44	69.90	1.38	0.97
	C4	25	0.24	10.78	88.38	11.50	1.02	0.72	87.64	1.05	0.74	0.37	8.66	72.44	9.10	0.62	0.44	71.16	1.81	1.28
	C5	37.5	0.22	10.45	89.10	11.12	0.95	0.67	88.27	1.17	0.83	0.33	8.45	73.55	8.85	0.57	0.41	72.20	1.92	1.35
	C6	50	0.21	10.16	89.75	10.81	0.93	0.66	88.80	1.33	0.94	0.28	8.25	74.44	8.65	0.57	0.40	72.97	2.08	1.47
	F		0.25									0.24								
	T																			
	T2		0.04									0.09								
	T3		0.04									0.09								
	Cc+Tt																			
	Mass Bal																			
		0																		
Run-02	C1	5	1.51	15.07	83.32							1.12	11.25	64.12						
3SPW	C2	10	0.24	13.44	85.33							0.35	10.24	67.05						
3 SPW + 880 ppm NO_3^-	C3	17.5	0.22	12.66	86.35							0.39	9.80	68.92						
	C4	25	0.19	12.22	86.89							0.32	9.53	69.88						
	C5	37.5	0.18	11.79	87.44							0.30	9.26	70.84						
	C6	50	0.17	11.47	87.86							0.27	9.06	71.50						
	F		0.27									0.26								
	T																			
	T2		0.06									0.11								
	T3		0.03									0.09								
	Cc+Tt																			
	Mass Bal																			

APPENDICES

	Sample	Time, min	Copper %	Copper Grade %	Copper Rec %	Ave Copper grade %	Std dev	Std error	Ave Copper rec %	Std dev	Std error	Nickel %	Nickel Grade 10%	Nickel Rec %	Ave Nickel grade %	Std dev	Std error	Ave Nickel rec %	Std dev	Std error
		0						0.00	0.00		0.00						0.00	0.00		0.00
Run-01	C1	5	1.09	10.87	81.96	12.11	1.76	1.25	83.33	1.93	1.36	0.87	8.72	63.73	9.14	0.59	0.42	65.09	1.92	1.36
3SPW	C2	10	0.29	10.12	84.19	11.21	1.54	1.09	85.47	1.80	1.27	0.37	8.25	66.50	8.60	0.50	0.35	67.86	1.93	1.37
3 SPW + 1760 ppm NO_3^-	C3	17.5	0.22	9.73	85.15	10.66	1.32	0.93	86.37	1.74	1.23	0.38	8.03	68.07	8.31	0.40	0.28	69.60	2.16	1.53
	C4	25	0.19	9.42	85.84	10.35	1.32	0.94	86.95	1.57	1.11	0.36	7.85	69.35	8.14	0.40	0.29	70.68	1.89	1.33
	C5	37.5	0.19	9.12	86.52	10.00	1.24	0.88	87.60	1.52	1.08	0.33	7.68	70.52	7.93	0.36	0.26	71.83	1.85	1.31
	C6	50	0.19	8.94	87.01	9.83	1.27	0.89	87.98	1.38	0.97	0.31	7.56	71.27	7.82	0.38	0.27	72.41	1.62	1.14
	F		0.27									0.25								
	T																			
	T2		0.03									0.09								
	T3		0.05									0.11								
	Cc+Tt																			
	Mass Bal																			
		0																		
Run-02	C1	5	1.34	13.36	84.69							0.96	9.56	66.45						
3SPW	C2	10	0.29	12.29	86.74							0.35	8.95	69.23						
3 SPW + 1760 ppm NO_3^-	C3	17.5	0.17	11.59	87.60							0.35	8.59	71.12						
	C4	25	0.19	11.29	88.06							0.33	8.42	72.02						
	C5	37.5	0.17	10.87	88.68							0.29	8.19	73.15						
	C6	50	0.20	10.72	88.95							0.27	8.09	73.56						
	F		0.27									0.26								
	T																			
	T2		0.03									0.09								
	T3		0.05									0.10								
	Cc+Tt																			
	Mass Bal																			

	Sample	Time, min	Copper %	Copper Grade %	Copper Rec %	Ave Copper grade %	Std dev	Std error	Ave Copper rec %	Std dev	Std error	Nickel %	Nickel Grade 10%	Nickel Rec %	Ave Nickel grade %	Std dev	Std error	Ave Nickel rec %	Std dev	Std error
		0						0.00	0.00		0.00							0.00		0.00
Run-01	C1	5	1.14	11.43	84.84	12.36	1.31	0.93	85.71	1.22	0.87	0.88	8.80	68.27	9.09	0.40	0.28	68.17	0.15	0.11
3SPW	C2	10	0.23	10.49	86.81	11.42	1.32	0.93	87.62	1.13	0.80	0.30	8.20	70.96	8.51	0.44	0.31	70.69	0.39	0.28
3 SPW + 1200 ppm SO_4^{2-}	C3	17.5	0.17	10.09	87.50	10.88	1.11	0.79	88.39	1.26	0.89	0.33	7.98	72.33	8.22	0.34	0.24	72.26	0.10	0.07
	C4	25	0.17	9.82	88.00	10.53	1.00	0.70	88.97	1.37	0.97	0.32	7.83	73.28	8.02	0.27	0.19	73.30	0.03	0.02
	C5	37.5	0.19	9.58	88.53	10.23	0.92	0.65	89.47	1.34	0.95	0.30	7.68	74.16	7.84	0.23	0.16	74.17	0.01	0.01
	C6	50	0.17	9.39	88.93	9.83	0.64	0.45	90.17	1.76	1.24	0.25	7.55	74.77	7.60	0.06	0.05	75.24	0.67	0.47
	F		0.27									0.25								
	T																			
	T2		0.05									0.10								
	T3		0.03									0.08								
	Cc+Tt																			
	Mass Bal																			
		0																		
Run-02	C1	5	1.33	13.28	86.57							0.94	9.37	68.06						
3SPW	C2	10	0.29	12.35	88.42							0.33	8.82	70.41						
3 SPW + 1200 ppm SO_4^{2-}	C3	17.5	0.17	11.66	89.28							0.32	8.46	72.19						
	C4	25	0.18	11.23	89.94							0.29	8.21	73.32						
	C5	37.5	0.16	10.88	90.42							0.25	8.01	74.18						
	C6	50	0.17	10.28	91.41							0.24	7.64	75.71						
	F		0.27									0.25								
	T																			
	T2		0.03									0.08								
	T3		0.03									0.08								
	Cc+Tt																			
	Mass Bal																			

	Sample	Time, min	Copper %	Copper Grade %	Copper Rec %	Ave Copper grade %	Std dev	Std error	Ave Copper rec %	Std dev	Std error	Nickel %	Nickel Grade 10%	Nickel Rec %	Ave Nickel grade %	Std dev	Std error	Ave Nickel rec %	Std dev	Std error
Run-01		0						0.00	0.00		0.00							0.00		0.00
3SPW	C1	5	1.11	11.11	86.74	10.81	0.42	0.30	86.02	1.02	0.72	0.94	9.37	70.34	8.67	0.99	0.70	67.91	3.44	2.43
3 SPW + 2400 ppm SO_4^{2-}	C2	10	0.22	10.01	89.19	9.73	0.40	0.28	88.78	0.59	0.42	0.30	8.59	73.54	7.96	0.88	0.62	71.49	2.90	2.05
	C3	17.5	0.16	9.53	90.07	9.31	0.32	0.23	89.72	0.50	0.35	0.35	8.30	75.33	7.73	0.80	0.56	73.34	2.81	1.99
	C4	25	0.18	9.30	90.62	9.07	0.32	0.23	90.31	0.43	0.30	0.31	8.14	76.21	7.59	0.78	0.55	74.33	2.65	1.87
	C5	37.5	0.17	9.04	91.19	8.82	0.31	0.22	90.90	0.41	0.29	0.27	7.95	77.12	7.43	0.75	0.53	75.32	2.54	1.80
	C6	50	0.19	8.91	91.53	8.70	0.30	0.21	91.25	0.40	0.28	0.26	7.86	77.56	7.34	0.73	0.52	75.78	2.52	1.79
	F		0.24									0.24								
	T																			
	T2		0.03									0.08								
	T3		0.03									0.09								
	Cc+Tt																			
	Mass Bal																			
		0																		
Run-02	C1	5	1.05	10.51	85.29							0.80	7.98	65.48						
3SPW	C2	10	0.25	9.44	88.36							0.32	7.34	69.44						
3 SPW + 2400 ppm SO_4^{2-}	C3	17.5	0.21	9.08	89.37							0.39	7.17	71.35						
	C4	25	0.19	8.84	90.01							0.33	7.04	72.46						
	C5	37.5	0.17	8.60	90.62							0.29	6.90	73.53						
	C6	50	0.19	8.48	90.96							0.25	6.82	73.99						
	F		0.26									0.25								
	T																			
	T2		0.03									0.09								
	T3		0.03									0.10								
	Cc+Tt																			
	Mass Bal																			

	Sample	Time, min	Copper %	Copper Grade %	Copper Rec %	Ave Copper grade %	Std dev	Std error	Ave Copper rec %	Std dev	Std error	Nickel %	Nickel Grade 10%	Nickel Rec %	Ave Nickel grade %	Std dev	Std error	Ave Nickel rec %	Std dev	Std error
		0							0.00		0.00						0.00	0.00		0.00
Run-01	C1	5	1.11	11.07	85.32	10.43	0.91	0.64	85.48	0.23	0.16	0.83	8.34	67.48	8.74	0.57	0.41	69.84	3.34	2.36
3SPW	C2	10	0.23	9.86	88.20	9.39	0.66	0.47	88.29	0.12	0.09	0.32	7.62	71.64	8.03	0.57	0.40	73.45	2.57	1.81
3 SPW + 60 ppm $S_2O_3^{2-}$	C3	17.5	0.19	9.41	89.24	9.01	0.56	0.39	89.26	0.03	0.02	0.37	7.40	73.74	7.81	0.58	0.41	75.27	2.17	1.54
	C4	25	0.20	9.12	90.01	8.76	0.51	0.36	89.98	0.04	0.03	0.29	7.23	74.89	7.64	0.58	0.41	76.30	1.99	1.41
	C5	37.5	0.16	8.82	90.67	8.51	0.44	0.31	90.63	0.06	0.04	0.23	7.03	75.87	7.46	0.60	0.43	77.19	1.87	1.32
	C6	50	0.16	8.64	91.09	8.36	0.40	0.28	91.04	0.07	0.05	0.21	6.91	76.45	7.34	0.61	0.43	77.70	1.77	1.25
	F		0.26									0.24								
	T																			
	T2		0.03									0.08								
	T3		0.03									0.08								
	Cc+Tt																			
	Mass Bal																			
Run-02		0																		
3SPW	C1	5	0.98	9.79	85.64							0.91	9.15	72.20						
3 SPW + 60 ppm $S_2O_3^{2-}$	C2	10	0.24	8.92	88.37							0.29	8.43	75.26						
	C3	17.5	0.20	8.62	89.28							0.38	8.22	76.81						
	C4	25	0.20	8.41	89.95							0.29	8.05	77.71						
	C5	37.5	0.19	8.20	90.59							0.26	7.89	78.51						
	C6	50	0.18	8.08	90.99							0.22	7.77	78.96						
	F		0.27									0.24								
	T																			
	T2		0.03									0.08								
	T3		0.03									0.08								
	Cc+Tt																			
	Mass Bal																			

APPENDICES

	Sample	Time, min	Copper %	Copper Grade %	Copper Rec %	Ave Copper grade %	Std dev	Std error	Ave Copper rec %	Std dev	Std error	Nickel %	Nickel Grade 10%	Nickel Rec %	Ave Nickel grade %	Std dev	Std error	Ave Nickel rec %	Std dev	Std error
		0							0.00		0.00							0.00		0.00
Run-01	C1	5	1.40	14.04	86.80	14.06	0.04	0.03	86.86	0.09	0.06	0.93	9.32	68.08	9.81	0.69	0.49	68.12	0.06	0.04
3SPW	C2	10	0.28	12.62	89.30	12.47	0.21	0.15	89.44	0.21	0.15	0.34	8.58	71.68	8.89	0.44	0.31	71.74	0.08	0.06
3 SPW + 78 ppm $S_2O_3^{2-}$	C3	17.5	0.23	12.05	90.23	11.77	0.40	0.28	90.39	0.22	0.16	0.47	8.37	73.96	8.56	0.27	0.19	73.95	0.01	0.01
	C4	25	0.21	11.72	90.78	11.35	0.52	0.37	91.00	0.32	0.22	0.32	8.19	74.96	8.31	0.16	0.11	75.03	0.09	0.06
	C5	37.5	0.22	11.38	91.40	11.01	0.52	0.37	91.55	0.22	0.16	0.33	8.02	76.06	8.11	0.13	0.09	75.95	0.15	0.11
	C6	50	0.21	11.16	91.80	10.79	0.53	0.38	91.93	0.18	0.13	0.27	7.90	76.67	7.97	0.10	0.07	76.50	0.23	0.16
	F		0.26									0.24								
	T																			
	T2		0.03									0.08								
	T3		0.03									0.08								
	Cc+Tt																			
	Mass Bal																			
Run-02		0																		
3SPW	C1	5	1.41	14.09	86.92							1.03	10.30	68.17						
3 SPW + 78 ppm $S_2O_3^{2-}$	C2	10	0.24	12.32	89.59							0.31	9.20	71.80						
	C3	17.5	0.16	11.49	90.54							0.33	8.75	73.95						
	C4	25	0.16	10.98	91.23							0.25	8.42	75.09						
	C5	37.5	0.15	10.64	91.71							0.22	8.20	75.84						
	C6	50	0.16	10.41	92.06							0.21	8.04	76.34						
	F		0.26									0.24								
	T																			
	T2		0.03									0.08								
	T3		0.03									0.08								
	Cc+Tt																			
	Mass Bal																			

Appendix B-1: Sequential flotation performance for all the water types and ions involved

	Cu-Ni Recovery			Cu-Ni Grade		Recovery_std		Grade_std	
Water (I.S)	Circuit	Cu Rec (%)	Ni Rec (%)	Cu Grade (%)	Ni Grade (%)	Cu Rec_std	Ni Rec_std	Cu Grad_std	Ni Grad_std
3SPW	Cu-circuit	70.16	55.75	8.72	3.95	0.08	0.91	0.62	0.45
	Ni-circuit	18.24	13.37	2.05	2.44	3.42	0.88	0.34	0.12
5 SPW	Cu-circuit	60.00	48.79	9.56	4.35	11.80	3.81	0.07	0.10
	Ni-circuit	23.41	15.92	2.03	3.68	3.26	2.72	0.04	0.19
10 SPW	Cu-circuit	54.59	44.51	9.41	4.70	0.60	5.41	0.49	0.31
	Ni-circuit	34.73	30.40	2.03	3.32	3.22	7.63	0.07	0.13
3 SPW + 400 ppm Ca^{2+}	Cu-circuit	71.61	53.34	11.55	6.17	0.60	5.41	0.60	0.12
	Ni-circuit	15.76	16.46	1.26	2.82	3.54	2.74	0.13	0.15
3 SPW + 800 ppm Ca^{2+}	Cu-circuit	67.55	56.68	8.44	5.46	1.77	0.42	1.42	0.81
	Ni-circuit	21.27	12.88	1.78	3.25	1.25	0.29	0.08	0.07
3 SPW + 350 ppm Mg^{2+}	Cu-circuit	65.22	53.05	10.57	6.57	1.83	0.72	0.39	0.29
	Ni-circuit	21.27	12.88	2.19	4.17	2.07	0.47	0.12	0.01
3 SPW + 700 ppm Mg^{2+}	Cu-circuit	57.99	43.90	10.83	6.72	1.00	1.58	0.86	0.23
	Ni-circuit	26.52	18.41	2.18	4.24	1.25	0.60	0.09	0.17
3 SPW + 880 ppm NO_3^-	Cu-circuit	63.83	51.80	10.48	6.25	1.20	0.78	0.81	0.50
	Ni-circuit	21.86	16.03	2.15	3.48	4.60	2.54	0.22	0.18
3 SPW + 1760 ppm NO_3^-	Cu-circuit	68.22	53.71	9.32	5.27	0.36	0.78	1.09	0.35
	Ni-circuit	17.25	14.16	1.89	3.33	0.54	0.09	0.10	0.14
3 SPW + 1200 ppm SO_4^{2-}	Cu-circuit	66.67	55.18	9.67	5.62	1.27	1.37	0.93	0.31
	Ni-circuit	20.95	15.50	1.75	2.90	4.93	2.41	0.02	0.15
3 SPW + 2400 ppm SO_4^{2-}	Cu-circuit	66.79	56.44	7.91	4.77	0.80	0.28	0.28	0.62
	Ni-circuit	21.98	15.05	1.81	3.19	0.40	0.15	0.09	0.11
3 SPW + 60 ppm $S_2O_3^{2-}$	Cu-circuit	64.81	57.50	7.53	5.08	0.42	2.05	0.47	0.41
	Ni-circuit	23.48	15.95	1.87	2.94	1.00	1.03	0.05	0.06
3 SPW + 78 ppm $S_2O_3^{2-}$	Cu-circuit	65.88	54.89	10.59	5.70	0.09	1.81	0.15	0.31
	Ni-circuit	23.57	16.85	1.88	3.19	0.17	0.75	0.31	0.50

Appendix C-1: 2-phase column studies

Ionic strenth	Froth	Solution	std_froth	std_pulp
3 SPW	247.36	516.77	8.98	5.03
5 SPW	910.82	990.87	1.12	2.43
10 SPW	1311.33	1311.33	0.01	0.01
3 SPW + 400 ppm Ca^{2+}	509.85	588.78	2.58	40.92
3 SPW + 800 ppm Ca^{2+}	583.80	585.72	3.74	6.343
3 SPW + 350 ppm Mg^{2+}	189.83	534.72	7.37	15.55
3 SPW + 700 ppm Mg^{2+}	85.28	532.78	0.92	1.92
3 SPW + 1200 ppm SO_4^{2-}	635.82	578.83	10.22	8.37
3 SPW + 2400 ppm SO_4^{2-}	507.78	647.92	6.65	15.75
3 SPW + 880 ppm NO_3^-	232.85	640.52	56.65	2.78
3 SPW + 1760 ppm NO_3^-	743.67	900.13	25.60	8.37
3 SPW + 60 ppm $S_2O_3^{2-}$	490.05	574.95	10.58	4.68
3 SPW + 78 ppm $S_2O_3^{2-}$	478.82	578.58	2.72	2.88

Appendix C-2: 3-Phase column studies linked to recovery

Ionic strenth	Froth	Pulp	Cu_Rec [%]	Ni_Rec [%]	std_froth	std_pulp	std_copper	std_nickel
3 SPW	4.68	5.42	90.92	74.03	0.28	0.35	0.46	1.05
5 SPW	6.26	5.76	86.12	70.43	0.11	0.14	11.44	2.25
10 SPW	9.74	11.06	93.01	82.12	0.37	0.33	0.74	5.68
3 SPW + 400 ppm Ca^{2+}	4.32	4.56	89.30	74.76	0.11	0.14	1.94	1.18
3 SPW + 800 ppm Ca^{2+}	4.40	4.38	91.18	73.48	0.15	0.31	1.58	0.54
3 SPW + 350 ppm Mg^{2+}	4.44	4.64	89.49	71.11	0.13	0.18	1.05	1.50
3 SPW + 700 ppm Mg^{2+}	3.73	4.62	88.61	69.24	0.60	0.10	1.07	0.86
3 SPW + 1200 ppm SO_4^{2-}	4.28	5.41	90.17	75.24	0.05	0.11	1.24	0.47
3 SPW + 2400 ppm SO_4^{2-}	3.96	5.10	91.25	75.78	0.00	0.04	0.28	1.79
3 SPW + 880 ppm NO_3^-	4.46	5.09	88.80	72.97	0.29	0.05	0.94	1.47
3 SPW + 1760 ppm NO_3^-	6.15	7.09	87.98	72.41	0.30	0.07	0.97	1.14
3 SPW + 60 ppm $S_2O_3^{2-}$	3.49	5.27	91.04	77.70	0.17	0.04	0.05	1.25
3 SPW + 78 ppm $S_2O_3^{2-}$	4.36	5.10	91.93	76.50	0.03	0.01	0.13	0.16